LIBRARY
UNIVERSITY OF UTAH

Journal of the Electrochemical Society

Engineering
Library

AS PARTNERS IN
YOUR PROGRESS . . .

PACKAGING – is a *plus* factor!

The painstaking care with which GLC carbon and graphite products are prepared for shipment is typical of the interest taken by our personnel—all along the line—to achieve unsurpassed quality.

The earnestness with which our people tackle their jobs —whether the task be large or small—is a substantial *plus factor* in the dependability of GLC electrodes, anodes, carbon brick and mold stock.

The high degree of integration between discoveries in our research laboratories, refinements in processing raw materials, and improved manufacturing techniques is further assurance of excellent product performance.

ELECTRODE
GLC®
DIVISION

Great Lakes Carbon Corporation

GRAPHITE ELECTRODES, ANODES, MOLDS and SPECIALTIES

ADMINISTRATIVE OFFICE: 18 East 48th Street, New York 17, N. Y. PLANTS: Niagara Falls, N. Y., Morganton, N. C. OTHER OFFICES: Niagara Falls, N. Y., Oak Park, Ill., Pittsburgh, Pa. SALES AGENTS: J. B. Hayes Company, Birmingham, Ala., George O. O'Hara, Wilmington, Cal. SALES AGENTS IN OTHER COUNTRIES: Great Northern Carbon & Chemical Co., Ltd., Montreal, Canada; Great Eastern Carbon & Chemical Co., Inc., Chiyoda-Ku, Tokyo, Japan

EDITORIAL STAFF

R. M. Burns, *Chairman*
Cecil V. King, *Editor*
Norman Hackerman, *Technical Editor*
Ruth G. Sterns, *Managing Editor*
U. B. Thomas, *News Editor*
Natalie Michalski, *Assistant Editor*
Eleanor Blair, *Assistant Editor*

DIVISIONAL EDITORS

W. C. Vosburgh, *Battery*
Joseph E. Draley, *Corrosion*
John J. Chapman, *Electric Insulation*
Abner Brenner, *Electrodeposition*
H. C. Froelich, *Electronics*
Herbert Bandes, *Electronics—Semiconductors*
Sherlock Swann, Jr., *Electro-Organic*
John M. Blocher, Jr., *Electrothermics and Metallurgy, I*
A. U. Seybolt, *Electrothermics and Metallurgy, II*
W. C. Gardiner, *Industrial Electrolytic*
C. W. Tobias, *Theoretical Electrochemistry*

REGIONAL EDITORS

Howard T. Francis, *Chicago*
Joseph Schulein, *Pacific Northwest*
J. C. Schumacher, *Los Angeles*
G. W. Heise, *Cleveland*
G. H. Fetterley, *Niagara Falls*
Oliver Osborn, *Houston*
Earl A. Gulbransen, *Pittsburgh*
A. C. Holm, *Canada*
J. W. Cuthbertson, *Great Britain*
T. L. Rama Char, *India*

ADVERTISING OFFICE

Jack Bain
Advertising Manager
545 Fifth Avenue
New York 17, N. Y.
Phone—*Murray Hill 2-3345*

Journal of the
Electrochemical Society

MAY 1956 VOL. 103 • NO. 5

CONTENTS

Editorial

The Electrochemist and the Atom. *Hans Thurnauer* 113C

Technical Papers

Dissolution of Cadmium in Chromic Chloride Solutions. *Cecil V. King and Edward Hillner* 261

High Pressure Oxidation of Metals—Tungsten in Oxygen. *J. P. Baur, D. W. Bridges, and W. M. Fassell, Jr.* 266

Oxidation of Oxygen-Free High Conductivity Copper to Cu_2O. *J. P. Baur, D. W. Bridges, and W. M. Fassell, Jr.* 273

Corrosion of Copper-Gold Alloys by Oxygen-Containing Solutions of Ammonia and Ammonium Salts. *J. I. Fisher and J. Halpern* 282

Acceleration of the Dissolution of Iron in Sulfuric Acid by Ferric Ions. *Harry C. Gatos* 286

Polymer Synthesis by Gamma Radiation. *T. D. Callinan* ... 292

Preparation of Pure Nickel by Electrolysis of a Chloride Solution. *W. A. Wesley* 296

Determination of the Activity of Sodium in Sodium-Lead Alloys at High Temperatures. *Bernard Porter and Morris Feinleib* 300

Electrochemical Characteristics of Melts in the $Sb\text{-}Sb_2S_3$ System. *Tsutomu Yanagase and Gerhard Derge* 303

Current Affairs

Tennessee Products & Chemical Corp.—ECS Sustaining Member 116C

News Items 117C
Section News 121C
New Members 122C
ECS Membership Statistics 123C
Personals 123C
Book Reviews 124C
Announcements from Publishers 126C
Literature from Industry .. 126C
Employment Situations ... 126C

Published monthly by The Electrochemical Society, Inc., Mount Royal and Guilford Aves., Baltimore 2, Md., combining the JOURNAL and TRANSACTIONS OF THE ELECTROCHEMICAL SOCIETY. Editorial offices: 216 West 102nd Street, New York 25, N. Y. Statements and opinions given in articles and papers in the JOURNAL OF THE ELECTROCHEMICAL SOCIETY are those of the contributors, and The Electrochemical Society assumes no responsibility for them. Nondeductible subscription to members $5.00; subscription to nonmembers $18.00. Single copies $1.25 to members, $1.75 to nonmembers. Copyright 1956 by The Electrochemical Society, Inc. Entered as second-class matter November 15, 1947, at the Post Office at Baltimore, Md., under the act of August 24, 1912.

CALL ON Mallinckrodt

in the development stage...

The ability of Mallinckrodt research and production chemists to control purity, maintain uniformity from the pilot plant through the production plant stages has played an important part in the growth of the electronics industry. This is particularly true of chemicals needed to manufacture phosphors for *fluorescent lamps.*

The year 1938 marked the advent of the first commercial fluorescent lamp. Production in 1945 was 37 million fluorescent lamps. During the last four years it has averaged over 90 million per year.

At the inception, the average life rating of a fluorescent lamp was only 100 hours . . . efficiency was extremely low. By 1948 life rating had been increased to approximately 3000 hours, but the efficiency drop was as much as 40% after only 1000 hours.

The problem: ***manufacturing the proper halo-phosphate phosphors.***

The pure *calcium phosphate dibasic* needed was not commercially available. The industry called on Mallinckrodt whose experienced technical staff produced laboratory samples in a matter of days. Large-scale factory production was underway within a month after laboratory samples were approved.

Mallinckrodt had again substantiated its reputation to provide the *right chemical* processed to the exact degree of purity and proper physical form *at a strategic time.*

Mallinckrodt maintains high purity standards in the following partial list of chemicals used extensively in the electronics industry:

ACIDS
Acetic Acid
Boric Acid
Chromic Acid
Hydrofluoric Acid
Nitric Acid
Sulfuric Acid

ALUMINUM
Aluminum Chloride
Aluminum Nitrate

AMMONIUM
Ammonium Bifluoride
Ammonium Carbonate
Ammonium Phosphate Dibasic

BARIUM
Barium Acetate
Barium Carbonate
Barium Chloride
Barium Nitrate

CADMIUM
Cadmium Chloride
Cadmium Nitrate
Cadmium Sulfate

CALCIUM
Calcium Carbonate
Calcium Chloride
Calcium Fluoride
Calcium Nitrate
Calcium Phosphate Dibasic

COPPER
Cupric Sulfate
Cuprous Chloride

LITHIUM
Lithium Carbonate
Lithium Chloride
Lithium Sulfate

MAGNESIUM
Magnesium Carbonate
Magnesium Oxide

MANGANESE
Manganese Carbonate
Manganese Sulfate

MERCURY
Mercury Metal
Mercuric Oxide

NICKEL
Nickel Nitrate

POTASSIUM
Potassium Cyanide
Potassium Dichromate

SILICA
Silicic Acid

SILVER
Silver Cyanide
Silver Nitrate
Silver Oxide

SODIUM
Sodium Carbonate
Sodium Dichromate
Sodium Hydroxide

SOLVENTS AND ORGANICS
Benzene
Carbon Tetrachloride
Chloroform
Ether
Ethyl Acetate
Isopropyl Alcohol
Methyl Alcohol
Toluene

STEARATES
Calcium Stearate
Magnesium Stearate
Zinc Stearate

STRONTIUM
Strontium Chloride
Strontium Nitrate

ZINC
Zinc Metal
Zinc Chloride
Zinc Oxide
Zinc Sulfate

MALLINCKRODT CHEMICAL WORKS

SECOND & MALLINCKRODT STREETS, ST. LOUIS 7, MO. · 72 GOLD STREET, NEW YORK 8, N. Y.

CHICAGO · CINCINNATI · CLEVELAND · DETROIT · LOS ANGELES · PHILADELPHIA · SAN FRANCISCO

IN CANADA: MALLINCKRODT CHEMICAL WORKS, LIMITED · MONTREAL · TORONTO

A dependable source of DEPENDABLE ANODES

(Plain or Treated Types)

STACKPOLE

CARBON COMPANY • *St. Marys, Pa.*

THIS IS OUR 50th Year

STACKPOLE

FOUNDED 1906

BRUSHES for all rotating electrical equipment • CONTACTS (carbon-graphite and metal powder types) • TUBE ANODES • CATHODIC PROTECTION ANODES • VOLTAGE REGULATOR DISCS • WATER HEATER and PASTEURIZATION ELECTRODES • BEARINGS • WELDING CARBONS • MOLDS and DIES SPECTROGRAPHITE • POROUS CARBON • SALT BATH RECTIFICATION RODS • SEAL RINGS • FRICTION SEGMENTS • CLUTCH RINGS • ELECTRIC FURNACE HEATING ELEMENTS • PUMP VANES . . . and many others.

Editorial

The Electrochemist and the Atom

IN YEARS TO COME, historians of the atomic age will refer to two official United States papers which describe in detail the status of atomic developments at the time of their publication. Eleven years ago the first document was published, the Smyth report, accounting for development of the atomic bomb. The author, Professor H. D. Smyth, gave an excellent review of the Manhattan project under the leadership of General Groves and a summary of scientific information (a semitechnical report, as he called it) which could be released to the public without violating national security.

It is to the credit of General Groves and his collaborators that they realized, even during times of great urgency, that nuclear energy might have far reaching applications in peace; he appointed the Tolman Committee to look into the possibilities of using nuclear energy for power production and radioactive by-products of fission processes for scientific, medical, and industrial purposes. Smyth, in his report, summarizes the findings of the Committee: "While there was general agreement that a great industry might eventually arise, comparable, perhaps, with the electronics industry, there was disagreement as to how rapidly such an industry would grow; the consensus was that the growth would be slow, over a period of many years. At least there is no immediate prospect of running cars with nuclear power or lighting houses with radioactive lamps, although there is a good probability that nuclear power for special purposes could be developed within ten years and that plentiful supplies of radioactive materials can have a profound effect on scientific research and perhaps the treatment of certain diseases in a similar period."

And now, eleven years later, we have before us the second document, the McKinney report on the present and future impact of the peaceful uses of atomic energy. The report has received wide publicity and has drawn many favorable comments all over the country. It should be required reading for every member of our Society.

It is surprising how close we came to the prognostications of the Tolman Committee. While we have made considerable progress in applying radioactive materials in science, medicine, agriculture, and many industrial processes, we are only at the threshold of the atomic age, as far as power production is concerned, and many problems must be solved before we can live in the world of Science Fiction. The McKinney panel predicts that electric power from nuclear fission will make its first impact not before 1965, but by 1980 the capacity of atomic power plants may exceed present United States electrical generating capacity.

It is hoped that the process of growth and development can be accelerated by reducing secrecy restrictions. There does not seem to be any doubt that sooner or later restrictions for the peaceful development of the atom will fall. This, however, will carry with it a responsibility by Industry to make use of the afforded opportunity.

Electrochemical developments have significantly contributed to atomic progress in the past and will do so in the future. One of the leading electrochemical enterprises of our country is in charge of the largest Government atomic installation and research laboratory.

Better and radically new materials are needed to solve the problems of heat resistance, corrosion, radiation damage, and others which arise in the design of power plants of tomorrow. The atomic power plant can be efficient and competitive with conventional installations only if it is operated at the high temperatures and pressures of conventional power systems.

Utilization of atomic energy for chemical processing has hardly been considered. The McKinney panel recommends that developments in this direction should be pursued. The Electrochemical Industry has a golden opportunity to render pioneer work in this field.

Perhaps it is proper to suggest, in the light of the McKinney report, that our Society should form a Committee to assess the possible contributions of the Electrochemical Industry toward peaceful atomic developments. Such a survey would provide a useful basis for Research and Industry to plan for the future and help to attract young people and scientists, so urgently needed for our growth.

—HANS THURNAUER

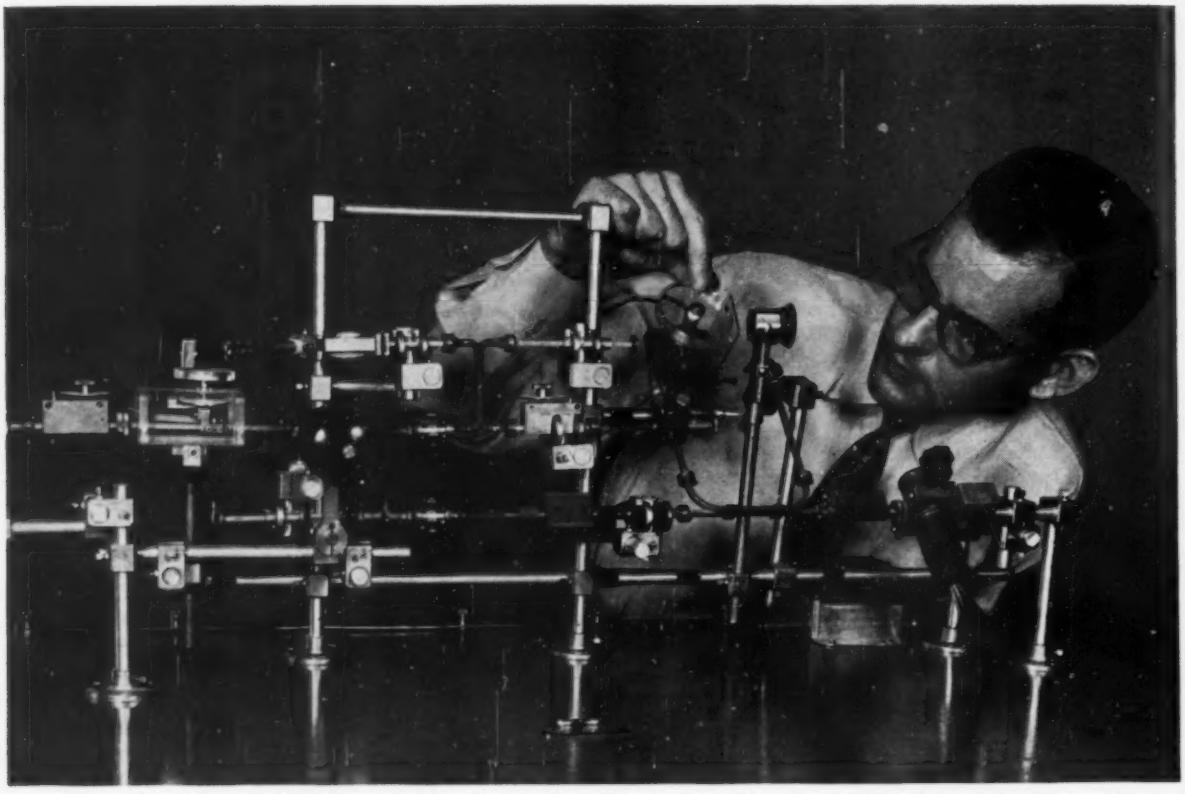

Physicist G. K. Farney checks the frequency of Bell's new klystron, which is located at far right. Tube's output is about 20 milliwatts.

Sixty billion vibrations per second

A great new giant of communications—a waveguide system for carrying hundreds of thousands of voices at once, as well as television programs—is being investigated at Bell Telephone Laboratories.

Such a revolutionary system calls for frequencies much higher than any now used in communications. These are provided by a reflex klystron tube that oscillates at 60,000 megacycles, and produces waves only 5 mm. long.

The resonant cavity that determines the frequency is smaller than a pinhead. The grid through which the energizing electron beam is projected is only seven times as wide as a human hair, and the grid "wires" are of tungsten ribbon 3/10,000 inch in width.

G. K. Farney, University of Kentucky Ph. D. in nuclear physics, is one of the men who successfully executed the development of the klystron. Dr. Farney is a member of a team of Bell scientists whose exciting goal is to harness the immense bandwidth that is available with millimeter waves . . . and to make certain that your telephone system remains the best in the world.

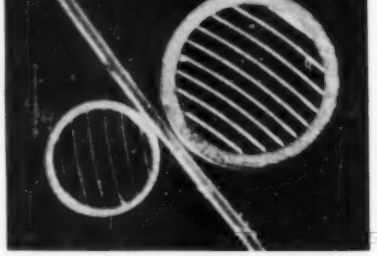

Grids in new tube, enlarged 30 times, with human hair for comparison. Electronic beam passes through smaller, then larger, grid.

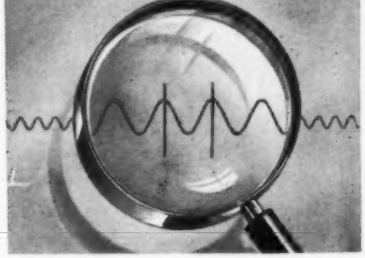

Wavelengths produced by the klystron tube are only .2 inch long—1/15 that of the transcontinental radio relay system.

BELL TELEPHONE LABORATORIES

WORLD CENTER OF COMMUNICATIONS RESEARCH

Dissolution of Cadmium in Chromic Chloride Solutions

CECIL V. KING AND EDWARD HILLNER

Department of Chemistry, New York University, New York, New York

ABSTRACT

The dissolution rate of cadmium has been determined in dilute chromic chloride solutions containing hydrochloric acid up to 4M as functions of concentration, stirring speed, and temperature. A small amount of hydrogen is produced, but the main reaction is the reduction of chromic to chromous ion. Reaction with the violet hexaaquo chromic ion is slow and under chemical or electrochemical control; with the green dichlorotetraaquo ion it is much faster and transport- or diffusion-controlled. In each case, the driving force is only a few millivolts. The potential of the metal in these solutions is essentially that of the cadmium-cadmium ion couple, and there is little if any anodic polarization.

INTRODUCTION

The research described below follows a general plan to study the corrosive dissolution of metals in such solutions that insoluble films are not formed, and that the driving force of the reaction is small. If cadmium is immersed in dilute, unacidified chromic chloride, oxide or hydroxide films are deposited, but this does not occu with 0.5–4M hydrochloric acid present.

The following standard reduction or electrode potentials are found in the literature:

$$Cd^{++} + 2e \rightarrow Cd \qquad E^0 = -0.402 \text{ v}$$

$$Cr^{+++} + e \rightarrow Cr^{++} \qquad E^0 = -0.40 \text{ or } -0.41 \text{ v}$$

The chromic-chromous potential cannot be measured on platinum, which catalyzes the chromous-hydrogen ion reaction, but has been measured on mercury (1). It is sensitive to traces of oxygen, and the standard potential E^0 is uncertain to ± 5 mv or more. Exact potentials for the solutions employed in the present research are even less certain, but it is evident that the reaction

$$Cd + 2Cr^{+++} \rightarrow Cd^{++} + 2Cr^{++} \qquad (I)$$

has little driving force, or only a small free energy change. The fact that cadmium ion forms stable chloride complexes helps the forward reaction, but even in 4M HCl it does not go to completion.

EXPERIMENTAL

Cylinders of best commercial cadmium (99.9%) were used, each approximately 2.5 cm long and 1.5 to 2 cm in diameter. They were mounted on a motor shaft with the ends protected. The rotational speed was established with a stroboscope (calibrated with the aid of a synchronous motor), and was adjusted to obtain the desired peripheral speed of the cylinder.

The reaction vessel was a 4-oz square bottle, fitted with a nitrogen inlet tube, and mounted in a 400 ml beaker. The square bottle allowed use of a small solution volume, preventing cavitation at the stirring speeds employed without introduction of baffle plates or sealing the cell. The vessel was kept at constant temperature (± 0.3°C) by circulating water from a thermostat through the beaker. All solutions were deaerated as well as possible by bubbling nitrogen through them for 30 min prior to, and during, each run. Nitrogen was passed over copper turnings at 450°C, then through water. A small space between the Bakelite sleeve of the motor shaft and the bottle neck allowed the nitrogen to escape.

Stock solutions of violet chromic chloride were prepared by dissolving the green crystals (Analytical or Reagent grade) in water and allowing to stand at least a week; as shown below, about 98% of the ion was then in the hexaaquo form $Cr(H_2O)_6^{+++}$. Green solutions were prepared by dissolving the salt in at least 2M hydrochloric acid, which makes hydrolysis of the green ion $CrCl_2(H_2O)_4^+$ to the violet very slow, since this rate is inversely proportional to hydrogen ion concentration (2). Fresh green stock solution was prepared every 7–10 days since lower rates were found with older solutions. Stock solutions were analyzed by oxidizing samples with sodium peroxide to chromate, then following a standard volumetric procedure.

Reaction solutions were made up by mixing the proper amounts of stock solution with standardized hydrochloric acid and water, with a final volume of 70 ml in all cases. The amount of dissolution in suitable time intervals was determined by weight loss of the cylinders and was corrected for weight loss in the acid alone to obtain the amount of chromic ion reduction. In several runs this was checked by analysis for chromous ion; excess deaerated dichromate was added to the solution, which was then titrated with ferrous sulfate.

Violet Solutions

The dissolution rate in violet solutions was small, a few mg/hr from a cylinder 15 cm² in area. The cylinders were polished with #600 silicon carbide paper, immersed at the proper rotational speed, and taken out each hour for weighing, without repolishing until a new solution was used. Dissolution was much greater in the first hour or two than in subsequent hours because of the small amount of green ion present. The latter reacts at a transport-controlled rate, and is essentially all used up in an hour or two with the solution volume and stirring speeds employed.

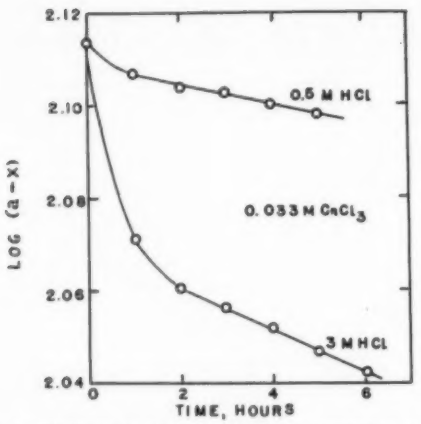

FIG. 1. Evaluation of first order rate constants in violet chromic chloride; 25°C, peripheral speed 15,000 cm/min.

TABLE I. *Rate constants k_c in cm/hr in violet chromic chloride, 25°C and 15,000 cm/min*

C_{HCl}, M	Concentration $CrCl_3$, M				Avg k_c
	0.033	0.066	0.10	0.133	
0.5	0.015	0.011	0.012	0.014	0.013
1.0	0.016	0.020	0.016	0.014	0.016
2.0	0.022	0.024	0.023	0.017	0.022
					0.021*
					0.021†
3.0	0.055	0.133	0.092	0.175	0.114
					0.096*
					0.102†
4.0	0.304	0.244	—	—	0.274

* At 7500 cm/min.
† N_2 bubbling only.

During the first-hour runs a gray deposit appeared on the cylinders, in a spiral pattern related to the paths of solution flow. The film could be wiped off with moist filter paper, and microanalysis of the resulting smudge showed no metal other than cadmium. In all other experiments the metal surface remained bright or at least had no loose deposit.

First order rate constants were obtained in accordance with the equation

$$k_c = \frac{2.3V}{At} \log \frac{a}{a - x} \qquad \text{(II)}$$

with V in cm³, A the measured area in cm², t in hours. The dissolving capacity of the solution a was calculated from the composition, since it was not practical to determine the extent of reaction at equilibrium. A comparatively small fraction of the reaction was followed, and thus k_c is a measure of the forward rate of reaction (I). As shown in Fig. 1, a plot of log $(a - x)$ vs. time becomes linear after an hour or two, and k_c is found from the slope. All weight losses were corrected for the amount dissolving in the acid alone, before making the plots.

Values of k_c for 25°C and a peripheral speed of 15000 cm/min are given in Table I. Most of these runs were repeated at 7500 cm/min, and with no stirring except nitrogen bubbling. Examples are included in the table.

TABLE II. *Activation energy in violet solutions*

C_{HCl}, M	0.5	1.0	2.0	3.0	4.0
E, cal/mole . . .	8900	10,500	12,800	14,300	15,400

While the experimental error is large in some cases, it is evident from Table I that there is no consistent trend in k_c with chromium chloride concentration or with stirring speed. Several qualitative experiments were done with no stirring at all; a cadmium cylinder was immersed in deaerated solution contained in a narrow tube about 25 cm long. The tube was sealed and allowed to stand. Within 24 hr the solution around the metal became light blue, and above the cylinder there was a sharp boundary between blue and violet solutions. With no stirring the dissolution is then diffusion-controlled.

Experiments were carried out at 15° and 35° with stirring at 7500 cm/min only. Results are similar to those at 25°, including the large effect of hydrochloric acid above 2M. Plots of log k_c vs. reciprocal of absolute temperature were linear within experimental error for each acid concentration. Activation energies are given in Table II.

Green Solutions

Dissolution is so much faster in green solutions that the runs took a few minutes rather than several hours. For example, in 0.033M $CrCl_3$, 1.0 M HCl, 35°C, same area and peripheral speed, the following weight losses were found: violet solution, 10.1 mg in 5 hr; green solution, 33.6 mg in 3 min. Because of the high rate, the weight loss was followed over a large per cent of the total reaction. Since in only a few of the solutions used does the reaction go nearly to completion, plots of log $(a - x)$ are not linear with time. Equation (II) must be modified as follows:

$$k_f + k_b = \frac{2.3V}{At} \log \frac{x_e}{x_e - x} \qquad \text{(III)}$$

where k_f is the rate constant for the forward reaction, k_b for the reverse reaction, and x_e is the amount of chromic ion reduction at equilibrium.

Values of x_e were determined by shaking cadmium cylinders with solution until equilibrium was attained, then measuring the weight loss. This was done in thermostatted flasks which were evacuated to deaerate the solutions, and which were attached to manometers through flexible glass capillary tubes. The pressure rise, calibrated with cadmium in acid alone, was used to make corrections for hydrogen evolution. At least two, generally three runs were made at each concentration, for example, of 6-, 7-, and 9-hr duration, to be sure that equilibrium had been reached. While determinations were made at 15°, 25°, and 35°C, most of the values were within a range of 15 mg and showed no trend with temperature. Therefore, average values are given in Table III.

Plots of log $(x_e - x)$ vs. time were linear from zero time as shown in Fig. 2, and rate constants $k_T (= k_f + k_b)$ were calculated from the slopes. Reproducibility was of the order of 5% and average deviation from the mean for the four concentrations was seldom greater. Average values

TABLE III. *Values of x_e, mg cadmium dissolved at equilibrium in 70 ml solution (corrected for hydrogen evolution)*
Average for 15°, 25°, 35°C

C_{HCl}, M	Concentration $CrCl_3$, M			
	0.033	0.066	0.10	0.133
0.5	100	208	318	435
1.0	104	227	342	462
2.0	119	243	366	481
4.0	123	248	374	492
Theory	130	257	393	523

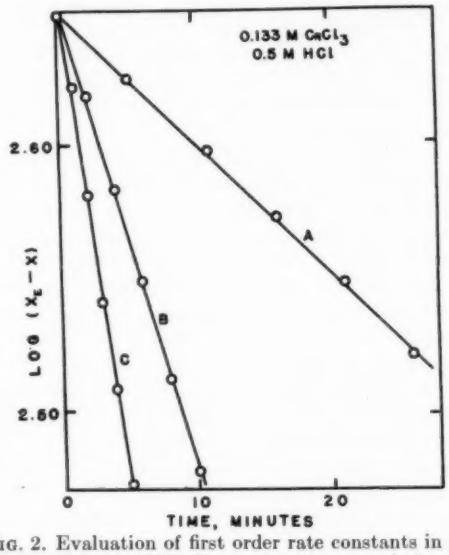

FIG. 2. Evaluation of first order rate constants in green chromic chloride; 25°C. Curve A, nitrogen stirring only; curve B, 7500 cm/min; curve C, 15,000 cm/min.

TABLE IV. *Values of k_T, cm/min, in green chromic chloride*

Temp.	C_{HCl}, M	N_2 bubbles	7500 cm/min	15000 cm/min
°C				
15	0.5	0.047	0.24	0.41
	1.0	—	0.23	—
	2.0	0.048	0.19	0.31
	4.0	0.041	0.21	0.31
25	0.5	0.057	0.30	0.49
	1.0	—	0.31	—
	2.0	0.055	0.25	0.40
	4.0	0.058	0.23	0.35
35	0.5	0.076	0.29	0.49
	1.0	0.068	0.32	0.55
	2.0	0.064	0.31	0.49
	4.0	0.071	0.36	0.52

of k_T are given in Table IV. The rate appears to be independent of acid concentration as well, greatest deviations being at the highest speed.

Plots of log k_T vs. $1/T$ are linear; activation energies are given in Table V.

Unacidified solutions.—A few runs were made in green solutions with no added acid. The dissolution rate decreased rapidly with time, and after 20 min the solution was violet rather than green. While hydrogen evolution is not rapid, the *p*H at the metal surface evidently rises to a value at which attainment of the green-violet equilibrium occurs quickly.

TABLE V. *Activation energy in green solutions*

Stirring	N_2	7500 cm/min	15000 cm/min
E, cal/mole	3700	3400	3300

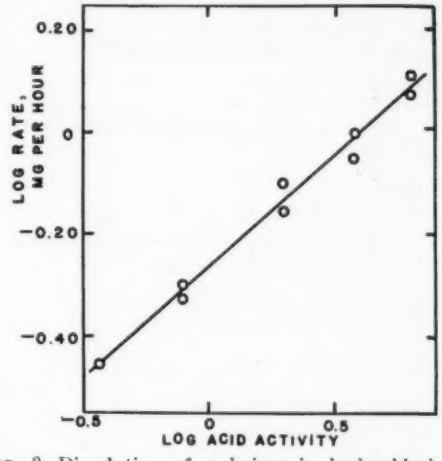

FIG. 3. Dissolution of cadmium in hydrochloric acid alone.

Dissolution in Acid Alone

The dissolution rate of the cadmium cylinders in deaerated hydrochloric acid is very small. The amount dissolved in the first hour is somewhat larger than in the following hours, when a "steady-state" value is attained. For example, 3M HCl dissolved 1.6 mg in the first hour, 1.0 mg in each subsequent hour (from 15 cm^2 surface area). The rate is independent of stirring speed, and while only a few runs were made at 15° and 35°C, the temperature coefficient appears to be small.

In Fig. 3, the log of the steady-state rate at 25°C is plotted vs. log of the mean ion activity of the hydrochloric acid (3). The slope of the straight line is 0.45, and therefore the equation

$$\text{rate} = k a_{\pm}^{0.45} \qquad \text{(IV)}$$

represents the rates at least empirically.

Potentials

The potential of the rotating cadmium cylinder vs. the saturated calomel electrode was measured first in deaerated hydrochloric acid, then with violet and green chromic chloride added, and with other salts for comparison. All measurements were at room temperature, 24°–28°C. Potentials became linear with time after a few minutes, as shown in Fig. 4. The straight lines were extrapolated to zero time to obtain representative values,[1] which

[1] Possibly the cadmium surface is not quickly cleaned in the more dilute acid (Fig. 4); the potential should drift slowly in a less negative direction as metal dissolves, after the initial clean-up.

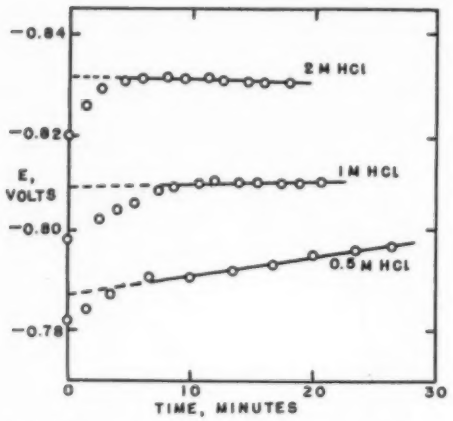

FIG. 4 Change in potential of cadmium with time in hydrochloric acid (vs. saturated calomel cell).

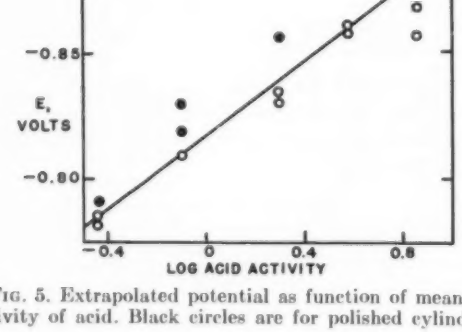

FIG. 5. Extrapolated potential as function of mean ion activity of acid. Black circles are for polished cylinders.

are plotted in Fig. 5 vs. log $a_{\pm}$ (HCl). The straight line shown has the slope, −0.070 v/log unit.

Mixtures such as 2M HCl, 2M NaCl give potentials in the same range as 4M HCl, showing the importance of the cadmium-chloride ion complex. Addition of 0.1M $CdCl_2$ shifts the potential in the cathodic (less negative) direction, to be expected with more free Cd^{++} present. Green chromic chloride does the same, since it dissolves considerable cadmium in a few minutes. The violet form has little effect and the same is true of sodium and aluminum chlorides at a concentration of 0.1M.

Potentials were measured with cadmium rotating in perchloric acid up to 4M to avoid the chloride complex. Values were erratic with time and about the same at each acid concentration. The average was −0.66 ± 0.01 v.

Discussion

It became obvious in this investigation that cadmium does not catalyze the reoxidation of chromous ion by hydrogen ion, nor is hydrogen evolution hastened in any other manner. Experiments in the evacuated flasks with attached manometers showed hydrogen evolution to be somewhat slower in the chromic chloride solutions, both green and violet, than in the acid alone. Zinc reacts quite differently in these solutions. There is always copious hydrogen evolution in the violet solutions, and whether chromous ion or hydrogen is formed in green solutions seems a matter of chance (4).

The low rates, lack of effect of stirring speed, and comparatively high temperature coefficients in the violet solutions show that the surface process is rate-controlling. There are no permanent anodic and cathodic areas on the cadmium; the cylinder may become roughened and eroded if run many hours without repolishing, but not pitted. The measured potentials do not indicate whether polarization of the cathodic reaction, reduction of chromic to chromous ion, accompanies its rate-determining role. The hydrogen evolution potential is of course highly polarized.

The gray film formed initially in violet solutions may have been cadmium deposited by the reverse reaction. When starting with far higher concentrations of the green ion, such redeposited metal should probably not be expected to show up in this way until the reaction was near the equilibrium point.

In the green solutions the magnitude of the rate constants indicate that convective-diffusive transport is the controlling step, and the effect of stirring speed and low temperature coefficients substantiate this. Using an estimated 4.5×10^{-4} cm²/min for the diffusion coefficient of chromic ion, the "effective" diffusion layer thickness is calculated to be similar to values found in other transport-controlled systems (5). Over the limited range of stirring employed, k_T is approximately proportional to the 0.7 power of stirring speed, which agrees with the relations found by other authors in unbaffled systems (6). At higher speeds we should expect a power near unity in a well-baffled system (5). In employing equation (III) it was assumed that the reverse reaction is first order, and the results seem to agree with this. It takes place only on the surface of the cylinder, i.e., cadmium never precipitates in the solution or on the vessel walls. The rate constant for the forward reaction can be calculated if desired, since $k_f a/x_e = k_T$, where a is the amount which would be dissolved with complete reaction (7). However, the important thing is that the constants for the chemical process (k_c) in the green solutions are larger than any values of k_f, and much larger than k_c for the violet solutions.

The obvious reasons for the different reactivities of the two ions lie in (*a*) the different charge types of the two chromium ions, and (*b*) the different compositions and polarizabilities (the structures being similar). The charge type is important in homogeneous reactions, for instance in anion catalysis of the nitramide reaction (8), and in the reaction of thiosulfate ion $S_2O_3^{=}$ with a bromo-ester or the corresponding bromo-anion (9).

Silver dissolves 15 or 20 times as fast in ferric sulfate solutions as in ferric perchlorate (10), reflecting the difference between the ions $FeSO_4^+$ and (hydrated) Fe^{+++} or $Fe(OH)^{++}$. However, it is believed that the silver surface is positively charged due to preferential adsorption of silver ions. In the present case one expects the cadmium surface to be negatively charged, and electrostatic effects would favor reaction with the triply charged violet ion.

The very great increase in rate in violet solutions above 2M HCl suggests that two reaction mechanisms are involved. This is supported by the increase in activation energy at high acidity. The kinetics must eventually be referred to the rate of formation and decay of one or more

activated states, which in chemical reactions are assumed to involve "critical complexes." The following mechanisms are postulated:

1. In violet solutions with low HCl concentration, the critical complex consists mostly of one or two adsorbed chromic ions associated with a cadmium atom or ion; decomposition results in Cd^{++} in solution, which then forms the chloride complex.

2. At high HCl concentration, Cl^- ions are found in the critical complex, which results in direct formation of cadmium-chloride ions in solution.

3. The green ion which already contains chloride should form chloride-containing critical complexes most rapidly.

The problem here is similar to that found in the electrodeposition of chromium from aqueous Cr(III) ion, which involves reduction to Cr(II) as the first step. Lyons (11) has pointed out that, in general, halo-aquo ions require less activation energy than aquo-ions for electroreduction.

Study of the dissolution in perchloric acid alone and with the violet ion, with chlorides and other salts, would be helpful.

Potential and rate.—In hydrochloric acid alone the following equation represents the cadmium potential (Fig. 5):

$$E = E' - 0.070 \log a_{\pm} \qquad (V)$$

At first sight, the slope may seem anomalous since other metals, especially iron, give a smaller slope of opposite sign (12, 13). However, this is a cadmium-cadmium ion potential, not a hydrogen or atomic hydrogen potential.

In these hydrochloric acid solutions most of the cadmium is present as $CdCl_3^-$ (14). The activity of the free cadmium ion is given by

$$a_{Cd^{++}} = K a_{CdCl_3^-}/a^3_{Cl^-} \quad \text{or} \quad K a_{CdCl_3^-}/a^3_{\pm} \qquad (VI)$$

At comparable stages of the dissolution it may be assumed from equation (IV) that

$$a_{CdCl_3^-} = k' a_{\pm}^{0.45} \qquad (VII)$$

Combining (VI) and (VII)

$$a_{Cd^{++}} = K k' a_{\pm}^{-2.55} \qquad (VIII)$$

The cadmium potential is given by

$$E = E^{0'} + 0.0295 \log a_{Cd^{++}} \qquad (IX)$$

From (VIII) and (IX), combining constants,

$$E = E'' - 0.075 \log a_{\pm} \qquad (X)$$

In view of the approximations made and neglect of other complexes than $CdCl_3^-$, agreement with the experimental slope is satisfactory. It would be difficult to calculate E'', but if 10^{-6} is assumed as a reasonable value for $a_{Cd^{++}}$ when $a_{\pm} = 1$,

$$E = -0.402 - 0.246 - 0.177 = -0.825$$

vs. the calomel cell (cf. Fig. 5).

Potentials of cadmium in perchloric acid are erratic but more cathodic, indicating that more free Cd^{++} is present; the buffering and stabilizing effect of the chloride ion is missing.

Spectrophotometry of Chromic Chloride Solutions

When the more rapid initial rates in violet solutions were found, a search was made for the cause. Preelectrolysis and experiments with small additions of Cu^{++} and Pb^{++} indicated that heavy metal impurities were not responsible. Addition of small amounts of green ion, either initially or after one or two hours, showed the reason. Extrapolation of log $(a - x)$ vs. t plots to zero time would most likely serve to analyze the mixtures.

The absorption spectra of violet and green solutions were determined in the range 300–750 mμ with a Beckman DU instrument, and the molar extinction coefficients were plotted vs. wave length. There are two absorption bands with peaks at 407 and 575 mμ for the violet form; the bands for the green form are very similar with the peaks displaced about 15 mμ toward longer wave lengths. The curves are not reproduced here, since they are almost identical with absorption curves found by Marks for violet and green chromic sulfates (15). Marks showed that by working somewhat off the absorption maxima, where the extinction coefficients differ most, a rather good analysis of mixtures of the two ions can be made. The method did not look promising in the present case, and exact analysis proved to be unnecessary.

Manuscript received August 30, 1955. This paper was prepared for delivery before the Pittsburgh Meeting, October 9 to 13, 1955. It was taken from the Ph.D. thesis submitted by Edward Hillner to the Graduate School Faculty of New York University. Work done under Contract No. DA-30-069-ORD-1113 of the Office of Ordnance Research.

Any discussion of this paper will appear in a Discussion Section to be published in the December 1956 JOURNAL.

REFERENCES

1. G. S. FORBES AND H. W. RICHTER, *J. Am. Chem. Soc.*, **39,** 1140 (1917).
2. A. B. LAMB, *ibid.*, **28,** 1710 (1906); A. B. LAMB AND G. R. FONDA, *ibid.*, **43,** 1154 (1921); R. E. HAMM AND C. M. SHULL, *ibid.*, **73,** 1240 (1951).
3. H. S. HARNED AND B. B. OWEN, "The Physical Chemistry of Electrolytic Solutions," p. 547, Reinhold Publishing Corp., New York (1943).
4. C. V. KING AND N. MAYER, *This Journal*, **100,** 473 (1953).
5. C. V. KING AND M. SCHACK, *J. Am. Chem. Soc.*, **57,** 1212 (1935).
6. M. EISENBERG, C. W. TOBIAS, AND C. R. WILKE, *This Journal*, **101,** 306 (1954).
7. S. GLASSTONE, "Textbook of Physical Chemistry," p. 1070, D. Van Nostrand Co., New York (1946).
8. R. P. BELL, "Acid-Base Catalysis," Oxford Press (1941).
9. E. S. AMIS AND W. J. BROACH, *J. Chem. Phys.*, **22,** 952 (1954).
10. H. SALZBERG AND C. V. KING, *This Journal*, **97,** 290 (1950); C. V. KING AND F. S. LANG, *ibid.*, **99,** 295 (1952).
11. E. H. LYONS, JR., *ibid.*, **101,** 363 (1954).
12. J. D'ANS AND W. BRECKHEIMER, *Z. Elektrochem.*, **56,** 585 (1952).
13. A. C. MAKRIDES, N. M. KOMODROMOS, AND N. HACKERMAN, *This Journal*, **102,** 363 (1955).
14. C. E. VANDERZEE AND H. J. DAWSON, *J. Am. Chem. Soc.*, **75,** 5659 (1953).
15. G. W. MARKS, *U. S. Bur. Mines Rept. Invest.* No. 4779, March 1951.

High Pressure Oxidation of Metals—Tungsten in Oxygen

J. P. Baur, D. W. Bridges, and W. M. Fassell, Jr.[1]

Department of Metallurgical Engineering, University of Utah, Salt Lake City, Utah

ABSTRACT

Tungsten rod and sheet were found to oxidize linearly in oxygen from 600° to 850°C at oxygen pressures ranging from 20 to 500 psia. Oxidation rate increased with increased oxygen pressure at temperatures 750°–850°C. Theoretical considerations indicate that an equilibrium adsorption process occurs prior to the rate-determining step. The assumption of a linear change of adsorption energy with increase of surface coverage allowed observed oxidation rates to be corrected for pressure effect. The activation energy was 48 kcal. Tungsten sheet volatilization losses were appreciable above 800°C. Only tungsten rod data were free from volatilization losses at 850°C. Photographs are included showing the effect of shearing samples at room temperature prior to oxidation on the final physical appearance of the oxide. Cold shearing produces exfoliated tungsten oxide.

Introduction

Tungsten has been the subject of many theoretical papers dealing with the adsorption of oxygen upon the metal surface (1). Langmuir's original work in the field of chemisorption dealt with tungsten-oxygen systems at extremely low pressures (2–4).

Gulbransen and Wysong (5) employed the microbalance technique in a study of the oxidation behavior of tungsten in the temperature range 25°–550°C (7.6 cm-Hg). The metal was reported to oxidize according to the parabolic rate law. Dunn (6) reported the parabolic rate law is obeyed in air from 700° to 900°C with an anomaly occurring at 850°–950°C, attributed to a phase change from alpha WO_3 to beta WO_3. The parabolic law was also reported by McAdam and Geil (7). Nachtigall (8) published some oxidation data for tungsten (500°–800°C). Published curves are neither ideally linear nor parabolic. Almost linear relationships were obtained by Scheil (9), and by Kieffer and Kolbl (10) between 500° and 900°C.

There is no recorded study of the effect of oxygen pressure variation upon the oxidation rate of tungsten. Also no information is available on the oxidation behavior of tungsten in oxygen at pressures in excess of 1 atm. The present work is an investigation of the oxidation behavior of tungsten over the temperature range 600°–850°C and oxygen pressures from 20 to 500 psia.

Experimental Procedure

Four different types of tungsten were employed: General Electric Co. sheet of approximately 20 mil thickness, Fansteel Metallurgical Corp. and Westinghouse Electric Manufacturing Co. sheet of approximately 5 mil thickness, and tungsten rod, $\frac{1}{10}$ in. diameter, of unknown manufacture.

Tungsten sheet sheared at room temperature exhibited markedly undesirable properties; it was necessary to resort to special sample preparation. The tungsten sheet was heated to about 800°C in an oxygen-natural gas burner. The samples were then hot sheared to the desired size (recorded in Table I) by means of a DI-ARCO precision shear. A $\frac{3}{32}$ in. diameter hole was hot punched at one end of each small sample The resulting oxide scale was removed by immersion in a boiling solution of potassium ferrocyanide and potassium hydroxide (11). Following washing in distilled water and drying, the sample was abraded with 6/0 garnet paper and the geometrical surface area was determined.

The high temperature-high pressure furnaces and the experimental techniques used to follow the reaction have been discussed in detail in a previous paper (12). Data are recorded in the form of curves showing weight gained as a function of time.

Experimental Results

Tungsten metal was oxidized from 600° to 850°C over an oxygen pressure range of 20–500 psia. Under the imposed conditions it was found that the oxidation rate is governed by the linear law. Deviations from the linear rate of oxidation for the first few minutes were observed at 600° and 650°C; however, subsequent long periods of observation show no deviation from linearity for 3 hr.

It was found that tungsten oxide, formed on tungsten sheet, sublimed at temperatures in excess of 850°C. This sublimation resulted in deviations from linear rate and caused the rate to change but slightly with temperature increase. Comparison with observed rates using tungsten rod seemed to indicate that the total surface area exposed is the most important factor in the influence of volatilization on the oxidation rate. Changes in surface roughness as well as accelerated attack of active centers during the initial phases of oxidation could also account for the high temperature deviations. However, it is felt that volatilization is probably the largest factor. It should be stressed that the experimental technique used is a static method; volatilization losses should be much greater in an oxygen flow system.

Table I is a compilation of tungsten oxidation data which represents selection of data in the respect that, although

[1] Present address: Howe Sound Co., Salt Lake City, Utah.

TABLE I. *Observed oxidation rates of tungsten in oxygen*

Temp	Type of tungsten	Oxygen pressure	Oxidation rate	Value of θ calculated by equation (XII)
°C		*psia*	$mg \cdot cm^{-2}\ hr^{-1}$	
600	A	50	0.2	
		100	0.2	
650	A	50	0.9	
		100	0.9	
700	B	20	3.1	
		30	2.9	
		50	3.4	
		100	3.3	
		150	3.2	
		200	3.4	
750	C	20	6.9	0.55
		50	8.1	0.64
		200	9.5	0.77
		300	9.9	0.81
		500	11.2	0.86
	B	30	8.7	
		100	9.2	
		200	12.4	
800	C	20	22.5	0.58
		50	27.6	0.69
		100	31.1	0.77
		150	29.9	0.81
		200	33.8	0.85
		300	34.7	0.89
		400	34.3	0.93
		500	33.5	0.95
850	C	20	40.2	0.32
		30	47.3	0.36
		50	54.1	0.53
		100	76.1	0.69
		200	85.2	0.84
		300	86.7	0.94

A—Westinghouse sheet (rolled by H. Cross Co., N. Y., N. Y.) $1\frac{1}{4}$ in. x $\frac{3}{4}$ in. x 0.005 in.; surface area: 6.25 cm^2.

B—Fansteel Metallurgical Corp. sheet, 2 in. x 0.4 in. x 0.005 in.; surface area: 8.2 cm^2.

C—Tungsten rod (unknown manufacturer) $\frac{3}{4}$ in. lengths x 0.1 in. dia. Surface area: 1.6 cm^2.

some 200 samples were oxidized; high temperature data on the sheet tungsten are not tabled since the material suffered from volatilization losses. Oxidation rates for the tabled metal in the region reported are quite satisfactorily reproducible. Low temperature tungsten rod data are lacking since the surface area of the rod was insufficient to allow a measureable rate to be obtained. It should be borne in mind that the specific gravity of tungsten is 19.3 and thus a sample of sufficient surface area and mass not exceeding two grams (the latter restriction is imposed by the use of the quartz spring technique) is difficult to obtain.

Originally the tungsten samples were sheared to size from the manufacturer's larger sheets at room temperature. This "cold shearing" disrupted the grain structure of the sheet in the vicinity of the sheared edge. This ruptured area permitted rapid oxidation to take place along these edges producing the exfoliated condition shown in Fig. 1. The samples, after oxidation for 20 min at 600°–850°C, consisted of a large number of plates. Each platelet contained unreacted tungsten embedded in the oxide. This sandwich effect resulted in an irregular increase in the mass change per unit time since the surface area increases as the plates form. Volatilization losses were markedly greater with the "cold sheared" tungsten occurring at lower temperatures. In order to eliminate this difficulty the later samples were "hot sheared" as described above. Fig. 2 shows the final appearance of hot sheared samples oxidized in the temperature and pressure range of Table I. The oxidation rates of these samples were highly reproducible. In spite of the hot shearing, preferential oxidation at higher temperatures occurred along the edges and around the hole, as shown in Fig. 3.

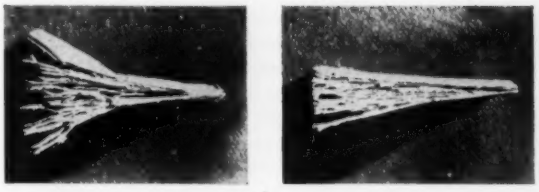

FIG. 1. Photographs showing effect of cold shearing on final appearance of oxidized tungsten sheet. *Left*, 800°C, 100 psia; oxidized 18 min; *right*, 750°C, 100 psia; oxidized 21 min.

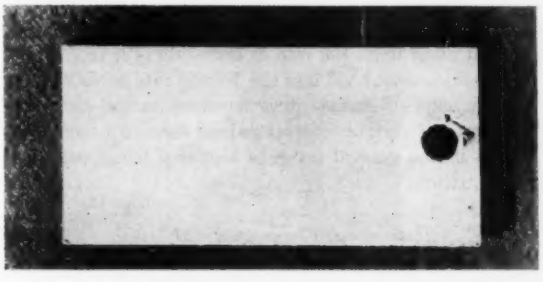

FIG. 2. Final appearance of hot sheared tungsten sheet in the temperature range of Table I. Hot sheared; oxidized 21 min, 700°C, 100 psia.

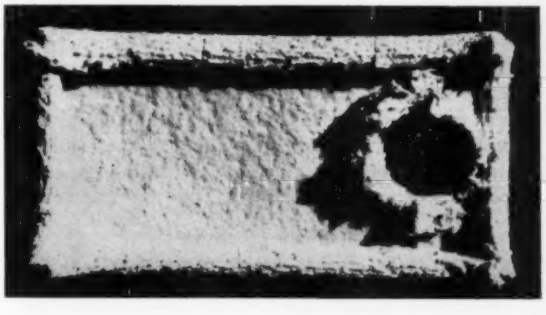

FIG. 3. Hot sheared tungsten sheet oxidized in excess of 850°C. Hot sheared; oxidized 25 min, 1000°C, 100 psia.

It was reported by Dunn (6) that the color of the oxide formed at ordinary temperatures (presumably below

850°C) was deep orange. Smithells (11) states that "tungstic oxide, WO_3, is yellow, the exact shade depending very much on particle size. On heating to about 500°C the color changes to an orange brown but reverts to yellow again on cooling" . . . (p. 47, *op cit*). All samples at all temperatures and pressures investigated in this study were yellow in color when removed from the furnace. One sample was purposely oxidized in air at 900°C to determine whether or not the other gases present affected the color. This sample was similar in color to the others.

Discussion of Experimental Results

Previous articles from this laboratory have discussed and developed a general treatment of the effect of oxygen concentration upon the rate of oxidation (12, 13). Briefly this development combines the Eyring rate equation (14) and the explicit surface oxygen concentration factor resulting from surface site saturation considerations. This results in the general pressure sensitive linear oxidation rate equation:

$$\text{Rate} = k_0 \cdot f(\theta) \cdot \frac{kT}{h} \cdot \exp[-\Delta F^*/RT] \qquad \text{(I)}$$

where k_0 is a proportionality constant with the dimensions of ML^{-2} and includes the correction factors for the true surface area involved in the oxidation reaction, i.e., the surface roughness factor, as well as the number of active sites per square centimeter. The other terms retain their customary significance as in the Eyring absolute reaction rate theory with the transmission coefficient assumed equal to unity (14). The concentration factor, $f(\theta)$, represents a function of θ, the fraction of the surface covered with oxygen molecules or atoms. The exact nature of this term depends on the type of adsorption mechanism postulated.

Molecular adsorption is assumed. Following Langmuir, one can write:

$$S + O_2 = S \cdots O_2 \qquad \text{(II)}$$

where S represents an active site at the zone of reaction; O_2, an oxygen molecule; and $S \cdots O_2$, the adsorbed oxygen molecule. If θ is the fraction of the corrected surface area covered with oxygen molecules, the vacant sites, S, are then $[1 - \theta]$.

The mechanism depicted is that of an oxygen molecule adsorbing upon an active site in molecular form. Decomposition of the adsorbed oxygen molecule or some subsequent phase boundary step is the slow rate-determining step. Hence, the surface sites are always in equilibrium with the external gas phase and the adsorption process may be treated as an equilibrium process.

Expression for $f(\theta)$ results from a consideration of the equilibrium expression for the appropriate surface mass balance equation, equation (II). The activity of the surface concentration of the adsorbed oxygen or oxygen phase immediately adjacent to the zone of reaction is assumed to be proportional to the fugacity of the external oxygen phase, $f(O_2)$, which leads to the expression:

$$f(O_2) = [O_2] = n/V = P/RT \qquad \text{(III)}$$

where R, the molar gas constant, is used as 0.08206 ltr-atmo/mole-degree Kelvin. If K_1 represents the molar equilibrium constant of equation (II), $f(\theta)$ can be derived as follows:

$$K_1 = \frac{\theta}{[1-\theta]\cdot[O_2]} = \exp\left[\frac{-(\Delta H - T\cdot\Delta S)}{RT}\right] \qquad \text{(IV)}$$

$$\theta = \frac{K_1\cdot[O_2]}{1 + K_1\cdot[O_2]} \,. \qquad \text{(V)}$$

$$\text{Rate} = K_0 \frac{K_1[O_2]}{1 + K_1[O_2]} \qquad \text{(VI)}$$

where K_0 represents the Eyring absolute reaction rate constant, $kT/h \cdot \exp[-\Delta F^*/RT]$.

In order to satisfy equation (VI) the following conditions must be satisfied:

1. Values of K_0 must be greater than any observed oxidation rate at the temperature in question. This would be expected as,

$$\lim_{[\theta \to 1]} dm/dt = K_0$$

2. Slope of plot, $\log_{10}K_0$ vs. 1/°K must be negative in order that the energy of activation for the oxidation process be positive.

3. Slope of plot, $\log_{10}K_1$ vs. 1/°K, must be positive, since the heat of chemisorption of oxygen must be exothermic.

4. Values of K_1, equilibrium constant for chemisorption of oxygen, must be greater than unity since it is necessary that

$$\Delta F_{ads} \leq 0 \text{ and } K_1 = \exp[-\Delta F/RT]$$

Where the effect of interaction between the adsorbed molecules on the energy of adsorption cannot be neglected, the classic Langmuir type derivation for θ, the fraction of the surface covered, equation (IV), must be amended. Langmuir recognized this and wrote an alternate expression for the fraction of the surface covered applicable for a varying energy of adsorption (15, 16):

$$\theta = \sum_i K_i P/(1 + K_i P) \qquad \text{(VII)}$$

K_i is no longer a constant but varies according to the extent and nature of the interaction energy. Most often the assumption is made that the enthalpy of adsorption is a linear function of surface coverage:

$$\Delta H_{ads} = \Delta H^0_{ads} + \theta z V \qquad \text{(VIII)}$$

where ΔH^0_{ads} is the enthalpy of adsorption for $\theta = 0$. Since V is defined as the positive molar energy of interaction, the enthalpy becomes less and less negative as the surface coverage approaches its equilibrium limit. The coordination number, z, of the monolayer ($0 \leq z \leq 6$) is dependent on the nature of the monolayer and the degree of completeness of coverage. Thus it is seen that under the above scheme the first adsorbed molecules are more strongly adsorbed than the last.

The assumption of equation (VIII) is not as artificial as may be thought at first glance. It results from consideration of the distribution of adsorbed molecules as completely random (14, 17) and has been experimentally observed in the case of hydrogen on tungsten (18–20).

Modification of the Langmuir derivation under the condition of equation (VIII) has been published by

Brunauer and co-workers (21). Their derivation (with slight alteration in definitive terminology) will be outlined briefly. Let an equilibrium constant for changeable adsorption enthalpy be defined as:

$$K_1 = \exp[-(\Delta F^0_{ads} + \theta zV)/RT] = K_1^0 \cdot \exp[-\theta zV/RT] \quad \text{(IX)}$$

where $K_1^0 = \exp[-(\Delta H^0 - T \cdot \Delta S^0)/RT]$, the value of the equilibrium constant for $\theta = 0$.

The expression for the surface coverage, θ, is now the summation of small differential units of coverage, θ_s, each involving a different enthalpy and valid over a small element of area, ds. Equation (V), with K_1 defined as in equation (IX), expresses θ_s. Then the fraction of the entire area covered with adsorbed molecules is:

$$\theta = \Sigma \theta_s \cdot ds = \int_0^\theta \theta_s \cdot ds = \int_0^\theta \frac{K_1^0 \cdot [O_2] \cdot \exp[-s \cdot zV/RT]}{1 + K_1^0 \cdot [O_2] \cdot \exp[-s \cdot zV/RT]} \cdot ds \quad \text{(X)}$$

This integral is of the form $\int dU/U$, where U is the denominator above. Integrating equation (X), one obtains:

$$\theta = 2.3RT/zV \log_{10}\left\{\frac{1 + K_1^0 \cdot [O_2]}{1 + K_1^0 \cdot [O_2] \cdot \exp[-\theta \cdot zV/RT]}\right\} \quad \text{(XI)}$$

where $K_1^0[O_2] \gg 1 \gg K_1^0[O_2] \cdot \exp[-z\theta V/RT]$

$$\theta \approx 4.6T/zV\{\log_{10}[O_2] + \log_{10} K_1^0\} = 4.6T/zV\left\{\log_{10}[P_{O_2}] + \log_{10}\left(\frac{K_1^0}{RT}\right)\right\} \quad \text{(XII)}$$

Equation (XII) is a result first derived semi-empirically by Frumkin and Slygin (22). These workers and also

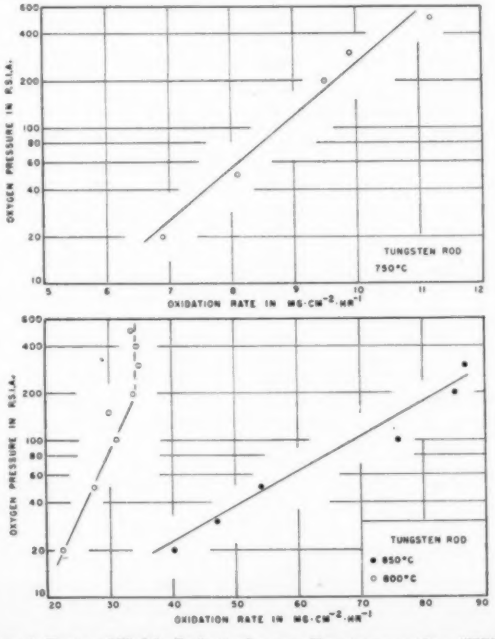

FIG. 4. Data of Table I plotted according to equation (XIII)

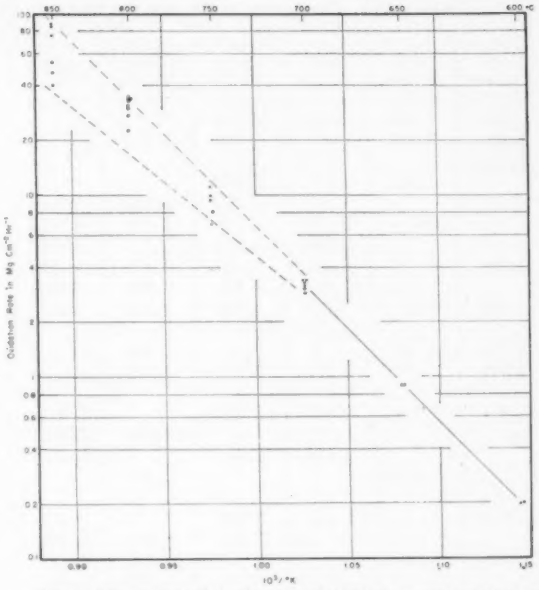

FIG. 5. Uncorrected Arrhenius plot of observed oxidation rate of tungsten, using data of Table I. (Note: Horizontal arrays of points indicate the same oxidation rate at the particular temperature.)

TABLE II. *Estimate of interaction energy and adsorption equilibrium constant*

Temp	Assumed K_0	zV in calories	K_1^0
°C			
750	11.5	21,285	3.24×10^4
800	35.0	18,874	1.82×10^4
850	89.0	9,850	4.57×10^2

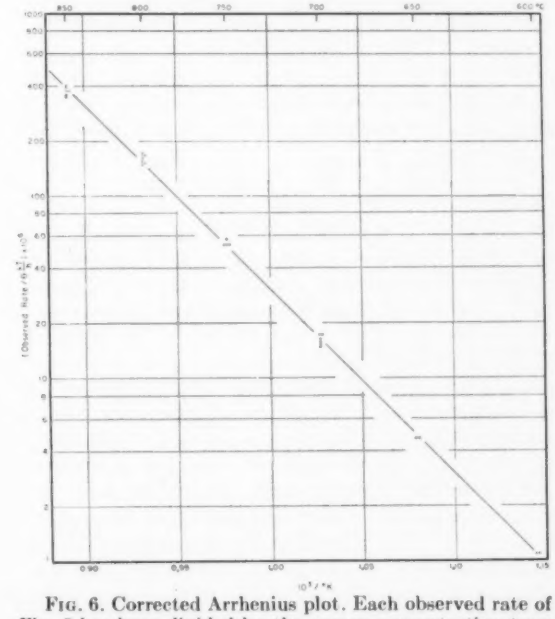

FIG. 6. Corrected Arrhenius plot. Each observed rate of Fig. 5 has been divided by the proper concentration term (θ). (Note: Horizontal arrays of points indicate the same oxidation rate at a particular temperature.)

TABLE III. *Tabulation of the experimentally determined interplanar spacings of oxidized tungsten with listing of the ASTM cards for comparison*

600°C 100 psia	650°C 100 psia	700°C 100 psia	750°C 100 psia	800°C 125 psia	850°C 100 psia	900°C 100 psia	900°C 100 psia Ground	Tungstite mineral	WO_3 5-0363,4	WO_2 5-0431	W_4O_{11}	$W_{20}O_{58}$ 5-0386,7
4.321	4.353	4.210	4.332							4.78		4.28
3.95	3.942		3.917	3.934							3.92	
3.883							3.867					3.89
	3.850		3.850					3.84	3.835			
3.770		3.818	3.770	3.825	3.786	3.818	3.786	3.76	3.762		3.78	3.77
	3.739	3.723		3.723	3.738	3.723	3.678					3.70
		3.633	3.648		3.663	3.619		3.63	3.642		3.63	3.64
3.414	3.414	3.414	3.414	3.479	3.562		3.376		3.411	3.45		
		3.314	3.351	3.401	3.225	3.314			3.342			
3.164	3.159	3.079	3.089	3.132	3.028	3.079	3.153	3.07	3.109			
							3.110		3.076	2.828		3.821
2.734	2.722			2.698			2.722		2.684		2.74	2.729
2.683	2.683	2.675	2.659	2.659		2.667	2.675	2.66	2.661			2.707
						2.644	2.644					2.640
2.564	2.556	2.629	2.622		2.621	2.600		2.62	2.617		2.62	2.620
				2.536	2.592		2.528		2.528			
		2.508	2.501		2.481	2.501			2.509	2.446		
	2.436			2.429						2.436	2.44	
										2.428		
2.392		2.404	2.398							2.418		
			2.287	2.321	2.265	2.254				2.393		
2.188	2.191		2.206	2.233	2.227		2.206				2.22	2.211
				2.176	2.181	2.171	2.161		2.172	2.181		
		2.151	2.151			2.146		2.15	2.149	2.150		
2.122	2.122	2.089		2.058	2.127				2.098			
	2.040	2.032	2.036	2.036		2.036			2.038			
		2.010	2.010	2.014	2.014	2.014	2.010		2.020			
									2.011			
	2.002			1.994	1.994	1.994			1.991		1.98	
		1.969	1.969		1.965	1.969	1.977	1.97	1.966			1.963
1.949	1.941			1.937	1.953		1.926					
1.914		1.914	1.918			1.914		1.92	1.917			1.898
	1.895	1.873	1.877	1.895	1.899	1.877	1.884	1.88	1.879			1.884
1.845	1.841				1.859					1.847	1.85	
1.828	1.824	1.817	1.824	1.838		1.821	1.828	1.82	1.820	1.827		
		1.798	1.797	1.811	1.784	1.807	1.804	1.79	1.807			
1.773							1.755		1.793		1.75	1.741
1.728	1.727			1.722			1.728			1.724		1.720
	1.704	1.705	1.713	1.703		1.707			1.707	1.709		1.700
			1.691		1.692		1.698	1.69		1.698	1.70	1.695
	1.684	1.684				1.687			1.687			1.680
1.664		1.664	1.669		1.675	1.670			1.670		1.67	1.674
	1.656			1.653			1.661	1.65	1.654			1.666
									1.646			
		1.639	1.642		1.626	1.639	1.642	1.64	1.638			
1.599									1.593	1.593		
	1.566	1.578		1.563			1.578		1.580			1.562
	1.554	1.554	1.554	1.551		1.553			1.554	1.545	1.55	1.550
1.542					1.542	1.537	1.534	1.53	1.538	1.537	1.53	1.537
		1.540	1.540						1.527			1.524
				1.510	1.528	1.514	1.508		1.514			
1.502	1.499		1.501			1.497		1.50	1.499			
1.486		1.486	1.488	1.475	1.490	1.484	1.484	1.48	1.486			
		1.467	1.467		1.478	1.463		1.47	1.464	1.464	1.46	
					1.457							
1.406	1.408						1.414		1.411	1.412		
									1.406	1.406		
1.388	1.393	1.400	1.399	1.400					1.399			
						1.388	1.386		1.390	1.391		
	1.384				1.379				1.381	1.387		1.365
							1.359		1.358			1.359
1.351	1.352			1.351					1.347	1.354		
		1.342	1.342	1.342		1.336	1.336		1.342		1.34	1.337
	1.331		1.336		1.334			1.33	1.331			
		1.310	1.312	1.318			1.316		1.322			
									1.317			
						1.307		1.31	1.308			
1.299					1.302				1.297	1.297		1.282
	1.287	1.280	1.281	1.287	1.274	1.281	1.287	1.28	1.283	1.284	1.29	1.275

TABLE III—*Continued*

600°C 100 psia	650°C 100 psia	700°C 100 psia	750°C 100 psia	800°C 125 psia	850°C 100 psia	900°C 100 psia	900°C 100 psia Ground	Tungstite mineral	WO_3 5-0363,4	WO_2 5-0431	W_4O_{11}	$W_{20}O_{58}$ 5-0386,7
1.268		1.258							1.264		1.26	1.269
	1.251			1.248			1.252		1.254			1.262
		1.242	1.242		1.237	1.237	1.242	1.24	1.245			1.255
									1.242			1.248
									1.238			
									1.235			
	1.222			1.220			1.218	1.22			1.21	
		1.215	1.217							1.215		
						1.212			1.213	1.212		
1.204					1.209					1.209		
										1.207		
1.196				1.197			1.197		1.201	1.195		1.207
1.183	1.181	1.175	1.176	1.181	1.172	1.175	1.168		1.191	1.184		1.196
	1.161	1.157	1.157	1.161	1.151	1.157	1.157					1.189
	1.145	1.139	1.141	1.144			1.143					1.147
1.131	1.131	1.125	1.128	1.130			1.130					1.141
1.122	1.124				1.123	1.126	1.120					1.133
	1.095	1.114	1.115	1.118	1.109	1.114	1.109					
	1.090	1.085	1.105	1.107	1.100	1.105						
	1.074	1.068	1.085	1.086	1.065	1.068						1.105
	1.041	1.037	1.068	1.071			1.050					
	1.031	1.028	1.046	1.050	1.045	1.037	1.031					
			1.037	1.041	1.034	1.026						
			1.028	1.029	1.025							
	0.9976	0.9934	0.9955		0.9934	0.9962						
				0.9871	0.9816		0.9864					
	0.9783											
	0.9684	0.9621		0.9646	0.9621	0.9609	0.9653					
0.9483	0.9469	0.9451	0.9457	0.9469	0.9434	0.9446	0.9469					
0.9354	0.9354				0.9321	0.9326	0.9337					
0.9166	0.9140	0.9135										
	0.9090	0.9066	0.9066	0.9070	0.9056	0.9080						

Temkin and Pyzkov (23) used it in connection with the explanation of the adsorption of NH_3 on iron catalyst. It is applied to NH_3 on a double promoted iron catalyst 931 by Love and Emmett (24). It should be noted that equation (XII) is not good at either limit of the allowed values for θ, the fraction of the surface covered. K^0 will only be a true measure of the adsorption potential where the change of adsorption enthalpy with surface coverage is linear over the entire range of θ values as $\theta \rightarrow 0$; this may not be universally applied at all temperatures.

Subsitution of equation (XII) into the general rate expression, equation (I), yields:

$$\text{Rate} = \frac{4.6T}{zV} \cdot K_0 \cdot \{\log_{10}[P_{O_2}] + \log_{10}(K_1^0/RT)\} \quad \text{(XIII)}$$

where $K_0 = k_0 \cdot (kT/h) \exp[-\Delta F^*/RT]$, the absolute reaction rate constant.

Plots of observed rate vs. the logarithm of oxygen pressure for 750°, 800°, and 850°C data of Table I are shown in Fig. 4. Correlation of the data seems to indicate that the adsorption of oxygen on tungsten in the observed range of this investigation is in accordance with equation (XIII). Assuming the limiting observed rate as an approximate value for K_0, the quantity zV may be estimated for the slopes of plots of Fig. 4. Results are tabulated in Table II.

The adsorption equilibrium constant descends with increasing temperature as is to be expected in accordance with energy considerations (see third condition stated above). However, it can be readily judged that a plot of $\log_{10}K_1^0$ vs. 1/°K would not be linear attesting to the fact that the approximation of completely random interaction is not valid over the entire range of surface coverage.

Fig. 5 is the uncorrected Arrhenius plot ($\log_{10}$ rate vs. 1/°K). Fig. 6 is the corrected Arrhenius plot for the oxidation of tungsten. Within the pressure sensitive range the observed rate has been divided by $\theta \cdot kT/h$, where θ is the fraction of the surface covered with oxygen. The activation energy (calculated from the slope of Fig. 6) is 48 kcal.

X-ray Diffraction Studies

Gulbransen and Hickman (25) state that WO_3 is the stable oxide below approximately 600°C, while WO_2 first forms at 700°C. Magneli (26) showed molybdenum and tungsten oxides existed as homologous series of the form Me_nO_{3n-1} and Me_nO_{3n-2}. No data exist on the oxides present on tungsten in the pressure range studied in this report. X-ray diagrams were made of the *in situ* oxide coatings and the interplanar spacings are shown on Table III. Difficulty arose in measuring the exact positions of the lines because of the diffuse broad peaks caused by the small particle size. Also, a certain amount of lattice strain may be present due to the rapid growth of the oxide. This strain effect is shown by a comparison of columns 7 and 8. Column 8 shows the interplanar spacings of the oxide coating formed at 900°C and 100 psia after the oxide had been scraped from the sheet and ground. The agreement between the values of column 8 and those

of the mineral tungstite (column 9) and the data on WO_3 of Magneli is quite satisfactory There appears to be no general shift in the "*d*" values, indicating no change in lattice parameter with temperature or no formation of a solid solution series. The presence of "*d*" values at about 3.4Å and 2.4Å suggests the presence of WO_2 in small amounts, but the similarity of the patterns of the various oxides and the large number of lines present make it almost impossible to state exactly which oxides are present unless a detailed analysis is made. The presence of lines at about 4.3Å and 3.93Å is difficult to explain unless the oxides present are W_4O_{11} and $W_{20}O_{58}$. There is some question as to the existence of W_4O_{11}.

Conclusions

The summary of the oxidation behavior of tungsten in oxygen from 600° to 850°C at pressures ranging from 20 to 500 psia (total oxygen pressure) is as follows:

1. Tungsten oxidizes linearly at all temperatures and pressures investigated.
2. The oxidation rate increases with increasing oxygen pressure at temperatures above 750°C.
3. Theoretical considerations indicate that an equilibrium adsorption process occurs prior to the rate-determining step. Interaction between adsorbed molecules is sufficient to require modification of the Langmuir idealized adsorption mechanism.
4. The ultimate end product is almost wholly WO_3, although some indication of the presence of WO_2 was detected.
5. The enthalpy of activation for the oxidation of tungsten (600°–850°C) is 48,000 cal.
6. Oxidation of tungsten is accompanied by subsequent volatilization of the oxide above 800°C.

Acknowledgments

The authors wish especially to thank Mrs. Gretta Scott Baur who performed the x-ray diffraction analysis summarized in Table III. The authors acknowledge the interest shown in this project by Dr. John R. Lewis, Head, Department of Metallurgy, and express their appreciation to the Office of Ordnance Research, U. S. Army and the Watertown Arsenal Laboratory for the funds that made the work possible.

Manuscript received August 22, 1955.

Any discussion of this paper will appear in a Discussion Section to be published in the December 1956 Journal.

References

1. The reader is referred to the following three references as representative: E. K. Rideal, and B. M. W. Trapnell, *Proc. Roy. Soc.*, **A205,** 409 (1951); J. K. Roberts, *Proc. Cambridge Phil. Soc.*, **36,** 53–68 (1940); R. C. L. Bosworth, *Proc. Roy. Soc., N. S. Wales*, **83,** 31–38 (1949).
2. I. Langmuir, *J. Am. Chem. Soc.*, **38,** 2269 (1916).
3. I. Langmuir, *Ind. Eng. Chem.*, **22,** 393 (1930).
4. I. Langmuir, *Chem. Rev.*, **13,** 150 (1933).
5. E. A. Gulbransen, and W. S. Wysong, *Metals Technol.*, **14,** 1 (1947).
6. J. S. Dunn, *J. Chem. Soc.*, **132,** 1149, (1929).
7. G. McAdams and G. Geil, J. Research Nat. Bur. Standards, **28,** 593–635, (1942).
8. E. Nachtigall, *Z. Metallkunde*, **43,** 23 (1952).
9. E. Scheil, *ibid.*, **29,** 209 (1937).
10. R. Kieffer and F. Kolbl, *Z. anorg. Chem.*, **262,** 229 (1950).
11. C. J. Smithells, "Tungsten," p. 122, 3rd ed., Chapman and Hall Ltd., London (1952).
12. R. C. Peterson, W. M. Fassell, Jr., and M. E. Wadsworth, *J. Metals*, **6,** 1038 (1954).
13. J. P. Baur, D. W. Bridges, and W. M. Fassell, Jr., *This Journal*, **102,** 490 (1955).
14. S. Glasstone, K. Laidler, and H. J. Eyring, "Theory of Rate Processes," McGraw-Hill Book Co., New York (1941).
15. I. Langmuir, *J. Am. Chem. Soc.*, **40,** 1361 (1918).
16. I. Langmuir, *Trans. Faraday Soc.*, **17,** 607 (1922).
17. R. Fowler and E. A. Guggenheim, "Statistical Thermodynamics," p. 429, Cambridge University Press, Cambridge (1949).
18. J. K. Roberts, *Proc. Roy. Soc., London*, **A152,** 445 (1935).
19. B. M. W. Trapnell, *ibid.*, **A206,** 39 (1951).
20. E. K. Rideal and B. M. W. Trapnell, *Chim Phys.*, **47,** 126 (1950).
21. S. Branauer, K. S. Love, and R. G. Keenan, *J. Am. Chem. Soc.*, **64,** 751 (1942).
22. A. Frumkin and A. Slygin, *Acta physiocochim., U.R.S.S.*, **3,** 791 (1935).
23. M. Temkin and V. Pyshev, *ibid.*, **12,** 327 (1940).
24. K. Love and P. Emmett, *J. Am. Chem. Soc.*, **63,** 3297 (1941).
25. J. W. Hickman and E. A. Gulbransen, *Metals Technol.*, **14,** T. P. 2144 (1947).
26. A. Magneli, *Acta cryst.*, **6,** 495 (1953).

Oxidation of Oxygen-Free High Conductivity Copper to Cu_2O

J. P. Baur, D. W. Bridges and W. M. Fassell, Jr.[1]

Department of Metallurgical Engineering, University of Utah, Salt Lake City, Utah

ABSTRACT

The effect of oxygen upon the oxidation behavior of OFHC copper was studied under conditions that assured that the involved system is $Cu/Cu_2O/O_2$. Oxidation rate was correlated through use of two parallel reaction rates: (*a*) a diffusion step (resulting in a pressure sensitive parabolic constant, k_p), and (*b*) a phase boundary reaction (pressure insensitive). Application of the equation: $k_p = \text{const.}\ (P_{O_2})^{1/n}$ led to values for n: 950°C, $n = 2.0$; and 1000°C, $n = 3.4$. Theoretical considerations are outlined to emphasize that surface site saturation will lead to a cessation of the increase in k_p with increased oxygen pressure when the oxygen concentration and adsorption potential are sufficient to accommodate oxygen on all available sites. Photomicrographs of the growth of CuO on Cu_2O are included.

Introduction

Oxidation of copper has been studied extensively (1). Study and interpretation of results are complicated by the fact that the system, $Cu/Cu_2O/CuO/O_2$, is stable at oxygen pressures in excess of 160 mm-Hg (the oxygen partial pressure of atmospheric air) over the entire temperature range below 1050°C. However, at reduced oxygen pressures, CuO becomes unstable and oxidation is possible involving the system $Cu/Cu_2O/O_2$. The dissociation pressure of CuO as a function of temperature has been reported (2, 3).

The classical theory of parabolic oxidation due to Wagner (4–6, 1) dealt with the systems $Cu/Cu_2O/O_2$ and $Ni/NiO/O_2$. He reported that the oxidation of copper to Cu_2O from 0.23 to 60 mm-Hg oxygen pressure and 1000°C was not ideally parabolic. Diffusion alone was not rate-determining, but a phase bounday reaction at the Cu/Cu_2O interface also effected the reaction rate. Jost (6) states, "If both processes, viz., reaction at an interface and diffusion, proceed with comparable speed, the 'reaction resistivities' might be expected to be additive (7)". The foregoing considerations yield an expression:

$$\Delta m/k_1 + \Delta m^2/k_p = t \qquad \text{(I)}$$

where Δm is the weight increase per unit surface area, k_1 and k_p are the linear and parabolic reaction rate constants, respectively, and t is the time. A more complete derivation of equation (I) can be found on page 44, reference (1).

Wagner plotted $t/\Delta m$ as a function of Δm from which k_1 could be determined from the reciprocal of the $t/\Delta m$ intercept ($\Delta m \rightarrow 0$) and k_p from the reciprocal of the slope. Values of k_1 found by Wagner were relatively pressure insensitive, thus leading him to the conclusion that the interface in question was the Cu/Cu_2O interface. K_p was found to be proportional to the seventh root of the oxygen pressure. These findings were in good agreement with theoretical considerations yielding a $\frac{1}{8}$ power dependency and the electrical conductivity measurements of Wagner and Dunwald (8) on the system Cu_2O-O_2 which yielded a seventh root dependency of oxygen pressure.

Wagner and Hammen (9) reported an oxygen pressure dependency of 1/5 root found by determining the concentration of cupric ions (lattice vacancies). This was justified by assuming the defect activity was not ideal. The assignment of an activity coefficient of $\frac{1}{2}$ yielded a theoretical oxygen dependency of the 1/5.2 root.

The present paper deals with the oxidation behavior of high purity Oxygen Free High Conductivity (OFHC) copper at temperatures of 900°, 950°, and 1000°C at oxygen pressures which permit the formation of Cu_2O alone. The purpose is to criticize the universal use of a limited approximation, equation (III*a*), for the explanation of the effect of oxygen pressure on the magnitude of the parabolic oxidation rate constant.

Experimental Procedure

The vacuum furnace employed is shown schematically in Fig. 1. It was patterned after the standard high temperature-high pressure furnaces designed in this laboratory (10). It consists of a central glass-zirconia vacuum chamber surrounded by a steel outer chamber, both of which can be evacuated or pressurized independently. This construction was necessary in order to maintain the same oxygen pressure on both sides of the central tube, thereby equalizing the heat conduction. Kanthal A-1 furnace windings are wound, not on the zirconia tube, but on a concentric alundum tube. This was to prevent the recurrence of an earlier implosion due to the slagging of the zirconia tube by the winding at 1000°C. A platinum, platinum-rhodium thermocouple is mounted within the zirconia tube less than an inch from the sample.

A helical quartz spring, on which the sample to be oxidized is suspended by means of a platinum chain, is mounted concentrically within a 4-ft vertical glass extension above the zirconia tube. The spring system can be raised and lowered by means of a small glass winch made from a standard glass tapered joint and located at the top of the vertical glass extension.

The copper samples, 1 in. x $\frac{3}{8}$ in. x 0.019 in., are etched

[1] Present address: Howe Sound Co., Salt Lake City, Utah.

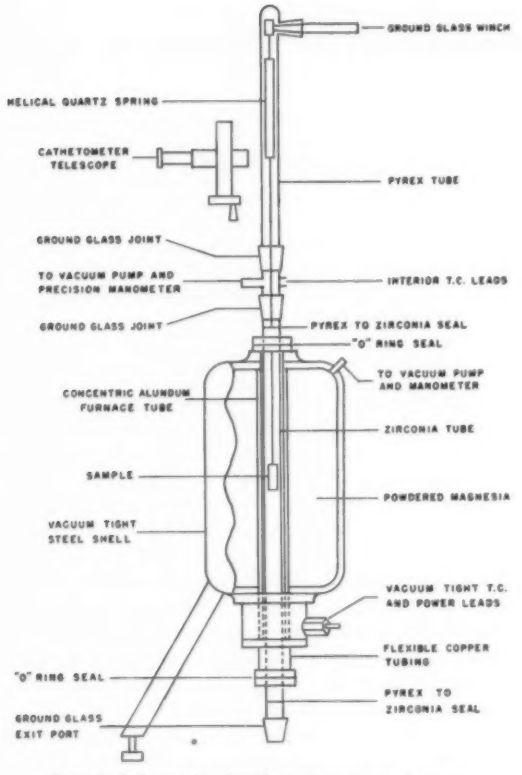

FIG. 1. Schematic drawing of vacuum furnace

for 15 min in 3–5% ammonium persulfate solution, washed in distilled water, rinsed in acetone, and dried. The sample is raised into the hot zone of the vacuum chamber following the obtainment of thermal equilibrium. The gain in weight is measured by following the deflection of the quartz spring by means of a cathetometer telescope.

The oxygen pressure is read on a precision dial manometer. Constant oxygen pressure is maintained through the use of a microleak valve connecting the system to the oxygen supply.

The results of spectrographic analysis of the copper revealed the following elements present: boron, 0.002%; silicon, 0.0015%. No other elements were detected.

EXPERIMENTAL RESULTS

At all temperatures and oxygen pressures investigated, the samples were found to oxidize in a "nonideal" parabolic manner. The oxidation behavior could not be expressed by the relationship (11):

$$(\Delta m)^2 = k \cdot t + C \qquad \text{(II)}$$

where k and C are constants, Δm is the weight gained per unit area, and t is the time. Fig. 2 shows a typical family of oxidation rate plots of (weight gained)^2 vs. time.

If one follows Wagner (4) and assumes that an interface reaction (Cu/Cu_2O interface) influences the reaction rate, the data could best be represented by equation (I). The parabolic rate constant k_p can then be found from the reciprocal of the slope and the linear constant k_l from the

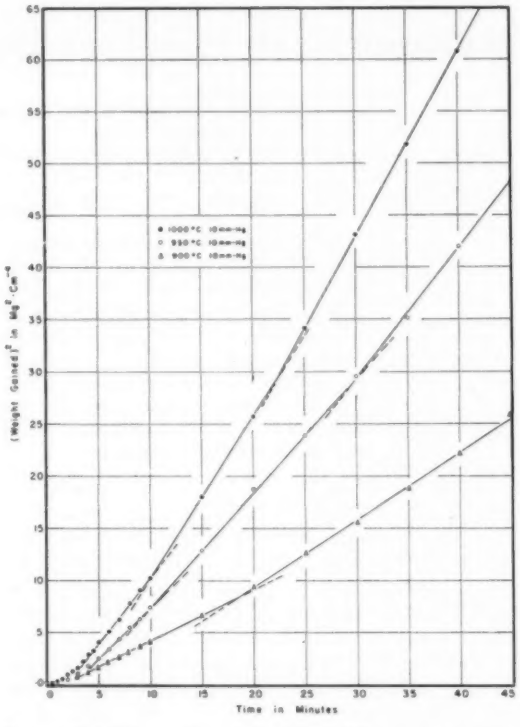

FIG. 2. Oxidation rate curves for OFHC copper in oxygen

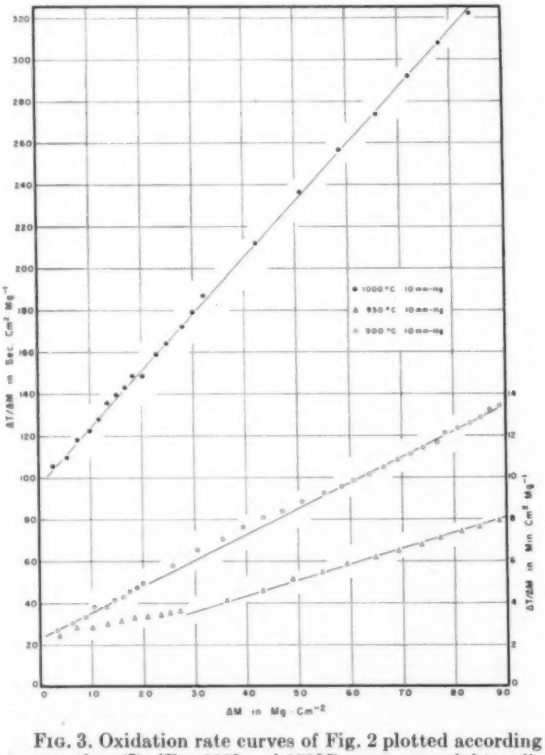

FIG. 3. Oxidation rate curves of Fig. 2 plotted according to equation (I). (For 900° and 950°C curves use right ordinate.)

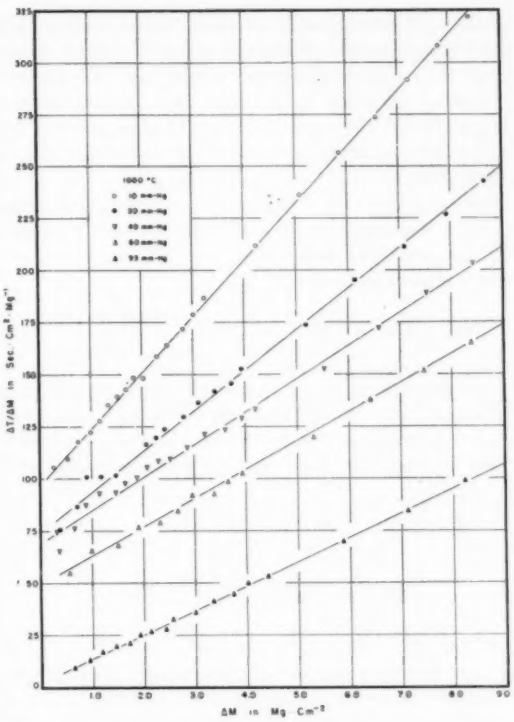

FIG. 4. Oxidation rate curves for OFHC copper, 1000°C at various pressures. (*Note*: add 10, 50, and 84 sec·cm²·mg⁻¹ to the ordinates of the 40, 60, and 95 mm Hg curves, respectively.)

TABLE I. *Summary of oxidation rate constants for high purity oxygen free high conductivity copper at 900°, 950°, 1000° C*

Temp	Oxygen pressure	Parabolic constant	Linear rate constant
°C	*mm Hg*	$mg^2cm^{-4}hr^{-1}$	$mg\ cm^{-2}hr^{-1}$
900	5	43.2	78.2
	10	48.2	26.0
950	10	81.5	40.4
	20	122.6	29.4
	30	136.0	33.2
	35	149.7	29.0
1000	5	126.7	49.3
	10	133.2	37.0
		152.3	42.7
	20	173.5	40.3
		190.8	41.6
	30	220.0	49.5
		225.4	40.4
	40	232.9	44.5
		239.0	34.1
	50	250.2	49.7
		249.1	39.5
	60	254.4	37.4
		236.5	48.6
	70	247.3	60.0
		256.7	52.3
	80	252.4	51.5
		268.2	51.9
	95	287.8	42.6

TABLE II. *Comparison of the parabolic rate constants obtained in this survey and those available in the literature for 1000° C for oxygen pressures of 10 mm-Hg to 95 mm-Hg**

Oxygen pressure	Parabolic constant in $g\cdot eq\cdot cm^{-1}\ sec^{-1} \times 10^9$ (12)		
	This project	Wagner (4)	Feitknecht (13)
mm-Hg			
10	3.37	4.5 (11 mm)	
	3.85		
20	4.39		
	4.82		
30	5.56		
	5.70		
40	5.89		
	6.04		
50	6.30		
	6.32		
60	5.98	6.2 (63 mm)	
	6.43		
70	6.25		
	6.49		
80	6.38		
	6.78		
95	7.27		7.29 (100 mm)

* Three experimental determinations of Moore and Lee (14) are within the temperature-pressure range of this investigation. The number following the investigators' initials are in the same units as Table II above. 1000°C, 5 mm-Hg: ML, 8.6×10^{-9}; BBF, 3.2×10^{-9}; 950°C, 5 mm-Hg: ML, 5.6×10^{-9}; BBF, (10 mm-Hg) 2.1×10^{-9}; 900°C, 5 mm-Hg: ML, 1.9×10^{-9}; BBF, 1.1×10^{-9}.

reciprocal of the intercept. Fig. 3 shows the family of curves of Fig. 2 plotted in accordance with equation (I). A series of 1000°C curves is plotted according to equation (I) on Fig. 4. The values of k_p and k_l determined as above are listed in Table I.

The relative constancy of k_l indicates that the phase boundary reaction is pressure independent. The pressure dependence of k_p can be estimated from a plot of log k_p vs. log P_{O_2} according to the equation:

$$k_p = K[P_{O_2}]^{1/n} \qquad \text{(IIIa)}$$

or,

$$\log k_p = 1/n \cdot \log P_{O_2} + \log K \qquad \text{(IIIb)}$$

Values of n for 950° and 1000°C are 2.0 and 3.4, respectively. A comparison of the values of k_p with those of other workers is shown by Table II.

Discussion of Experimental Results

Effect of Surface Concentration of Oxygen

Theoretical considerations of the effect of oxygen concentration on the oxidation rate of copper to Cu_2O are discussed in detail elsewhere (1, 4, 6, 15, 16). It is universally agreed that the migration of copper through the Cu_2O lattice occurs by diffusion of copper ions through cation vacancies (17). Wagner (4, 5, 8) expresses the production of vacancies by the equilibrium consideration:

$$4\,Cu^+ + 4e + O_2(gas) = 4h(Cu^+) + 4h(e) + 2\,Cu_2O \qquad \text{(IV)}$$

where Cu^+ is a cuprous ion, e is an electron, and $h(\ )$ terms represent vacancies (holes). The equilibrium con-

stant, K', for the above equation can then be written:

$$K' = \frac{[h(Cu^+)]^4 \cdot [h(e)]^4 \cdot [a_{Cu_2O}]^2}{[a_{Cu^+}]^4 \cdot [e]^4 \cdot [P_{O_2}]} \quad (V)$$

Assuming the activities of cuprous ions, electrons, and cuprous oxide to be essentially constant (this is equivalent to assuming a small density of vacancies), the concentration of vacancies, $[h(Cu^+)]$, is expressed as:

$$[h(Cu^+)] = \{K'' \cdot P_{O_2}\}^{1/8} \quad (VI)$$

since electroneutrality considerations lead to, $[h(Cu^+)] = [h(e)]$. Acceptance of equation (VI) as an expression of vacancies led Wagner to his parabolic oxidation equation, pressure dependency of which for constant temperature is of the form of equation (III*a*).

This equation is applicable only for the region of small surface coverage where the approximation of linear change of surface coverage with oxygen pressure can be made. Returning to equation (IV), one notes that for general discussion the term, O_2(gas), should not be used. The correct expression should read O_2(surface). This is correctly formulated elsewhere by Wagner (18) and also by Mott and Gurney (15).

Expression for the surface activity, or surface concentration, of oxygen must include consideration of the fact that there can be only a definite finite number of available sites for the accommodation of oxygen per unit surface area of the oxide-oxygen interface. Statistically Fermi-Dirac statistics would apply (19). Less formal formulation can be accomplished in the manner attributed to Langmuir (20, 21). One writes the expression:

$$S + O_2 = S \cdots O_2 \quad (VII)$$

where S represents an available site; O_2, an oxygen molecule; $S \cdots O_2$, an adsorbed molecule. An equilibrium expression for this equation can be written in terms of θ, the fraction of the total sites covered with adsorbed oxygen ($S \cdots O_2$ units). The equilibrium constant for this adsorption process is:

$$K_a = \frac{\theta}{[1-\theta] \cdot [O_2]_{gas}} \quad (VIII)$$

Expression for the concentration of the external oxygen phase, $[O_2]_{gas}$, can be formulated by assumption of the perfect gas law, $[O_2]_{gas} = n/V = P/RT$. It is noted that at constant temperature the only variable is the oxygen partial pressure. If the adsorption of oxygen is assumed much faster than the rate-determining steps [both this survey and Wagners' (4) indicate that the slow phase boundary reaction is at the Cu/Cu_2O interface], the fraction of the surface sites covered, θ, can then be used as an expression for the surface oxygen concentration, $[O_2]_{surface}$:

$$[O_2]_{surface} = \theta = \frac{K_a \cdot [O_2]_{gas}}{1 + K_a \cdot [O_2]_{gas}} \quad (IX)$$

It is seen that the approximate solution, equation (VI), can apply only where $K_a[O_2]_{gas} \ll 1$. Thus, eventually an oxygen pressure will be reached for any constant temperature above which the surface oxygen concentration will not be proportional to the external oxygen pressure. Moreover, a pressure will be reached above which the surface concentration of oxygen will not change at all, i.e., $\theta \approx 1$. Thus, regardless of whether the internal structure of the oxide were that of an "ideal dilute solution" (5) or not, the concentration of lattice vacancies will not continue indefinitely to increase with increase of oxygen pressure.

Using equation (VI) (with P replaced by θ) and equation (IX), the expression for the concentration of vacancies assuming molecular adsorption with no interaction between adsorbed molecules is:

$$[h(Cu^+)] = \{K'' \cdot \theta\}^{1/8} = \left\{K'' \cdot \frac{K_a \cdot [O_2]_{gas}}{1 + K_a \cdot [O_2]_{gas}}\right\}^{1/8} \quad (X)$$

If the assumption of constant adsorption equilibrium constant, K_a (i.e., K_a assumed invariant with change of surface coverage) is not valid, an alternate expression for the concentration of vacancies can be formulated:

$$[h(Cu^+)] = \{K''\theta\}^{1/8} \approx \left[K'' \cdot (4.6T/zV) \cdot \log_{10}\left(\frac{1 + K_a^0[O_2]}{1 + K_a^0[O_2] \cdot \exp(-\theta zV/RT)}\right)\right]^{1/8} \quad (XI)$$

Complete derivation of the equation is included in the Appendix to this paper and elsewhere (22–24). Although the above equality is exact it must be understood that the logarithmic approximation that follows is not proposed for universal application. The extent of its suitability is brought out in the Appendix. Considerations of the type presented by Wagner and Hammen (9) would cause K'' to be no longer a function of temperature alone [see equation (XIV)].

A General Reaction Rate Expression

A general rate equation for pressure sensitive oxidation processes which are diffusion controlled was recently proposed (15):

$$m \cdot \frac{dm}{dt} = k_p = C_0 \cdot f(\theta) \cdot kT/h \cdot \exp\left[\frac{-\Delta F^*}{RT}\right] \quad (XII)$$

Equation (XII) is applicable only if the gain of weight is directly proportional to the gain in the rate-controlling oxide thickness. Thus, for the case of two or more thermodynamically stable oxides variation in percentage composition of the oxides with temperature would result in the necessity for the inclusion of a temperature sensitive function for the conversion of weight increase to increase in thickness. Even for constant temperature the ratio of the two oxides must not change with time and oxygen concentration (pressure). For the oxidation of copper to cuprous oxide, $C_0 = 2\lambda^2 \cdot (-\Omega) \cdot k_0$, where λ is the vacancy jump distance of diffusing cuprous ions, Ω is the ratio of the metal oxide volume to an equivalent volume of metal, k_0 is a proportionality constant with dimensions of ML^{-2} and includes the correction factor for the true surface area (surface roughness and number of active sites per unit surface area) involved in the oxidation reaction. $kT/h \cdot \exp[-\Delta F^*/RT]$ results from the temperature dependence of the diffusion constant according to the Eyring theory

(25). ΔF^* is the activation free energy for vacancy migration and kT/h is the traditional Eyring frequency factor. The resulting function of surface coverage, $f(\theta)$, for the process is:

$$f(\theta) = [h(Cu^+)] = (K'' \cdot \theta)^{1/3} \quad \text{(XIII)}$$

where K'', the equilibrium constant for the production of vacancies, is:

$$K'' = \exp(-\Delta F_1/RT) \quad \text{(XIV)}$$

where ΔF_1 is the free energy involved in vacancy formation. The formulation of this factor has been discussed already (26–28).

Thus, for the oxidation of copper to cuprous oxide, the parabolic rate constant as a function of surface oxygen concentration and temperature is:

$$k_p = \theta^{1/3} \cdot C_0 \cdot kT/h \cdot \exp[-(\Delta F^* + \Delta F_1/8)/RT] \quad \text{(XV)}$$

For constant temperature and adsorption phenomena departing from ideal Langmuir behavior, the parabolic constant would be expressed by

$$k_p = \theta^{1/3} \cdot K_0 \approx K_0' \cdot \sqrt[5]{\log_{10}(1 + K_a^0[O_2])} \quad \text{(XVI)}$$

where $K_0 = C_0 \cdot kT/h \cdot \exp[-(\Delta F^* + \Delta F_1/8)/RT]$

$$K_0' = (4.6T/zV)^{1/3} \cdot K_0$$

and assuming in equation (XI) that,

$$K_a^0[O_2] \cdot \exp[-\theta \cdot zV/RT] \ll 1$$

The data of Table I plotted in accordance with equation (XVI) is shown in Fig. 5. Correlation is good enough to warrant the assumptions made, i.e., the adsorption potential varies linearly with surface coverage, or expressed more precisely, postulation of a random distribution of surface sites occupied by oxygen molecules with interaction between the pairs of nearest neighbors. K_a^0, the adsorption equilibrium constant for 950° and 1000°C, respectively, are 83,900 and 79,390. These values yield a mean adsorption free energy, ΔF^0, of approximately −12,000 calories per mole oxygen.

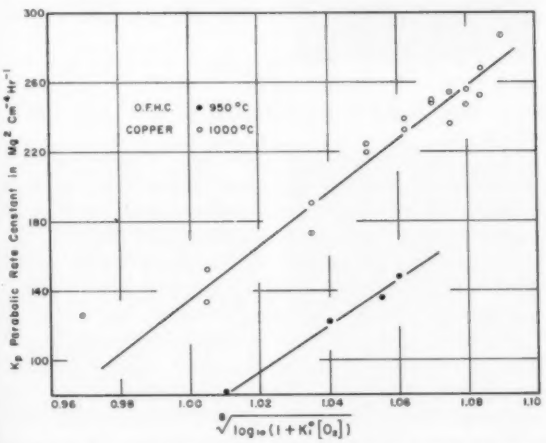

FIG. 5. Data of Table I plotted according to equation (XVI).

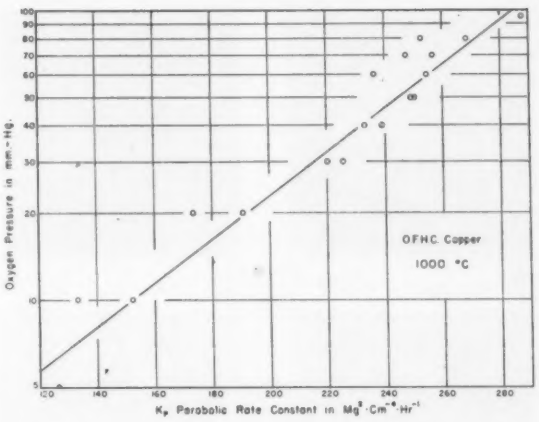

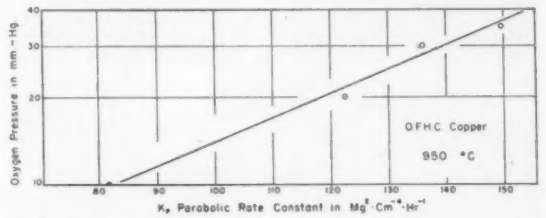

FIG. 6. Data of Table I plotted according to equation (XVII).

According to the boundary exhaustion layer theory of Hauffe and Engell (29, 30), the data of Table I could also be represented by an equation of the form

$$k_p \approx \text{const } \{\log_{10}(P_{O_2}) + \text{const}'\} \quad \text{(XVII)}$$

This correlation is shown in Fig. 6. Equation (XVII) assumes small surface coverage and a migration velocity controlled by an electrical field. This electric field strength is a function of the concentration of adsorbed oxygen ions.

PHOTOMICROGRAPHIC STUDY

In spite of the fact that the copper samples were oxidized under conditions of temperature and oxygen pressure such that Cu_2O was the only stable oxide present, x-ray diffraction patterns of the oxide coatings formed showed that a small amount of CuO was present in all samples formed during the period the sample was lowered from the hot zone (30 sec). It was felt that a photomicrographic study of the formation and growth of CuO on the surface of the Cu_2O layer would be of interest. Fig. 7 shows these photomicrographs under the experimental conditions of temperature and oxygen pressures wherein only Cu_2O can be formed in the hot zone. In all cases these surfaces are as formed and have not been etched or polished in any manner. The micrograph at 900°C and 5 mm-Hg oxygen pressure is typical of the oxide surface formed under conditions wherein only Cu_2O can exist. Several interesting features are apparent:

1. Sharp, well-defined crystals of a variety of sizes.
2. Deep angular recesses between the crystals possibly extending to the base metal.

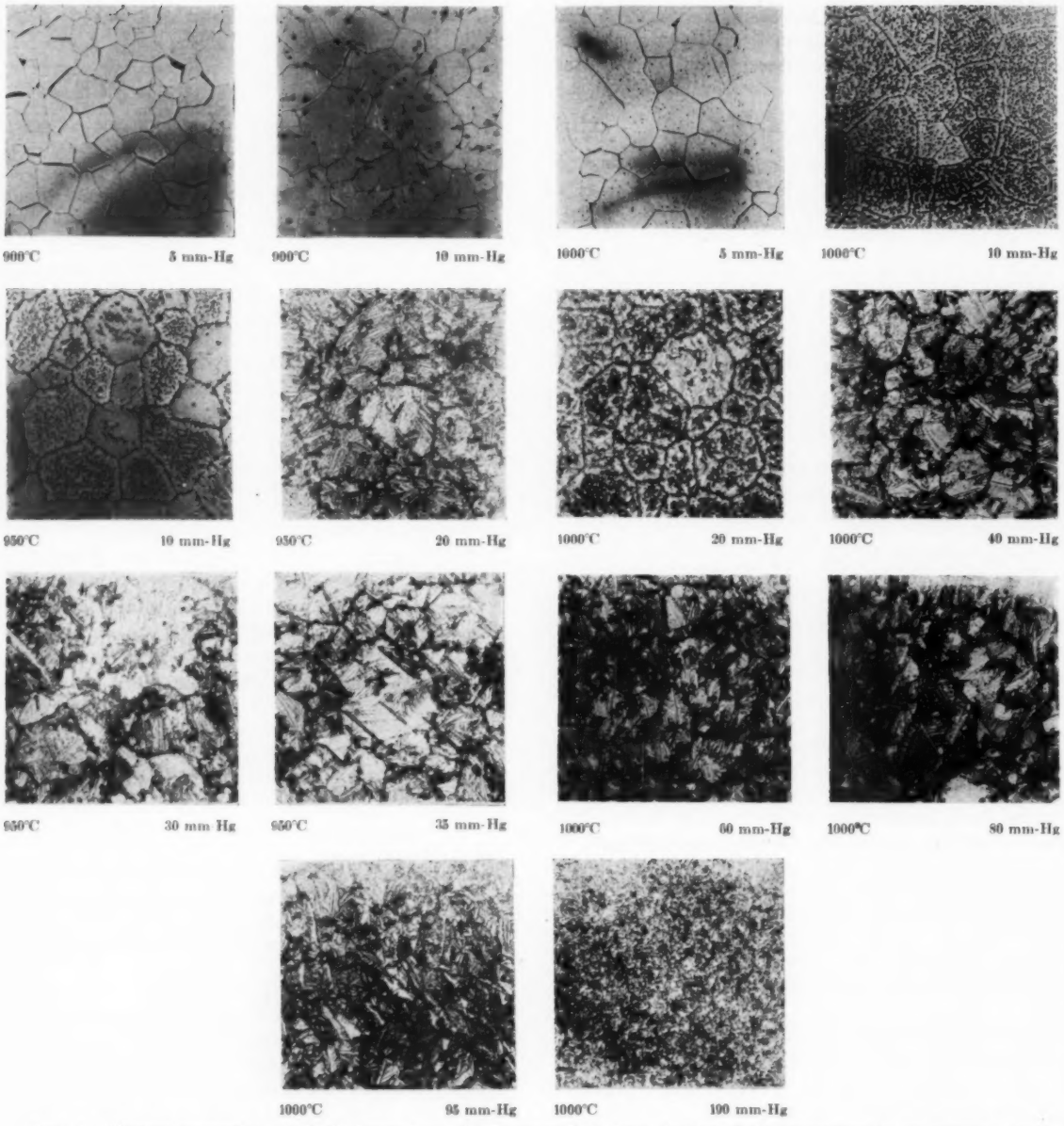

FIG. 7. Photomicrographs of CuO formed on Cu_2O quenched from indicated temperatures in an oxygen atmosphere of indicated partial pressure. 169× before reduction for publication.

3. Predominant appearance of one type of crystal face.

4. All flat faces are the same height above the base metal lying within the focal plane of the microscope objective.

This specimen had a hard mirror-like surface ruby red in color. The x-ray diffraction pattern of this surface showed no CuO to be present, and that the surface was oriented.

As the temperature and pressure increase, the amount of CuO increases from a few scattered dendrite-like formations at 950°C and 10 mm-Hg oxygen pressure through the fern leaf-like structures at the intermediate pressures to the fine grained structures shown in the photomicrograph at 1000°C and 190 mm-Hg which is characteristic of those surfaces formed above the dissociation pressure of CuO and at higher pressures, i.e., greater than 1 atm.

Fig. 8 shows successively higher magnifications of the CuO formed at 1000°C and 80 mm-Hg. The beautiful leaf-like patterns are clearly in evidence.

The oxide surface formed at 900°C and 5 mm-Hg was observed under crossed nicol prisms. Photomicrograph A of Fig. 9 in which the microscope is focused on the surface shows the bright and dark patches of ruby red under the surface grains whose boundaries are visible. Photograph B of Fig. 9 represents the same area except the focal plane is now on the oxide-metal interface. Closer inspection

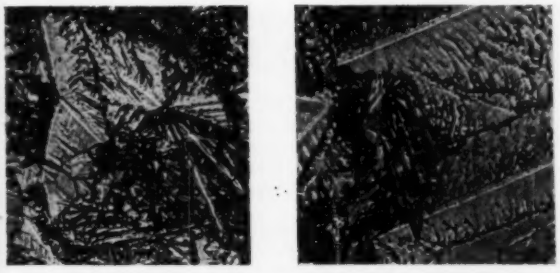

FIG. 8. Higher magnifications of 1000°C, 80 mm-Hg oxidized surface. *Left*, 500×, *right*, 800× before reduction for publication.

shows the grain boundaries of the annealed copper visible in the bright patches. Photograph C of Fig. 9 is a superposition of the negatives of micrographs A and B.

In order to demonstrate that the CuO was formed as a result of the lowering of the sample from the hot zone, a simple experiment was performed. The sample was oxidized in the usual fashion at 1000°C and 80 mm-Hg. Before the sample was lowered from the hot zone, the system was evacuated, thereby preventing the rapid formation of CuO. Fig. 10*a* which shows a comparison of the surfaces formed under both methods definitely establishes the fact that only one oxide Cu_2O exists in the hot zone. X-ray analysis of this surface again showed only Cu_2O

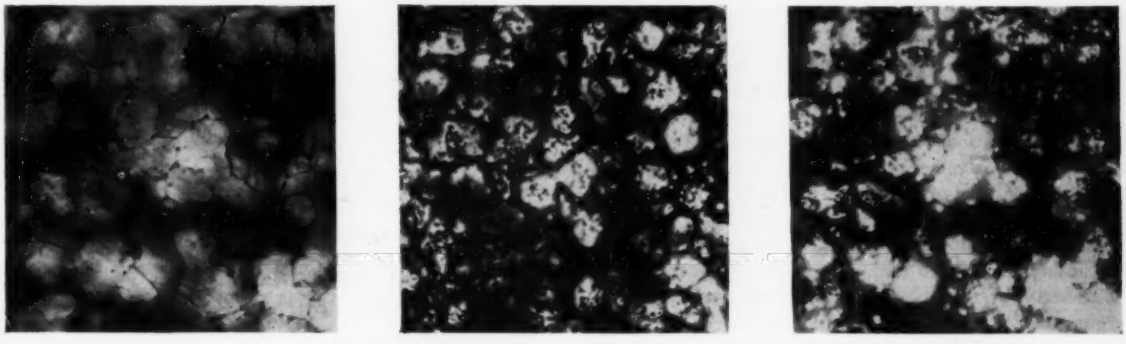

A B C

FIG. 9. Observation of cuprous oxide, Cu_2O, formed at 900°C, 5 mm-Hg under crossed nicol prisms. A—Focal plane on oxide surface; B—focal plane on oxide-metal interface; C—photographs A and B superimposed. 169× before reduction for publication.

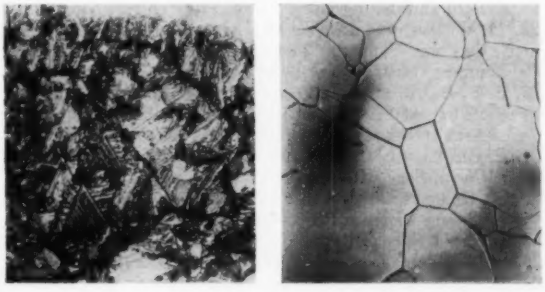

FIG. 10*a*. Sample oxidized at 1000°C, 80 mm-Hg for 45 min. *Left*, quenched in 80 mm-Hg; *right*, quenched in vacuum. 169× before reduction for publication.

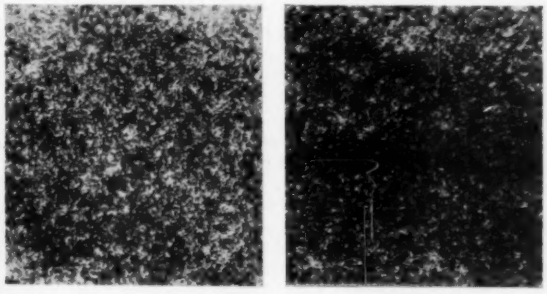

FIG. 10*b*. Sample oxidized at 1000°C, 190 mm-Hg for 45 min. *Left*, quenched in 190 mm-Hg; *right*, quenched in vacuum. 169× before reduction for publication.

to be present in a similarly oriented manner as the 900°C −5 mm-Hg surface. To establish the existence of both oxides, CuO and Cu_2O, above 98 mm-Hg at 1000°C, a sample was lowered after evacuation of the system as before. A comparison of the photomicrographs of Fig. 10*b* shows the same structure in both cases. X-ray diffraction patterns of both samples show the presence of both Cu_2O and CuO.

Fig. 11 is an example of the structure of the boundaries

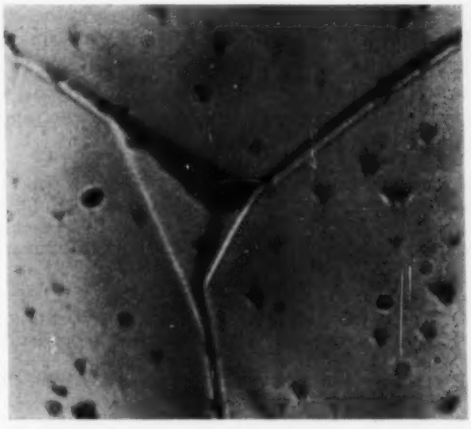

FIG. 11. An example of the structure of the boundaries between the oxide grains. Sample oxidized at 1000°C and 5 mm-Hg. 1250×.

between the oxide grains formed at 1000°C, 5 mm-Hg oxygen pressure.

The inclusion of this photomicrographic study showing the growth of CuO on the Cu_2O substrate as a layer is not intended to indicate that such growth is the case under conditions of temperature and pressure wherein both oxides are stable. The phenomena illustrated in Fig. 7 to 11 occurred under nonisothermal conditions.

Concluding Remarks

The explanation of Wagner (5, 9) of the deviation from ideality cannot be disregarded. The departure from the predicted eighth root dependency has sometimes been attributed to association of the defects (17, 31). Complete association results in the limit of one-fourth power dependency. Correlation of data obtained in the present investigation by use of equation (III*a*) led to values for the parameter n of less than four for both the 950° and 1000°C isotherms. Clearly it is not a case of deviation from ideal solution behavior alone. The effect of surface saturation of oxygen must be included in any general discussion of pressure sensitive oxidation. This will become even more apparent when the results of the high pressure oxidation study of nickel performed by two of the authors is reported (32).

The adsorption equilibrium step is not essential to the argument. A form identical to equation (IX) results from the so-called "steady-state" method employed by other workers (33, 34).

A reviewer brought out a well-founded objection to the authors' conclusions of the origin of the departure from true parabolic behavior. He suggested that the nonideality could arise from the fact that the surface is obviously not plane. Photomicrographs displaying the same phenomenon as Fig. 11 have been recorded on nickel oxide surfaces (32) and on cobalt oxide surfaces (35). Nickel oxidation data requires the use of equation (I). Cobalt seems to obey equation (II) quite rigorously.

Acknowledgments

The authors especially thank H. M. Schleicher, Metallurgical Department, American Metal Co., Limited, who graciously supplied the OFHC Copper used in this study.

They thank Dr. J. R. Lewis, Head, Department of Metallurgy, University of Utah, for his support of this project. Thanks are due to the Watertown Arsenal Laboratory, Department of Ordnance Research, who supplied the funds which made this work possible.

Manuscript received August 29, 1955. This paper was presented at the Pittsburgh Meeting, October 9 to 13, 1955.

Any discussion of this paper will appear in a Discussion Section to be published in the December 1956 Journal.

REFERENCES

1. O. Kubaschewski and B. E. Hopkins, "Oxidation of Metals and Alloys," Academic Press Inc., New York (1953).
2. F. Hastings Smith and H. R. Robert, *J. Am. Chem. Soc.*, **42**, 2582 (1920).
3. F. Becker, Physikalisch-chemische Tabellen 3. Erganzungsband, 3. Teil. Berlin, Springer (1935).
4. C. Wagner and K. Grunewald, *Z. Physik Chem.*, **B40**, 455 (1938).
5. C. Wagner, "Diffusion and High Temperature Oxidation of Metals" in the American Society of Metals publication, "Atom Movements," ASM, Cleveland (1951).
6. W. Jost, "Diffusion in Solids, Liquids, and Gases," Academic Press Inc., New York (1952).
7. K. Fishbeck, L. Neundeubel, and F. Salzer, *Z. Elektrochem.*, **40**, 517, (1934).
8. H. Dunwald and C. Wagner, *Z. physik Chem.*, **B22**, 212 (1933).
9. C. Wagner and H. Hammen, *ibid.*, **B40**, 197 (1938).
10. R. C. Peterson, W. M. Fassell, Jr., and M. E. Wadsworth, *J. Metals*, **6**, 1038 (1954).
11. O. Kubaschewski and B. E. Hopkins, *op cit*, p. 37.
12. *Ibid.*, p. 122. This reference outlines the method of conversion from direct mass increase units to gram-equivalent type units.
13. W. Feitknecht, *Z. Elektrochem.*, **35**, 142 (1929).
14. W. J. Moore and B. Selikson, *J. Chem. Phys.*, **19**, 1539 (1951). The conversion to units of Table II is: const. in gram-equivalents of copper times ($cm^{-1}sec^{-1}$) equals $(\frac{1}{2}V_{eq})^{-1}$ times Moore's constant (cm^2sec^{-1}). V_{eq} is the volume of Cu_2O containing an equivalent. The factor $\frac{1}{2}$ occurs as Cu_2O contains two equivalents of copper per gram-equivalent of Cu_2O.
15. N. F. Mott and R. W. Gurney, "Electronic Processes in Ionic Crystals," 2nd ed., Oxford Press, London, (1948).
16. J. P. Baur, D. W. Bridges, and W. M. Fassell, Jr., *This Journal*, **102**, 490 (1955).
17. J. Bardeen, W. H. Brattain, and W. Shockley, *J. Chem. Phys.*, **14**, 714 (1946).
18. H. Dunwald and C. Wagner, *op cit*, p. 224, section 8, second paragraph.
19. R. Fowler and E. Guggenheim, "Statistical Thermodynamics," chap. 10, Cambridge (1949).
20. I. Langmuir, *Ind. Eng. Chem.*, **22**, 393 (1930).
21. P. H. Emmett, Editor, "Catalysis," Vol. I, chapter by K. Laidler entitled 'Chemisorption,' chap. 3, Reinhold Publishing Corp., New York (1954).
22. D. W. Bridges and W. M. Fassell, Jr., "Niobium in Oxygen," Interim-Technical Report 9, Army Ordnance Contract DA-04-495-ORD-237.
23. J. P. Baur, D. W. Bridges, and W. M. Fassell, Jr., "Tungsten in Oxygen," Interim Technical Report 8, Army Ordnance Contract DA-04-495-ORD-237.
24. S. Brunauer, K. S. Love, and R. G. Keenan, *J. Am. Chem. Soc.*, **64**, 751 (1942).
25. S. Glasstone, K. Laidler, and H. Eyring, "The Theory of Rate Processes," McGraw-Hill Book Co., New York (1950).
26. N. F. Mott, *Trans. Faraday Soc.*, **36**, 472 (1940).
27. E. A. Gulbransen, *Trans. Electrochem. Soc.*, **83**, 391 (1943).
28. E. A. Gulbransen, Proceedings of the International Symposium on the Reactivity of Solids, Gothenburg 1952, Part II, 899, Goteborg, Elanders Boktryckeri Aktiebolag (1954).
29. B. Chalmers, Editor, "Progress in Metal Physics," Vol. 4, Chap. 2 by K. Hauffe entitled "Mechanism of Oxidation of Metals and Alloys," p. 101, Equation 71, Interscience Publishers Inc., New York (1953).
30. K. Hauffe, Proceedings of the International Symposium on the Reactivity of Solids, Gothenburg 1952, Part II, p. 842, Equation 46, (This article is in German), Goteborg, Elanders Boktryckeri Aktiebolag (1954).
31. N. F. Mott, *Nature*, **145**, 996 (1940).
32. J. P. Baur and W. M. Fassell, Jr., Work begun under an International Nickel Co. fellowship and continued under the Office of Ordnance Research Project DA-04-495-ORD-237. The system $Ni/NiO/O_2$ is stable over the entire oxygen pressure range. Over the majority of the pressure range (10 mm-Hg to 300 psia O_2) there is relatively little change in the magnitude

of the parabolic constant for 1100°, 1150°, and 1200°C, respectively.
33. W. J. Moore and J. K. Lee, *Trans. Faraday Soc.*, **47**, 501, (1951).
34. K. Hauffe and H. Pfeiffer, *Z. Elektrochem.*, **56**, 390 (1952).
35. Unpublished data.

APPENDIX

Where the effect of interaction between the adsorbed molecules on the energy of adsorption cannot be neglected, the original Langmuir derivation for θ (1), the fraction of the surface covered, equation (IX) of the text, must be amended. Langmuir recognized this and wrote an alternate expression (2) for the fraction of the surface covered applicable for a varying energy of adsorption (1, 2)

$$\theta = \sum_i K_i/(1 + K_i \cdot P) \qquad \text{(I)}$$

K_i is no longer a constant, but varies according to the extent and nature of the interaction energy. Most often the assumption is made that the enthalpy of adsorption is a linear function of surface coverage:

$$\Delta H_{ads} = \Delta H^0_{ads} + \theta z V \qquad \text{(II)}$$

where ΔH^0_{ads} is the enthalpy of adsorption for $\theta = 0$. As V is defined as the positive molar energy of interaction, the enthalpy becomes less and less negative as the surface coverage approaches its equilibrium limit. The coordination number, z, of the monolayer ($0 \leq z \leq 6$) is dependent on the nature of the monolayer and the degree of completeness of coverage. Thus, it is seen that under the above scheme the first adsorbed molecules are more strongly adsorbed than the last.

The assumption of equation (II) is not as artificial as may be thought at first glance. It results from consideration of the distribution of sites with adsorbed molecules as completely random (3, 4) and has been experimentally observed in the case of hydrogen on tungsten (5–7).

Modification of the Langmuir derivation under the conditions of equation (I) has been published by Brunauer (8). Their derivation (with slight alteration in definitive terminology) is outlined briefly. Let an equilibrium constant for changeable adsorption enthalpy be defined as:

$$K_a = \exp\left[-(\Delta F^0_{ads} + \theta \cdot zV)/RT\right] = K^0_a \exp\left[-\theta \cdot zV/RT\right] \qquad \text{(III)}$$

where $K^0_a = \exp\left[(-\Delta H^0 - T \cdot \Delta S^0)/RT\right]$, the value of the equilibrium constant for $\theta = 0$.

The expression for the surface coverage, θ, is now the summation of small differential units of coverage θ_s, each involving a different enthalpy and valid over a small element of area, ds. Equation (IX) of the text, with K_a defined as in equation (III) expresses θ_s. Then the fraction of the entire area covered with adsorbed molecules is:

$$\theta = \Sigma\, \theta_s \cdot ds = \int_0^s \theta_s \cdot ds = \int_0^s \frac{K^0_a \cdot [O_2] \cdot \exp\left[-s \cdot zV/RT\right]}{1 + K^0_a \cdot [O_2] \cdot \exp\left[-s \cdot zV/RT\right]} \cdot ds \qquad \text{(IV)}$$

This integral is of the form $\int dU/U$, where U is the denominator. Integrating equation (IV), one obtains:

$$\theta = \frac{RT}{zV} \cdot 2.3 \log_{10}\left\{\frac{1 + K^0_a \cdot [O_2]}{1 + K^0_a \cdot [O_2] \cdot \exp\left[-\theta \cdot zV/RT\right]}\right\} \qquad \text{(V)}$$

where

$$K^0_a[O_2] \gg 1 \gg K^0_a[O_2] \exp\left[-z\theta V/RT\right]$$

$$\theta \approx 4.6\, T/zV \{\log_{10}[O_2] + \log_{10} K^0_a\} = 4.6\, T/zV \left\{\log_{10}[P_{O_2}] + \log_{10}\left(\frac{K^0_a}{RT}\right)\right\} \qquad \text{(VI)}$$

Equation (VI) is a result first derived semi-empirically by Frumkin and Slygin (9). These workers and also Temkin and Pyzkev (10) used it in connection with the explanation of the adsorption of NH_3 on iron catalyst. Love and Emmett (11) applied it to a similar system. It should be noted that equation (VI) is not good at either limit of the allowed values for θ, the fraction of the surface covered. A completely different derivation of equation (VI) accredited to Roginski (12) arises from considerations of surface nonuniformity.

REFERENCES TO APPENDIX

1. I. Langmuir, *J. Am. Chem. Soc.*, **40**, 1361 (1918).
2. I. Langmuir, *Trans. Faraday Soc.*, **17**, 607 (1922).
3. R. Fowler and E. A. Guggenheim, "Statistical Thermodynamics," p. 429, Cambridge (1949).
4. S. Glasstone, K. Laidler, and H. Eyring, "Theory of Rate Processes," p. 364, McGraw Hill Book Co., New York (1941).
5. J. K. Roberts, *Proc. Roy. Soc. London*, **A152**, 445 (1935).
6. B. M. W. Trapnell, *ibid.*, **A206**, 39 (1951).
7. E. K. Rideal and B. M. W. Trapnell, *J. chim. phys.*, **47**, 126 (1950).
8. S. Brunauer, K. S. Love, and R. G. Keenan, *J. Am. Chem. Soc.*, **64**, 751 (1942).
9. A. Frumkin and A. Slygin, *Acta physicochim., U.R.S.S.*, **3**, 791 (1935).
10. M. Temkin and V. Pyskev, *ibid.*, **12**, 327 (1940).
11. K. Love and P. Emmett, *J. Am. Chem. Soc.*, **63**, 3297 (1941).
12. "Advances in Catalysis, V", Chapter by J. G. Tolpin and coauthors entitled 'Contributions of Russian Scientists to Catalysis,' pp. 240, Academic Press, Inc., New York (1953).

Corrosion of Copper-Gold Alloys by Oxygen-Containing Solutions of Ammonia and Ammonium Salts

J. I. Fisher[1] and J. Halpern

Department of Mining and Metallurgy, University of British Columbia, Vancouver, B.C., Canada

ABSTRACT

Copper-gold alloys, ranging in gold content from zero to 15 at. %, were exposed to stirred aqueous solutions of ammonia and ammonium salts under oxygen partial pressures of up to 6.8 at. Only copper dissolved under these conditions, a gold-rich film being left behind on the surface of the alloy. As the gold content of the alloys was increased, the rate of solution of copper generally fell off and the rate law shifted from linear, usually to parabolic. Alloys containing 15 at. % gold corroded slowly in solutions containing ammonia only, but were passive in the presence of ammonium sulfate. The effect on the kinetics of solution composition, oxygen pressure, and temperature are described, and some of the factors which limit the rate of corrosion are discussed. It is concluded that, under certain conditions, copper oxides are formed which contribute to the film structure and to limiting the corrosion rate.

Introduction

A kinetic study of the solution of copper in oxygen-containing aqueous solutions of ammonia and ammonium salts was described in an earlier paper (1). The over-all reaction in ammonia solutions is:

$$Cu + 4NH_3 + \tfrac{1}{2}O_2 + H_2O \rightarrow Cu(NH_3)_4^{++} + 2OH^- \quad (I)$$

and in solutions containing, also, ammonium salts,

$$Cu + 2NH_3 + 2NH_4^+ + \tfrac{1}{2}O_2 \rightarrow Cu(NH_3)_4^{++} + H_2O \quad (II)$$

It was shown that the rate-determining step is the chemical attack of a NH_3 molecule or NH_4^+ ion on the oxygen-covered copper surface. The observed rate is thus comprised of two independent contributions, of first order with respect to the concentrations of NH_3 and NH_4^+, respectively. Both rates are independent of the concentration of dissolved oxygen, provided that the latter is present in excess, so that its transport to the metal surface does not become rate-limiting. Where such limitation occurs, the kinetics are altered so as to obscure the mechanism of the chemical reaction (1, 2).

The object of the present study was to determine the effect on this reaction of alloying copper with another metal which is itself thermodynamically immune to attack by the corroding solutions. Gold, which fulfills this condition, was selected as the alloying element, since copper forms with it a continuous solid solution of well-known structural properties. There have been several earlier studies of the corrosion of copper-gold alloys in other media (3–5), but these have been concerned mainly with the determination of practical parting limits.

Experimental

Specimen ingots of pure copper and of four copper alloys, containing 2.0, 5.0, 10.0, and 15.1 at. % gold (designated as alloys 2, 5, 10, and 15, respectively), were prepared by induction melting in carbon crucibles under purified argon. Spectroscopic analysis of the final alloy specimens indicated a total foreign metal impurity content of less than 0.01%.

Ingots were homogenized in an argon atmosphere at 850°C for 70 hr, furnace cooled to 500°C, and finally quenched in water to ensure a disordered structure. Machined cylindrical specimens were then mounted in Bakelite so as to leave exposed a circular cross section of accurately measured geometrical area. Prior to re-use, each specimen was refaced in a lathe to remove the surface effects resulting from the previous experiment, and the freshly exposed surface was polished by standard metallographic techniques. This procedure was found to give reproducible results.

Corroding solutions were prepared from C. P. reagents and distilled water.

The stainless steel autoclave used for the experiments has been described earlier (1). The Bakelite mount containing the electrically insulated metal specimen was positioned, face downward, in the solution with the exposed surface about 5 mm above the impeller. The latter was 10.9 cm in diameter and rotated at 720 rpm, throwing the solution upward against the specimen face. The temperature of the solution and the partial pressure of oxygen were held constant at desired values. Most of the experiments were made at 25°C and O_2 partial pressure of 6.8 at.

The reaction was followed by withdrawing samples of the solution periodically for analysis. The concentration of dissolved copper was measured with a Beckman DU spectrophotometer using the carbamate method (6). A colorimetric procedure, involving the addition of rhodanine (7), was used to test the solutions for gold, concentrations of less than 1 mg/l being readily detectable. NH_3 concentrations were determined by potentiometric titration with standard HCl.

Following completion of the experiment the specimen was removed and subjected to visual and microscopic in-

[1] Present address: Physical Metallurgy Div., Mines Branch, Department of Mines and Technical Surveys, Ottawa, Ont., Canada.

spection. In some cases surface film scrapings were taken for chemical and x-ray diffraction analysis.

Results

In general, the copper and alloy specimens were found to undergo corrosion when exposed to solutions containing ammonia and oxygen, either in the absence or presence of added ammonium sulfate. An exception was alloy 15 which did not corrode in the presence of ammonium sulfate. The corrosion reaction comprised, essentially, dissolution of copper in accordance with equations (I) and (II). At no time could any gold be detected in the solution.

Some typical rate plots for solutions containing NH_3 only are shown in Fig. 1 and for those containing both NH_3 and $(NH_4)_2SO_4$ in Fig. 2. For pure copper the rate plots were always linear and solution rates were usually in agreement with those reported earlier (1). On the other hand, solution rates of copper from the copper-gold alloys generally fell off with time, the rate plots sometimes assuming complex shapes. This made it impossible to compare corrosion rates for different experiments in terms of a uniform rate constant. Instead, the amount of Cu dissolved in the first 3 hr of each experiment was arbitrarily adopted as a measure of the corrosion rate for comparative purposes, the relatively long reaction time being chosen in order to minimize spurious initial effects.

Corrosion in solutions containing NH_3 only.—Rate plots for the solution of copper from the various alloys in solutions containing NH_3 but no added ammonium salts are shown in Fig. 1. The curves for the alloys are of complex shape and cannot be fitted by either a linear or parabolic relation. Some of them are characterized by two apparent regions, an initial period of relatively rapid corrosion during which the rate falls off with time, and a final slower stage during which the rate remains essentially constant.

The results are summarized in Fig. 3 where the corrosion rates are plotted as functions of the gold content of the alloy and of the NH_3 concentration of the solution. It is seen that alloying the copper with gold even in concentrations as low as 2 at. % drastically reduces its rate of solution. Increasing the gold content between 2 and 15 at. % has relatively little further effect.

Increasing the NH_3 concentration of the solution between zero and 2 mole/l results in an increased corrosion rate for pure copper and for each of the alloys. The apparent levelling off of the rate at high NH_3 concentrations in the case of pure copper has been attributed to the influence of limitation by oxygen transport (1). With the alloys whose corrosion rates and hence oxygen requirements are much lower, this effect is less pronounced.

Corrosion in solutions containing NH_3 and $(NH_4)_2SO_4$.—No corrosion, either of pure copper or of the alloys, could be detected when they were exposed to solutions containing only $(NH_4)_2SO_4$ and no free NH_3. Apparently, some free NH_3 is required to form the soluble cuprammine salt, as suggested by equations (I) and (II). However, in the presence of NH_3, addition of small amounts of $(NH_4)_2SO_4$ was found to have a profound effect both on the corrosion rates and on the shapes of the rate plots.

The rate plots shown in Fig. 2 are typical of those obtained for the alloys in solutions containing both NH_3 and $(NH_4)_2SO_4$ and are seen to conform to a parabolic relation. As shown in Fig. 4, the rate for each alloy increases with increasing NH_4^+ concentration and finally levels off at a value which depends inversely on the gold content.

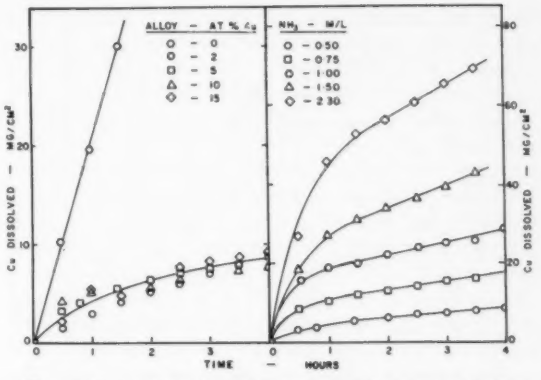

FIG. 1. Rate plots for the corrosion of copper and alloys in NH_3 solutions containing no NH_4^+ salts; 25°C, 6.8 at. O_2. (*a*) Corrosion of different alloys in 0.5M NH_3 solution; (*b*) corrosion of alloy 5 in solutions of different NH_3 concentration.

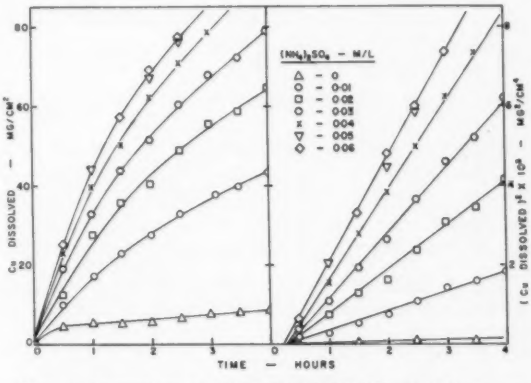

FIG. 2. Corrosion of alloy 10 in 0.5M NH_3 solutions containing various amounts of $(NH_4)_2SO_4$, 25°C, 6.8 at. O_2.

For a specified solution the rate falls off as the gold content of the alloy increases until the latter reaches about

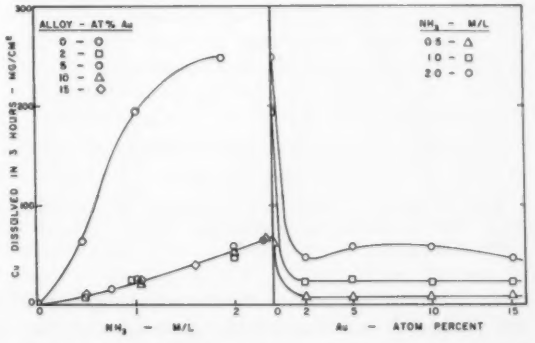

FIG. 3. Effect of NH_3 on the corrosion rate of copper and alloys, 25°C, 6.8 at. O_2.

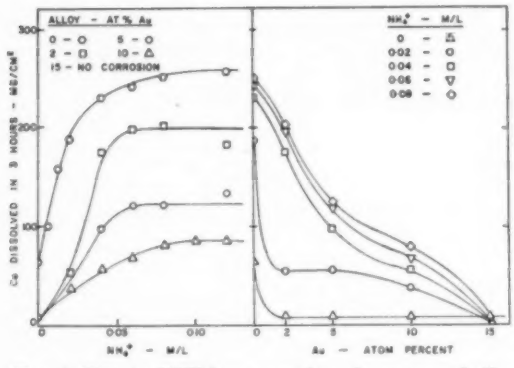

FIG. 4. Effect of NH_4^+ on corrosion of copper and alloys in solutions containing 0.5M NH_3, 25°C, 6.8 at. O_2.

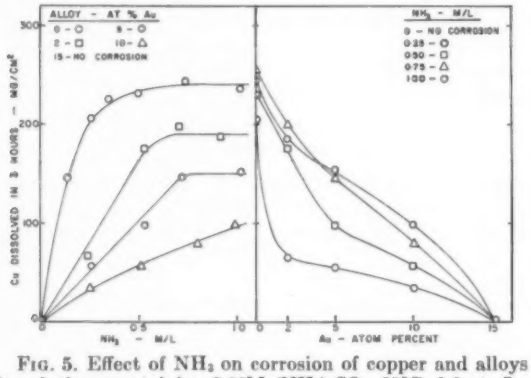

FIG. 5. Effect of NH_3 on corrosion of copper and alloys in solutions containing 0.02M $(NH_4)_2SO_4$, 25°C, 6.8 at. O_2.

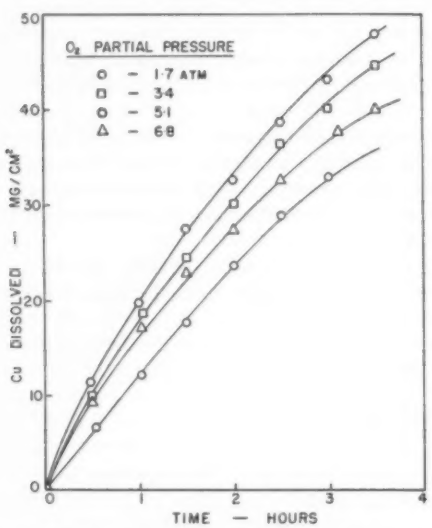

FIG. 6. Effect of varying O_2 pressure on corrosion of alloy 10 in solutions containing 0.5M NH_3, 0.01M $(NH_4)_2SO_4$, 25°C.

15 at. %. In no case, where solutions containing both NH_3 and $(NH_4)_2SO_4$ were used, could any corrosion of alloy 15 be detected either by examination of the specimen surface or by analysis of the solution.

Fig. 4 reveals that the effect of $(NH_4)_2SO_4$ addition is particularly marked for the alloys of low gold content, i.e., alloy 2, and diminishes as the gold content increases. Surprisingly, with alloy 15, addition of $(NH_4)_2SO_4$ appears to have a reverse effect since it inhibits completely the corrosion observed in its absence, i.e., in solutions containing NH_3 only. As shown in Fig. 5, the effect of varying the NH_3 concentration in solutions containing a constant amount of $(NH_4)_2SO_4$ parallels that obtained on varying the NH_4^+ concentration, except that the sensitivity of the rate to NH_3 is considerably lower. Thus about 10 times as much NH_3 is required to produce an effect of comparable magnitude. The limiting rate reached by increasing the NH_3 concentration approximates, for each alloy, that attained with NH_4^+. Inspection of Fig. 5 reveals that, as with NH_4^+, the effect of NH_3 is particularly pronounced for alloys of low gold content.

Effect of oxygen partial pressure.—With each alloy, measurements were made at several O_2 partial pressures ranging from zero to 6.8 at. No corrosion was observed in the absence of O_2. For pure copper the rate increases with the O_2 pressure until about 5 at., above which it remains substantially constant. It has been shown earlier (1) that in this region the transport of O_2 is sufficiently rapid so that the corrosion rate is chemically determined.

Typical of the results which were obtained for the alloys are the rate plots shown in Fig. 6. The rate increased slightly as the O_2 partial pressure was raised from 1.7 to 5.1 at., passed through a maximum, and then fell again as the O_2 pressure was further increased.

Effect of temperature.—The rate of solution of pure copper increases systematically with the temperature corresponding to an apparent activation energy of 5540 cal/mole (1). With the alloys, however, it was found that, while the initial rates followed a similar trend, corrosion rates were soon attained in each experiment which showed an inverse dependence on temperature. This is illustrated in Fig. 7 where rate plots for alloy 2, typical of those obtained for all the alloys, are shown for several temperatures ranging from 15° to 50°C.

Examination of corroded surfaces.—Apart from etching,

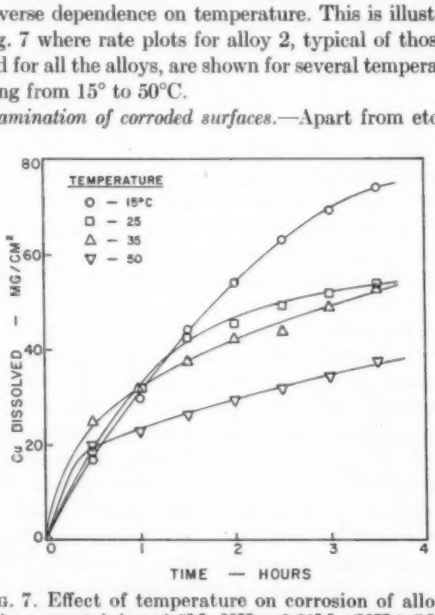

FIG. 7. Effect of temperature on corrosion of alloy 2 in solutions containing 0.5M NH_3, 0.01M $(NH_4)_2SO_4$, 6.8 at. O_2.

no surface changes, i.e., no film formation, could be observed following corrosion of the pure copper specimens. Examination of the alloy specimens generally revealed that corrosion had been accompanied by the formation of a surface film, presumably containing the gold which was left behind as the copper dissolved. In many cases, particularly with the gold-rich alloys, the appearance of the surface left little doubt that a phase rich in metallic gold had been formed.

Microscopic examination of the surface usually revealed complicated film structures which varied considerably with alloy composition and with the conditions of the experiment, but which could not be interpreted or correlated in any conclusive manner. In general, it was noted that the films on alloy 2 were rather more porous than those on alloys of higher gold content and that they tended to become denser and more compact as the corrosion temperature was increased. Often inclusions of very fine black particles were observed in the film. A sufficient quantity of this material could not be isolated for identification, but its appearance suggested that it was an oxide, i.e., CuO or Cu_2O, rather than a metal.

Attempts were made to characterize the film by x-ray diffraction analysis of powdered surface scrapings. However, excessive broadening of the lines precluded any positive identification. Qualitatively, the pattern appeared to resemble that for Cu_2O.

Discussion

With pure copper the reaction has been shown (1) to proceed by essentially chemical attack of NH_3 and NH_4^+ on the metal surface, following rapid chemisorption of oxygen, and resulting in solution of copper as the cuprammine ion. The surface of the corroding metal remains substantially unchanged with no indication of any film formation. Hence, the rate plots are consistently linear.

Judging from the continuity and over-all similarity of the results, it would appear that, initially at least, solution of copper from the alloys proceeds by a similar mechanism. It is clear, however, that as corrosion of the alloy proceeds, a surface film is formed and that, as the film thickens, it impedes to an increasing extent the transport of reactants and products between the reacting metal and solution, thus limiting the rate. In the first instance, at least, this film appears to be associated with the gold or gold-rich metal phase which is left behind as the copper dissolves. These considerations are supported by the observations that corrosion rates of the alloy specimens usually decrease with time and with increasing gold content. The parabolic rate relation which was observed in many of the experiments is characteristic of other corrosion systems in which the rate is determined by transport through a surface film of reaction products which thickens as the reaction proceeds (8).

There is a further strong suggestion both from the kinetic results and from the physical characteristics of the surface films that, in addition to the gold which is left behind, an oxide, probably Cu_2O and/or CuO, may form on the surface of the corroding alloy and that this deposit may also contribute to the film structure and to the slowing of the reaction. Such a deposit might be expected to accompany or result from the formation of the initial gold-rich film skeleton, since the latter would give rise to stagnant solution regions, i.e., in the film pores, protected from the bulk of the solution, which would be deficient in NH_3 and NH_4^+ and in which corrosion products, i.e., Cu^{++}, Cu^+, and OH^-, would tend to accumulate. Such a condition would favor the precipitation of CuO and Cu_2O. This picture is particularly helpful in explaining the results of experiments at very low NH_3 and NH_4^+ concentrations where unusually low corrosion rates were observed for the alloys of low gold content, i.e., alloy 2, despite the fact that the gold films formed were apparently very porous. The very marked effect of increasing the NH_3 and, particularly, the NH_4^+ concentrations on the corrosion rate of these alloys suggests that passivation is largely due to deposited oxides.

Oxide formation is apparently of greatest importance in solutions low in NH_4^+, i.e., those to which no $(NH_4)_2SO_4$ was added. This is understandable in terms of the buffering effect of NH_4^+ in whose presence solution of copper oxides is facilitated by the following reactions:

$$CuO + 2NH_3 + 2NH_4^+ \rightarrow Cu(NH_3)_4^{++} + H_2O \qquad \text{(III)}$$

$$Cu_2O + 2NH_3 + 2NH_4^+ \rightarrow 2Cu(NH_3)_2^+ + H_2O \qquad \text{(IV)}$$

This may explain the insensitiveness of the corrosion rate in such solutions to the gold content of the alloy (*see* Fig. 1 and 2), i.e., the readily formed copper oxide inhibits corrosion even of the low-gold alloys whose porous gold films are not, themselves, protecting. Increasing the gold content of the alloy has little effect since the copper oxide deposit continues to be controlling and may even act physically to prevent the formation of a coherent gold film. The oxide film itself cannot be completely protecting since it dissolves slowly in the ammonia solutions. Hence even the gold-rich alloys, i.e., alloy 15, continue to corrode in solutions containing NH_3 only. The linear regions of the rate plots (*see* Fig. 1) corresponding to the later stages of corrosion of the alloys in such solutions are consistent with a steady-state condition in which a copper oxide film dissolves at the same rate at which it is being restored.

The generally observed increase in corrosion rates of most of the alloys with increasing NH_3 and NH_4^+ concentration, to limiting values, may be due to higher rates of transport of these reactants through the film to the underlying dissolving copper, coupled with a reduced tendency for the precipitation of copper oxides, as suggested earlier. However, ultimately, at high NH_3 and NH_4^+ concentrations, the rate must become controlled by the transport of oxygen or corrosion products through the gold film whose formation is favored under these conditions and whose thickness and permeability should depend inversely on the gold content of the alloy. This corresponds to the region in which a limiting rate, characteristic of the alloy composition, is reached and further increases in the NH_3 and NH_4^+ concentrations are without effect. In this region, transport of oxygen through the film, from the solution to the underlying copper-rich metal, or transport of copper in the opposite direction is presumably rate-controlling. The existence of an analagous region for the corrosion of pure copper, where it has been

shown that transport of oxygen to the metal surface is rate-limiting (1), favors the former alternative.

The fact that the rate passes through a maximum with increasing oxygen pressure and then falls off again can also be explained in these terms. At low oxygen pressures, transport of O_2 either through the film or the solution may be, in whole or part, rate-limiting and, hence, the corrosion rate increases with the O_2 pressure. At the same time depletion of NH_3 and NH_4^+ and accumulation of Cu^{++} and OH^- are enhanced with the resulting formation of a protective copper oxide film. A point thus exists beyond which an increase in oxygen pressure impedes the reaction. This is somewhat analagous to the well-known behavior of iron exposed to neutral or alkaline solutions, where increasing the oxygen concentration may first accelerate corrosion, while a still higher oxygen concentration inhibits it by favoring the formation of a passivating oxide film (9).

The inverse dependence of corrosion rates of the alloys on temperature may be similarly understood. At higher temperatures the precipitation of copper oxides and the formation of denser film structures are both favored. The appearance of the films supports this explanation.

ACKNOWLEDGMENT

Support of this work through a research grant from the National Research Council of Canada is gratefully acknowledged.

Manuscript received September 13, 1955.
Any discussion of this paper will appear in a Discussion Section to be published in the December 1956 JOURNAL.

REFERENCES

1. J. HALPERN, *This Journal*, **100**, 421 (1953).
2. G. A. DEITZ AND J. HALPERN, *J. Metals*, **5**, 1109 (1953).
3. G. TAMMANN, *Z. anorg. u. allgem. Chem.*, **142**, 61 (1925).
4. W. J. MULLER, H. FREISSLER, AND E. PLETTINGER, *Z. Elektrochem.*, **42**, 366 (1936).
5. R. LANDAU AND C. S. OLDACH, *Trans. Electrochem. Soc.*, **81**, 521 (1942).
6. E. B. SANDELL, "Colorimetric Determination of Traces of Metals," p. 204, Interscience Publishers Inc., New York (1950).
7. Reference (6), p. 306.
8. U. R. EVANS, "Metallic Corrosion, Passivity and Protection," pp. 134–147, Edward Arnold & Co., London (1946).
9. E. C. GROESBECK AND L. J. WALDRON, *Proc. Am. Soc. Testing Materials*, **31** Part II, 279 (1931).

Acceleration of the Dissolution of Iron in Sulfuric Acid by Ferric Ions

HARRY C. GATOS[1]

Engineering Research Laboratory, Engineering Department, E. I. du Pont de Nemours and Company, Inc., Wilmington, Delaware

ABSTRACT

The dissolution of iron in H_2SO_4 solutions was studied as a function of Fe^{+++} concentration. In 1*N* H_2SO_4 the dissolution rate (5-hr period) increased at first with Fe^{+++} concentration and then decreased beyond 0.47 Fe^{+++} g ion/l until at 4.00 Fe^{+++} g ions/l, it became approximately equal to the rate in 1*N* H_2SO_4 containing no Fe^{+++}. The hydrogen evolution rate decreased with time and with Fe^{+++} concentration. For a given Fe^{+++} concentration, the dissolution rate decreased, and the hydrogen evolution rate increased with increasing H^+ concentration.

The accelerating effect of Fe^{+++} is due to the direct reduction of the Fe^{+++} to Fe^{++}. Consumption of Fe^{+++} was related to iron dissolution according to Faraday's law. Decrease in hydrogen evolved was considered the result of unfavorable electrode conditions for the reduction of H^+, created by the reduction of Fe^{+++} to Fe^{++}.

INTRODUCTION

In nonoxidizing acids, like dilute H_2SO_4, the dissolution of iron can be described:[2]

$$\text{anodic reaction: } Fe \rightarrow Fe^{++} + 2\epsilon^- \qquad [1]$$

$$\text{cathodic reaction: } 2H^+ + 2\epsilon^- \rightarrow 2[H]_{\text{nascent}} \rightarrow H_2 \qquad [2]$$

Ferric ions in acid media are spontaneously reduced to Fe^{++}, which in turn are quite stable. The thermodynamic stability of the Fe^{+++} and Fe^{++} in acids can be appreciated by the following potential diagram (1):

$$Fe \xrightarrow{E_o = -0.440\text{ v}} Fe^{++} \xrightarrow{E_o = 0.771}$$

$$Fe^{+++} \xrightarrow{E_o > 1.9} FeO_4^-$$

Because of their oxidizing properties, ferric ions accelerate the dissolution of iron in acids. This acceleration constitutes a problem during acid-cleaning operations of ordinary steel equipment bearing ferric oxide scale. In the presence of Fe^{+++}, a number of corrosion inhibitors become ineffective (2).

The accelerating action may be brought about either

[1] Present address: Lincoln Laboratory, Massachusetts Institute of Technology, Lexington, Mass.

[2] All ionic symbols in this paper omit specific reference to solvation.

by the acceleration of reaction [2] as a result of the following reaction:

$$Fe^{+++} + [H] \rightarrow Fe^{++} + H^{+} \quad [3]$$

or by the direct reduction of Fe^{+++}:

$$Fe^{+++} + e^{-} \rightarrow Fe^{++} \quad [4]$$

By combining the anodic reaction [1] and cathodic reaction [4], the following over-all reaction is obtained:

$$Fe + 2\ Fe^{+++} \rightarrow 3\ Fe^{++} \quad [5]$$

Van Name and Hill (3), in studying the dissolution of iron in Fe^{+++} solutions, considered the kinetics of reaction [5] without reference to the electrochemical aspects of the dissolution process.

Alquist, Wasco, and Robinson (2) concluded that in HCl solutions, reactions [3] and [5] take place simultaneously. According to these authors, the fact that the hydrogen evolved during the dissolution of iron is decreased in the presence of Fe^{+++} indicates that reaction [3] takes place; the fact that the presence of Fe^{+++} increases the amount of iron attacked indicates that reaction [5] takes place. Cardwell (4) stated that in Fe-HCl systems reaction [3] prevails.

However, it is quite possible that reaction [4] becomes the main cathodic reaction, and reaction [2] is partially or completely suppressed. In fact, experimental results reported in the present paper show that reaction [4] is primarily responsible for the acceleration of the dissolution of iron in nonoxidizing acid by Fe^{+++}.

Because of the importance of the Fe^{+++} action both from the theoretical and practical points of view, it was felt worth while to investigate quantitatively the role of Fe^{+++} on the dissolution of iron in acids. The present work also concerns the changes in hydrogen evolution which result from the presence of Fe^{+++}.

Experimental

Weight-loss and hydrogen-evolution tests.—The metal was SAE 1030 steel: 0.29% C, 0.37% Mn, 0.04% S, 0.01% P, 0.002% Si, 0.09% Cu, and the balance Fe. Test metal specimens measured 1 x 1.5 x ¼ in. Prior to testing, they were abraded with 120-grit paper, scrubbed with liquid soap, degreased in benzene, and desiccated.

The weight-loss and hydrogen evolution tests were performed in an apparatus consisting of an Erlenmeyer flask and a gas buret with a mercury leveling bulb. One specimen at a time was suspended by a glass rod and was totally immersed in the solution contained in the flask. The solution was 600 ml of 1*N* H_2SO_4, containing the desired amount of Fe^{+++}. Ferric sulfate served as the source of Fe^{+++}. The H_2SO_4 solution was saturated with hydrogen in the apparatus at the test temperature, and the whole apparatus was flushed with hydrogen before immersing the steel specimens. All dissolution experiments were performed at 25°C. The hydrogen evolved was collected in the gas buret. Its volume was corrected to S.T.P. No correction was made for hydrogen entering the steel specimens since it was considered insignificant for the present study.

Determination of Fe^{+++} and Fe^{++}.—The original concentration of the Fe^{+++} was determined volumetrically. Ferric ions were reduced to Fe^{++} in a Jones reductor and then titrated with standard $KMnO_4$. Upon completion of each test, a portion of the 1*N* H_2SO_4 was titrated directly with $KMnO_4$ to determine the total amount of Fe^{++} present. Another aliquot was passed through the Jones reductor, and then titrated with $KMnO_4$. This titration yielded the total amount of Fe^{++} and Fe^{+++} in the acid after the test. The amount of unreduced ferric ions was obtained by subtracting the amount of Fe^{++} from the total amount of iron ions.

Potential measurements.—The potential-measuring apparatus could accommodate six specimens at a time. Each specimen was partially immersed in 250 ml of solution. Both sides of a one-half inch square of the immersed part of the specimen were exposed to the solution. The remaining immersed part of the specimen was electrically insulated with a transparent cement. In order to minimize motion during measurements, specimens were suspended by rigid copper rods mounted on a Lucite plate. Electrical contact between test solutions and the reference electrode was established with agar gel bridges containing small amounts of KNO_3. These led to a saturated KCl solution, in which the capillary tip of a saturated KCl calomel reference electrode was also immersed. All agar bridges were renewed with every run. A *p*H meter with an impedance of 10^{10} to 10^{12} ohms was connected in series with the potentiometer and served as null current indicator. This arrangement yielded very reproducible results.

All electrode potential data have been converted to the standard hydrogen electrode scale.

Dissolution of Iron as a Function of Time in the Presence of Fe^{+++}

Before determining the effect of Fe^{+++} concentration on the dissolution rate of iron in 1*N* H_2SO_4 it was considered necessary to establish the dissolution of iron as a function of time at specific Fe^{+++} concentrations. In the absence of Fe^{+++} the dissolution rate of iron remains constant for at least 45 hr and is equal to 0.33 mg/cm²/hr. Dissolution of iron in $Fe^{+++} - H_2SO_4$ has been reported as a first-order reaction [3]. This was confirmed for 1*N* H_2SO_4 containing 0.042 and 0.416 g ions/l. Reaction constant K_1 is approximately 0.03 cm/sec. It was determined from the following equation describing a first-order reaction involving the dissolution of a metal:

$$K_1 = \frac{2.3\ V}{At} \log \frac{a}{a - n} \quad (I)$$

where V = volume of solution in ml, A = area of metal in cm², t = time in seconds, a = initial amount of Fe^{+++} in oxidation equivalents, and n = amount of Fe^{+++} in oxidation-equivalents reacting in time t. The dissolution rate in the 0.042 and 0.416 g ions/l solutions did not change detectably within 20 and 6 hr, respectively. Results for one concentration are shown in Fig. 1. The presence of moderate amounts of Fe^{++} does not affect the dissolution of iron in acids (5).

Dependence of dissolution rate on time was also reflected in the electrode potential of iron (Fig. 1).

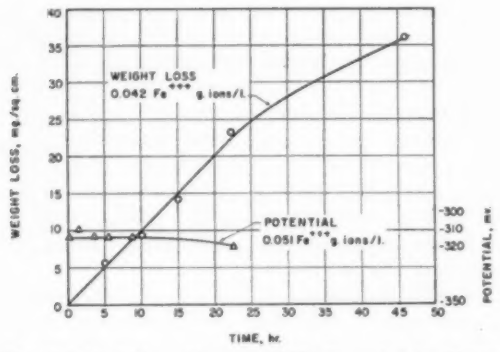

FIG. 1. Dissolution of iron in 1*N* H_2SO_4 containing Fe^{+++}

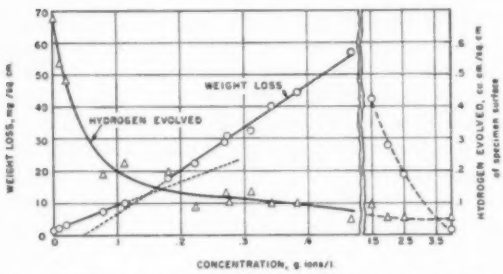

FIG. 2. Dissolution of iron in 1*N* H_2SO_4 containing Fe^{+++}; dissolution time, 5 hr.

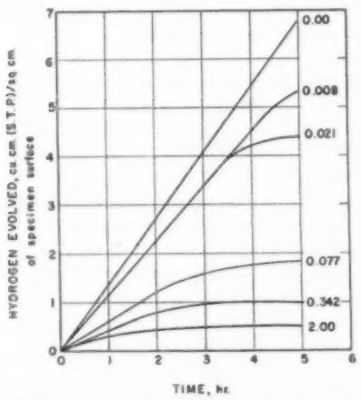

FIG. 3. Hydrogen evolved during dissolution of iron in 1*N* H_2SO_4 containing Fe^{+++}. The concentration of Fe^{+++} is indicated for each curve in g ions/l.

Effect of Fe^{+++} *Concentration on Dissolution of Iron and Evolution of Hydrogen*

On the basis of the results described above, a 5-hr period was chosen for studying this effect. During this period, the dissolution rate remained constant for Fe^{+++} concentrations up to about 0.47 g ions/l and was characteristic of the original concentration of Fe^{+++}. Above 1.5 Fe^{+++} g ions/l, the dissolution rate changed somewhat abnormally with time and approached zero within a few hours. For comparison purposes, however, all dissolution data are expressed in terms of weight loss of iron in mg/cm² of specimen surface/5 hr.

Fig. 2 illustrates the effect of Fe^{+++} concentration on the dissolution of iron at 25°C and on the amount of hydrogen evolved during dissolution. A concentration range up to 4 Fe^{+++} g ions/l was covered. The amount of hydrogen evolved is expressed in cubic centimeters per square centimeter of specimen surface. In this way, errors due to small variations in the size of the specimens are eliminated.

Fig. 2 shows that the weight loss of iron increases with Fe^{+++} concentration up to about 0.47 Fe^{+++} g ions/l in 1*N* H_2SO_4. At this concentration, the weight loss is about 35 times as great as in the absence of Fe^{+++}. Beyond 0.47 Fe^{+++} g ions/l, the weight loss gradually decreases and eventually approaches the weight loss value of iron in 1*N* H_2SO_4 containing no Fe^{+++}.

The hydrogen evolved during the dissolution of iron decreases rapidly at first, and then slowly, with increasing Fe^{+++} concentration (Fig. 2). This represents a twelvefold decrease in the amount of hydrogen at the highest Fe^{+++} concentration employed.

Hydrogen was not evolved at a constant rate during the 5-hr tests, except at zero Fe^{+++} concentration. The amount of hydrogen evolved as a function of time for various Fe^{+++} concentrations is shown in Fig. 3. For any given time, within the 5-hr period, the amount of hydrogen evolved decreases as the Fe^{+++} concentration increases. For a given Fe^{+++} concentration, the amount of hydrogen evolved increases linearly at first with time; then its rate of evolution decreases, and eventually becomes zero. The higher the Fe^{+++} concentration, the sooner the rate of evolution becomes zero. At concentrations higher than those indicated in Fig. 3, the hydrogen evolution stops within a few minutes.

These experiments, plus the fact that the iron dissolution continues even after the hydrogen evolution stops, indicate that reactions [2] and [4] proceed simultaneously at first; reaction [2], however, is gradually suppressed until reaction [4] becomes the principle cathodic reaction.

Reaction [3] most likely does not enter into the dissolution process. If the consumption of Fe^{+++} were due to their reduction by hydrogen, this reduction should proceed with 100% efficiency, while no hydrogen was being evolved. Such efficiency is unlikely under the present experimental conditions. Furthermore, on the basis of the reduction of Fe^{+++} by hydrogen it is difficult to explain why a minimum amount of time is required before the hydrogen is completely consumed as fast as it is generated.

Effect of Fe^{+++} *as a Function of* H^+ *Concentration*

A series of experiments was performed by means of which the effect of a specific concentration of Fe^{+++} was determined in various H_2SO_4 concentrations. The Fe^{+++} concentration chosen was 0.135 g ions/l, with a H_2SO_4 concentration range from 0.25 to 2.0*N*. Both weight-loss and hydrogen-evolution measurements were made. The weight loss of iron decreases slowly with increasing normality of H_2SO_4 (Fig. 4). The effect of H_2SO_4 concentration is in contrast to that observed in the absence of Fe^{+++}; in this case, the weight loss of iron (W, mg/cm²/5 hr)

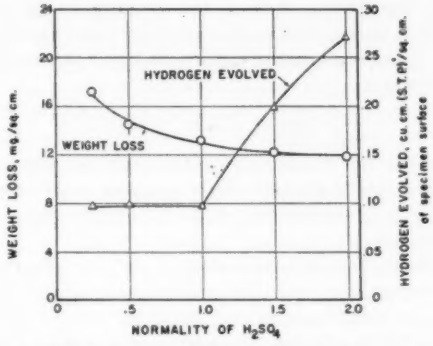
HYDROGEN EVOLVED
WEIGHT LOSS
WEIGHT LOSS, mg./sq. cm.
HYDROGEN EVOLVED, cu. cm. (S.T.P.)/sq. cm. of specimen surface
NORMALITY OF H_2SO_4

FIG. 4. Dissolution of iron in H_2SO_4-solutions containing 0.135 Fe^{+++} g ions/l. Dissolution time, 5 hr.

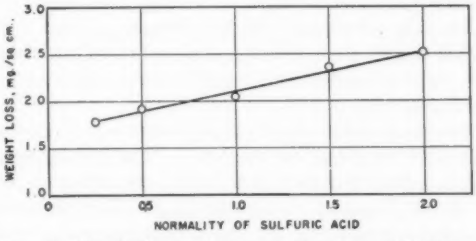

FIG. 5. Dissolution of iron as a function of H_2SO_4 concentration; dissolution time, 5 hr.

increases with the normality of H_2SO_4 (N), as described by equation:

$$W = 2.1\ N^{0.25} \qquad \text{(II)}$$

(*See* Fig. 5).[3] Hydrogen evolved in the presence of Fe^{+++} increases with increasing normality of H_2SO_4, particularly above the value of 1N. The fact that acceleration of Fe^{+++} decreases with hydrogen ion concentration, whereas the amount of hydrogen evolved increases, suggests that the direct reduction of Fe^{+++} (reaction [4]) is gradually suppressed in favor of the direct reduction of H^+ (reaction [2]), which becomes the principle cathodic reaction at about 1N H_2SO_4. These results are consistent with the ones described above, which showed that for a constant hydrogen ion concentration, reaction [2] is gradually suppressed by reaction [4], as the Fe^{+++} concentration increases.

Consumption of Fe^{+++}

By employing the analytical procedures described earlier in this paper, it was possible to determine the consumption of Fe^{+++}, and at the same time confirm the mass balance among the various quantities of Fe^{++} and Fe^{+++} ions involved during the 5-hr dissolution tests.

The results obtained for the tests reported in Fig. 2 up to a concentration of 0.47 Fe^{+++} g ions/l are shown in Table I.

The consumption of Fe^{+++} is plotted in Fig. 6 as a function of Fe^{+++} concentration. It is apparent that this consumption as a function of Fe^{+++} concentration resembles very closely the weight loss of iron as a function of Fe^{+++} concentration, shown in Fig. 4.

[3] The curve must go through the origin.

By calculating the weight loss of iron from the Fe^{+++} consumed on the basis of equation [5], and the weight loss corresponding to the hydrogen evolution (Fig. 2), it was found that the sum of the two weight losses is equal, within experimental error, to the actual weight loss determined gravimetrically, as shown in Table II. The weight loss corresponding to the amount of hydrogen represents a very small fraction of the total weight loss, except at low Fe^{+++} concentrations. Apparently no catalytic effects or side reactions are caused by the presence of Fe^{+++}.

Potential Measurements

The data reported above were supplemented by potential measurements of iron in 1N H_2SO_4, containing 0–2.5 Fe^{+++} g ions/l. Results are shown in Fig. 7. The potentials are the values obtained after the iron was immersed for 2 hr. As a general rule, in all Fe^{+++} concentrations, the potential reached a steady state in less than 2 hr and remained constant for several hours thereafter

TABLE I. *Experimental values for the various quantities of* Fe^{++} *and* Fe^{+++} *involved in dissolution tests*

$(Fe^{+++})_{original}$†	$(Fe^{+++})_{total}$†	$(Fe^{++})_{dissolution}$†	$(Fe^{++})_{Fe^{+++}}$§	$(Fe^{+++})_{unreduced}$§	$(Fe\ ions)_{solution}$†
10*	3	2	2	7	—
21	5	2	2	19	24
77	19	7	13	100	120
113	21	8	14	99	117
180	36	13	23	157	188
221	54	19	35	186	240
269	57	19	37	232	288
274	64	22	42	232	293
311	65	22	43	269	328
342	89	30	59	283	376
383	92	32	61	322	412
467	105	36	69	398	—

* All quantities in this table are expressed in mg ions/l.
† Values obtained directly by titration.
‡ Values obtained from weight loss measurements.
§ Values calculated from first and second columns.

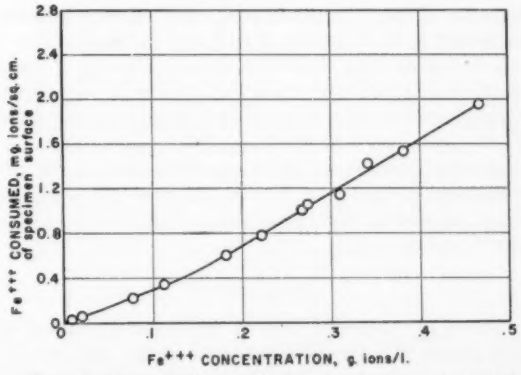

FIG. 6. Consumption of Fe^{+++} by iron in 1N H_2SO_4; time, 5 hr.

TABLE II. *Weight loss of iron in 1N H_2SO_4 containing Fe^{+++}; dissolution time 5 hr*

$(Fe^{+++})_{original}$	$(Fe)_{H_2}$	$(Fe)_{Fe^{+++}}$	$(Fe)_{H_2} + (Fe)_{Fe^{+++}}$	Actual weight loss
g ions/l				
0.010	1.3	1.0	2.3	2.1
0.021	1.2	1.7	2.9	3.2
0.077	0.4	9.6	10.0	7.8
0.113	0.7	9.9	10.6	10.8
0.180	0.5	17.0	17.5	17.7
0.221	0.3	22.6	22.9	23.9
0.270	0.4	28.6	30.0	29.3
0.274	0.3	29.7	30.0	31.1
0.311	0.4	32.0	32.4	32.4
0.342	0.2	40.0	40.2	40.2
0.383	0.2	42.7	42.9	44.3
0.467	0.1	55.0	55.1	57.0

$(Fe)_{H_2}$ = wt loss corresponding to the hydrogen evolved.
$(Fe)_{Fe^{+++}}$ = wt loss due to Fe^{+++} on the basis of equation [5].
Weight loss is expressed in mg/cm² of iron surface.

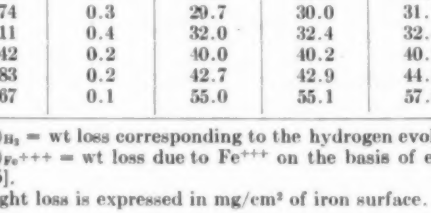

FIG. 7. Potential of iron after 2 hr in 1N H_2SO_4 containing Fe^{+++}.

(Fig. 1). Eventually, it drifted toward the potential of iron in 1N H_2SO_4, containing no Fe^{+++}.

As shown in Fig. 7, the potential of iron shifts toward more cathodic values with increasing Fe^{+++} concentration. At first this shift is rapid (Part A of the curve), then it becomes slow (Part B), then rapid again (Part C), and finally slow (Part D). It is of interest to note that the weight loss of iron and the hydrogen evolution plotted as a function of Fe^{+++} concentration, (Fig. 2) are reflected somewhat in the potential of iron as a function of Fe^{+++} concentration. Thus, Part A of the curve in Fig. 7 corresponds to the rapid decrease in hydrogen evolution; Part B corresponds to the slow decrease in hydrogen evolution; Part C corresponds to the change of the weight-loss function from increasing to decreasing with increasing Fe^{+++} concentration; and Part D corresponds to the relatively sharp decrease of the weight loss of iron with increasing Fe^{+++} concentrations.

Discussion

Nernst (6) suggested that on the boundary surface of two phases the chemical potential varies considerably between neighboring points. As a result, at such surfaces chemical reactions take place at extremely high rates. Thus, the diffusion rate of the reactants to the surface becomes the reaction rate-determining step. According to these views, the reaction rate dm/dt is given by the following equation

$$dm/dt = K(C - C_s) \qquad \text{(III)}$$

where K is the reaction constant, C is the concentration of the reactants in the bulk of the solution, and C_s the concentration in the solution at the boundary surface of the two phases.

These views were supported by Van Name and Hill (3), who stated that metal dissolution processes in many cases are diffusion-controlled, including the dissolution of iron in Fe^{+++} solutions. The latter case was studied by the above authors with Fe^{+++} concentrations below 0.1 g ions/l. They found that the dissolution rate increased linearly with concentration, according to equation (III), which is in agreement with the diffusion control theory. Similar results were recently obtained in HCl containing Fe^{+++} and other depolarizers by Makrides, Komodromos, and Hackerman (7).

The results of the present investigation are in agreement with those of the above authors, i.e., the dissolution rate of iron increases linearly with Fe^{+++} concentration below 0.1 Fe^{+++} g ions/l and in the range of approximately 0.15–0.47 g ions/l (Fig. 2). The slope, however, in the two ranges of concentration is 70 and 130, respectively, in units of Fig. 2. Any stirring effects caused by hydrogen evolution at low Fe^{+++} concentrations should, if anything, increase the slope in this range. Thus, the diffusion control theory alone appears inadequate to explain the dissolution of iron in the presence of Fe^{+++}, particularly when considering concentrations higher than the ranges mentioned above and the hydrogen evolution associated with the dissolution process.

It is believed that the electron transfer from the metal to the H^+ or its hydrated form is preceded by adsorption of these ions on the metal surface. In the presence of Fe^{+++},

TABLE III. *Potential of iron in H_2SO_4 containing 0.135 Fe^{+++} g ions/l*

Normality of H_2SO_4	Potential in v
0.25	−0.266
0.50	−0.268
1.00	−0.272
1.50	−0.272
2.00	−0.276

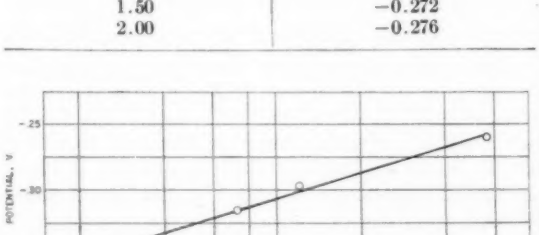

FIG. 8. Potential of iron in 1N H_2SO_4 containing Fe^{+++} as a function of log current density, calculated from weight loss.

both ions compete for the available sites, which are not necessarily restricted to specific areas on the surface. At low Fe^{+++} concentration, both H^+ and Fe^{+++} are adsorbed and subsequently reduced simultaneously (Fig. 2). In this case hydrogen ion reduction contributes appreciably to the dissolution process (Table II) and undoubtedly interferes with the reduction of Fe^{+++}. Hydrogen ions and hydrogen atoms on the surface limit the number of sites available for the reduction of Fe^{+++}. As the concentration of Fe^{+++} increases, the potential shifts toward more positive values (Fig. 7), resulting in a decrease of the hydrogen reduction rate (8). Thus, the interference of the reduction of Fe^{+++} by the hydrogen evolution process decreases as the concentration of Fe^{+++} increases. Above approximately 0.15 g ions/l the reduction of hydrogen is suppressed considerably (Fig. 3), and its contribution to the dissolution process becomes negligible (Table II). Thus, in the range 0.15–0.47 g ions/l the reduction of Fe^{+++} becomes the principal cathodic reaction which is under diffusion control. Below this concentration range it is difficult to define the rate-determining step of the dissolution process, although phenomenologically the dissolution process appears to be under Fe^{+++} diffusion control. The fact that a certain amount of H_2 is evolved in the beginning of the dissolution process, even at high Fe^{+++} concentration, is probably due to the finite time necessary for the cathodic potential shift.

The above views are further supported by the results of Fig. 4, where the interference of the Fe^{+++} reaction by hydrogen ions is demonstrated unambiguously. For a given Fe^{+++} concentration by increasing the hydrogen ion concentration the dissolution rate decreases slowly. In the absence of Fe^{+++}, by increasing the hydrogen ion concentration the dissolution rate increases (Fig. 5). Thus, in Fig. 4 the Fe^{+++} reduction is being suppressed by the increasing hydrogen ion reduction rate. This is consistent with the observed slow shift of the potential toward more anodic values as the hydrogen ion concentration was increased (Table III). The increase of the dissolution rate expected from the increase in the hydrogen reduction rate is masked by the corresponding relatively large decrease due to decrease of the Fe^{+++} reduction rate.

By plotting the potential obtained as described earlier against the logarithm of the current density for Fe^{+++} concentrations up to 0.4 g ions/l, a linear relationship is observed (Fig. 8). Current density was calculated from weight loss and by assuming a roughness factor of 4.0 (7). The equation describing this relationship is:

$$\text{Potential} = -0.3 + 0.06 \log i \qquad \text{(IV)}$$

where i is the current density in ma/cm². The same type of relationship was first observed by Makrides, Komodromos, and Hackerman (7) in the dissolution of iron in hydrochloric acid solutions containing Fe^{+++} and other depolarizers. This plot could be considered as an approximate polarization curve for the anodic reaction (7). The limitations of this approximation are pointed out by the above authors.

Above 0.47 Fe^{+++} g ions/l the dissolution rate (or current density) decreases with increasing Fe^{+++} concentration (Fig. 2) while the potential shifts rapidly toward more cathodic values. In this range the dissolution process obviously ceases to be under diffusion control. If the shift of potential is still indicative of the polarization of the anodic reaction, then in the above Fe^{+++} concentration range there is a rapid polarization of the anodic reaction. No clear explanation can be given for this at present, other than that the potential of iron becomes so noble in these Fe^{+++} concentrations that the anodic reaction becomes the rate-determining step with a high activation energy.

Conclusions

1. The dissolution of iron in H_2SO_4 solutions is greatly accelerated by Fe^{+++} as a result of adsorption and subsequent cathodic reduction of Fe^{+++} to Fe^{++}. It is diffusion controlled only within limited ranges of Fe^{+++} concentration.

2. The accelerating effect of Fe^{+++} follows Faraday's law and is quantitatively expressed by the over-all equation [5].

3. In 1*N* H_2SO_4, the accelerating effect increases with Fe^{+++} concentration up to 0.47 Fe^{+++} g ions/l. It decreases at higher concentration. For a given Fe^{+++} concentration, the accelerating effect decreases slowly with increasing H^+ concentration.

4. The rate of the hydrogen evolution associated with the iron dissolution process decreases with increasing Fe^{+++} concentration, and for a given Fe^{+++} concentration decreases with time.

5. For a given Fe^{+++} concentration, the hydrogen evolution rate increases with increasing H^+ concentration particularly above 1*N*.

6. At high Fe^{+++} concentrations (greater than 0.47 g ions/l), the accelerating effect becomes less pronounced, probably due to polarization of the anodic reaction.

Acknowledgment

The author wishes to express his appreciation to A. M. Madarassy for his skillful assistance and many suggestions during the course of this investigation.

Manuscript received July 27, 1955. This paper was prepared for delivery before the Pittsburgh Meeting, October 9 to 13, 1955.

Any discussion of this paper will appear in a Discussion Section to be published in the December 1956 Journal.

REFERENCES

1. W. M. Latimer, "Oxidation Potentials," 2nd ed., p. 228, Prentice-Hall, Inc., New York (1952).
2. F. N. Alquist, J. L. Wasco, and H. A. Robinson, *Corrosion*, **3**, 482 (1947).
3. R. G. Van Name and D. U. Hill, *Am. J. Sci.*, (4), **42**, 307 (1916).
4. P. H. Cardwell, *Trans. Am. Soc. Mech. Engrs.*, **76**, 47 (1954).
5. H. C. Gatos, *Corrosion*, in press.
6. W. Nernst, *Z. physik. Chem.*, **47**, 52 (1904).
7. A. C. Makrides, N. M. Komodromos, and N. Hackerman, *This Journal*, **102**, 363 (1955).
8. G. Kortüm and J. O'M. Bockris, "Textbook of Electrochemistry," Vol. II, p. 425, Elsevier Publishing Co., New York (1951).

Polymer Synthesis by Gamma Radiation

T. D. Callinan

U. S. Naval Research Laboratory, Washington, D. C.

ABSTRACT

Monomers have been polymerized successfully by the action of gamma rays to high molecular weight solids without the employment of elevated temperatures or catalysts. Among the monomers polymerized were ethylene, styrene, methylstyrene, acrylonitrile, and methyl methacrylate. Low molecular weight polyester syrups have been solidified into hard transparent solids without the use of the usual catalysts and accelerators. Some chemical and physical properties of these polymers have been determined. Observed values are compared with the properties of polymers obtained by thermal and catalytic activation. Radiation energies required for causing polymerization have been determined.

Introduction

The widespread demand for nonpolar, lossless dielectrics presents problems in synthesis which are frequently uneconomical. For example (1), while polyethylene in theory is both nonpolar and almost lossless, the economical production of this item entails the addition of judicious quantities of oxygen to the ethylene, without which low yields and exorbitant temperatures and pressures are encountered. The commercial product, while exceptional electrically and used extensively in pulse cables, possesses a slight but measurable permanent polarity and a moderate molecular weight. The temperature at which this material undergoes fairly sharp softening is 110°C. The molecular weight varies, depending on the conditions of synthesis, from 3000 to 50,000.

The use of catalysts in the polymerization of monomers is widespread, frequently consisting of the addition of benzoyl peroxide or lauryl peroxide, both sources of free radical initiators. It follows that these materials tend to produce polymers having permanent electric moments also. Since not all of the catalyst is used completely, it is often found that with time the reaction continues and changes in the physical, mechanical, and electrical properties occur.

Gamma radiation offers a tool for synthesizing high-melting, cross-linked dielectric solids from simple reagents without the use of adulterants (2). Through this technique the contaminating effect of catalysts is avoided. Where cost is not a factor, it offers a means of producing truly tailor-made dielectrics. Where the use of gamma radiation is economically feasible, it offers still other advantages. For these two reasons this study on polymer synthesis was undertaken.

Monomers have been polymerized successfully by the action of gamma rays to high molecular weight solids without the employment of elevated temperatures or catalysts. In these studies three distinct classes of compounds have been investigated, viz., (*a*) vinyl derivatives, (*b*) polyesters, and (*c*) polysiloxanes.

Experimental

The 2,300-curie source of Cobalt 60 located at the Naval Research Laboratory was employed in these tests. The radiation which emanates from the radioactive cobalt arises from the radiative decay of the metal to a stable isotope of nickel (3). The radioactive cobalt is located at the bottom of the well, under 12 ft of water, to protect personnel against the rays. In the case of reactions induced by the radiation, which happen to be exothermic, the water also acts as a cooling medium; the amount of heat liberated by the source itself is insignificant. The procedure for irradiating materials consists in placing an ampoule or glass container in one or two cells which can be lowered into the radiation field. Mechanisms by which gamma rays transform organic compounds have been described elsewhere in detail (3). Samples of liquids in glass containers were placed in the gamma field and the time required for solidification noted. Dosages were calculated from known field constants (4). No effort was made to exclude air (except in the case of ethylene) from the sample, nor to remove stabilizers incorporated by the producer, nor to control the temperature, since one of the purposes of the work was to determine the immediate feasibility of using gamma radiation under the fewest limitations. The significance of such variables as oxygen content, temperature, and volume is being investigated. Suffice it to say, lower dosages have been found necessary in solidifying large volumes than in converting small quantities of similar reagents. More of the radiationally generated free radicals are quenched at the container walls when small volumes are used. Similarly, lower dosages are needed when lower radiation rates are employed for solidifying equal volumes. This is because the reaction mixture has time, when irradiated slowly, to solidify by conventional means as well as by radiational means. In establishing the constant describing the amount of energy required to solidify a given amount of sample a necessary distinction is between compounds which become increasingly viscous and those which yield precipitates. Thus Type I may be described as polymers which are soluble in the mother liquor and which have as a general effect the increase in viscosity of the liquid being irradiated. Type II polymerizations yield solids which are insoluble in the reagent and, hence, appear as precipitates almost immediately on being introduced into the field. No particular increase in the viscosity of the reagent is noticed.

Calculations of the energy required for solidification involve simply determining the amount of precipitate formed through a unit of dose. In the case of Type I polymerizations the energy required is determined when the entire sample has solidified. Styrene, methyl styrene, methyl acrylate, methyl methacrylate, and 1-vinyl-2-pyrrollidone are typical Type I polymerizations, while ethylene and acrylonitrile form insoluble precipitates and are Type II polymerizations. Each of these syntheses is described and some of the characteristics which have been determined are presented.

Ethylene

A steel cylinder (2 in. in diameter, 14 in. high) containing 112 g of ethylene gas (molecular weight 28.03; melting point −169.4°C; boiling point −104°C; density, 1.245 g/l; purity, 99.94%) at an initial pressure of 1200 psi was placed in gamma fields having an intensity of 5×10^5 r/hr for a period of 72 hr. On removing and opening the cylinder, 14 g (12.5% yield) of a white semifibrous solid was obtained, having the following properties: softening point, 129°C, specific gravity, 0.88; Shore "A" durometer hardness, 45; water absorption after immersion for 24 hr, 0.005%; soluble in chlorinated aliphatic and aromatic compounds at elevated temperatures. The sharpness of the softening point is qualitative evidence for uniformity of molecular weight and freedom from cross-linking. The solid was found to be readily moldable in standard plastic forming equipment at a temperature of 125°C and a pressure of 5000 psi. Under these conditions the material discolored to a deep brown. Pressing at lower temperatures and higher pressures yielded white soap-like products similar in appearance to commercial polyethylene.

Additional syntheses of polyethylene from compressed ethylene gas resulted in yields presented graphically in Fig. 1. It would appear that there is an induction period after which the polymerization proceeds at a satisfactory rate. The reaction is a Type II polymerization.

Methyl Methacrylate

Five grams of commercial methyl methacrylate (mobile, colorless liquid, molecular weight, 100; melting point, −48°C; boiling point, 101°C; specific gravity, 0.940) containing 0.1% benzophenone as a stabilizer were sealed under air in a glass tube (15 × 100 mm) and found to have solidified after being subjected to a total dose of 10×10^6 r gamma.

The product was a clear transparent solid which could be molded at 187°C and 6000 psi, but suffered distortion under mechanical stress at 146°–153°C. This latter is apparently a phase transition similar to that suffered by electron cross-linked polyethylene at 120°C. The solid was found to have the following properties: specific gravity 1.20; Shore "D" durometer hardness, 90; water absorption after immersion for 24 hr, 0.21; solubility, affected by ketones.

Properties of this radiationally prepared polymer are similar to conventional polymethyl methacrylate except that the former has a heat distortion temperature from 16°–23° higher. It is thought that this process might offer a solution to the problem of aircraft canopies distorting at the temperatures arising from aerodynamic heating at high velocities.

Methyl Acrylate

Five grams of commercial methyl acrylate (colorless, mobile liquid, molecular weight 86.05, specific gravity 0.956; boiling point 80.5°C; melting point −75°C) were sealed under air in a glass ampoule (15 × 100 mm) and subjected to 40×10^6 r, whereupon it was removed from the field. The polymerization was Type I, the sample becoming increasingly viscous with time; obviously the sample could have been removed sooner, but the plastic product would have had a lower heat distortion temperature. The particular product obtained was a clear, transparent, colorless elastomer, which became brittle at 10°–20°C but which did not distort without pressure even at 195°C. The material had the following properties: specific gravity, 1.19; Shore "D" durometer hardness, 5; water absorption after immersion for 24 hr, 0.4%; soluble in ketones and chlorinated compounds. This sample was 25% denser than conventional polymethyl acrylate; its mechanical stability at elevated temperatures indicated a high degree of cross-linking.

The properties obtained indicate the versatility and usefulness of radiationally polymerized methyl acrylate both *per se* and in copolymerizations. These latter possibilities are reported under another heading.

Styrene

Ten grams of commercial styrene (colorless liquid, molecular weight 104.06; melting point −31°C; boiling point 146°C; specific gravity, 0.9074) were irradiated under air in a sealed glass ampoule (15 × 100 mm) and removed from the field after receiving 31×10^6 r. The orange-brown clear, transparent solid had a specific gravity of 1.04, distorted at 102°C, possessed a Shore "D" durometer hardness of 85, and absorbed 0.005% water after being immersed for 24 hr. This substance had density and hardness characteristics similar to conventional polystyrene, but differed appreciably in distortion temperature (14°–20°C higher than conventional), absorbed less water, and, on being removed from the gamma field, was colored. On standing at room temperature for 2 months or on being heated to 90°C, the radiationally prepared sample "bleached" appreciably.

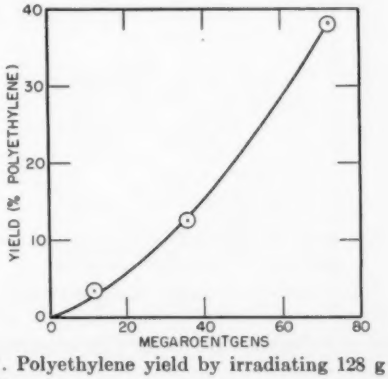

FIG. 1. Polyethylene yield by irradiating 128 g of ethylene gas.

Methyl Styrene

A sample consisting of 146 g of commercial methyl styrene (colorless, liquid; melting point, −131; boiling point, 164; specific gravity 0.88) was irradiated in the presence of air until solid. It had been subjected to 38 × 10^6 r, and the solid product was orange colored, had a specific gravity of 1.30, a heat distortion temperature of 187°C, Shore "D" durometer hardness of 91, and absorbed 0.14% water on being immersed 24 hr. This product was 20% denser than conventional polymethyl styrene and its heat distortion temperature was 40°C higher. On being heated the color of the radiationally prepared polymer "bleached" and approached that of the conventionally colorless polymethyl styrene.

1-Vinyl-2-Pyrrolidone

One hundred and fifty grams of commercial 1-vinyl-2-pyrrolidone were sealed in glass under air and were subjected to 2.2 × 10^6 r of gamma radiation and transformed into a hard, water-dispersible red solid. Considerable heat was evolved during the Type I polymerization. The monomer (colorless liquid, molecular weight 111, boiling point 96_{14} mm°C; specific gravity, 1.07) was transformed into a solid which swells in water, has a specific gravity of 1.51, and a Shore "D" durometer hardness of 75. The density of the material was 20% greater than conventional polyvinylpyrrolidone. The red color faded after 2 months at room temperature or after 2 hr at 135°C, or on being dispersed in water, and a slightly yellow solid was obtained.

TABLE I. *Dosages* for 50–50 copolymers*

	Acrylonitrile	Methyl methacrylate	Styrene	Methyl acrylate
Acrylonitrile	1.2	3.6	6.0	8.0
Methyl methacrylate	3.6	6.0	8.2	9.2
Styrene	6.0	8.2	11.0	19.0
Methyl acrylate	8.0	9.2	19.0	24.0

Relative dosages for 50–50 copolymers*

Acrylonitrile	1	3	5	7
Methyl methacrylate	3	5	7	8
Styrene	5	7	10	16
Methyl acrylate	7	8	16	20

* Megaroentgens at 0.5 mg/hr using 3-g sample.

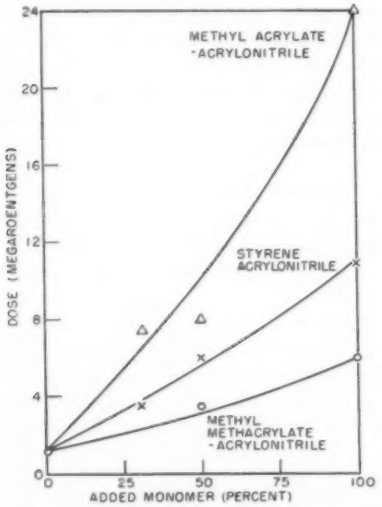

FIG. 2. Polymerization dosages for copolymers

Acrylonitrile

Eight grams of acrylonitrile (straw yellow, mobile water soluble liquid; molecular weight 53.03; melting point −84; boiling point, 77.3; specific gravity 0.80) were converted totally into a white powder on being subjected to 3.1 × 10^6 r of gamma radiation. Considerable heat was evolved during the Type II polymerization and care must be exercised to prevent an explosion occurring. The solid polyacrylonitrile obtained decomposed without melting and was found to be insoluble in common organic solvents. It was very slightly soluble in butyl lactone.

Copolymers

Of the myriad of copolymers conceivable from the monomers studied 50–50 pairs of the following four monomers were prepared and subjected to irradiation, viz., acrylonitrile, methyl methacrylate, styrene, and methyl acrylate. In every case, 3-g samples of each of the mixtures in the presence of air were irradiated at the rate of 5 × 10^5 r/hr and removed on becoming solid. In Table I the dosages in megaroentgens are listed and the relative dosages calculated. In general, it would appear that a Maxwell-type law of mixtures governs the dosages required, the dosages for a 50–50 mixture being intermediate between the dosages required for either of the components

TABLE II. *Copolymers of acrylonitrile*

% Acrylonitrile	% Styrene	Dose	Appearance	Sp gr	Hardness
100	0	1.2	White powder	0.99	90
67	33	4.0	Gray transparent solid	1.13	86
50	50	6.0	Brown transparent plastic	1.25	83
33	67	7.0	Green transparent plastic	1.18	86
0	100	11.0	Straw-colored transparent plastic	1.04	85
% Acrylonitrile	% Methyl methacrylate	Dose	Appearance	Sp gr	Hardness
100	0	1.2	White powder	0.99	90
50	50	3.6	Dark transparent solid	1.37	90
0	100	6.0	Clear transparent plastic	1.20	90
% Acrylonitrile	% Methyl methacrylate	Dose	Appearance	Sp gr	Hardness
100	0	1.02	White powder	0.99	90
70	30	7.5	Two-phase solid; *top:* crepe elastomer, *bottom:* straw-colored transparent plastic	1.25	10/85
30	70	9.5	Green transparent solid	1.39	83
0	100	24.0	Clear transparent solid	1.19	0–10

according to some simple logarithmic relation. This is shown in Fig. 2 where the effect of blending various quantities of more slowly polymerizing monomers on the dosages required for solidifying acrylonitrile is shown. Table II lists some physical qualities of acrylonitrile copolymers showing the variety of characteristics available. In Table III characteristics and dosage requirements of methyl acrylate, styrene, and methyl methacrylate copolymers are listed for those who require transparent plastics.

Casting and Potting Compounds

Samples of commercial polyesters liquids (Paraplex P-43, Laminac 4116, Laminac 4128) were subjected to irradiation and found to be readily convertible into clear hard transparent solids. Such liquids require conversion dosages of 2–4 $\times$ 10^5 r for equal quantities of the monomers previously reported (except vinyl pyrrolidone). The radiationally solidified polyester differs from the conventionally prepared solids in the following ways: they are 10–12% denser, usually have color (yellow-pink), shrink more on curing, and frequently absorb less water on being immersed for 24 hr. Continued irradiation of the polymer after initial solidification has the effect of increasing the hardness, coloration, and heat distortion temperature of the plastic. Thus, 10 g of Paraplex P-43 were solidified after absorbing 3 $\times$ 10^5 r and found to have a heat distortion temperature of 135°C; further irradiation resulting in the polymer receiving a total dose of 10 $\times$ 10^5 r produced a solid having a heat distortion temperature of 146°C, while continued irradiation up to 270 $\times$ 10^5 r gave a final heat distortion temperature of 154°C. The hardness of samples increased slightly during irradiation.

Elastomers

Silicone oils on being subjected to gamma radiation are converted into solid elastomers and products resembling rubber. For this reason the cross-linking and polymerization of polysiloxanes by gamma rays is sometimes referred to as vulcanization. Dosages required to vulcanize some Dow-Corning 200 silicone fluids of different viscosities are shown in Fig. 3. Silicone oils of low molecular weight 300–20,000 on being irradiated have been found to yield clear transparent solids by Type I polymerization. These crumble into soft gels on handling. On the other hand, irradiation of 10 g of silicone oil having an initial molecular weight of 400,000 yields a clear transparent elastomer having a tensile strength of 110 psi, a density of 0.932, a heat distortion temperature of −68°C, and a water absorption value of 0.2% after 24 hr of immersion. By judiciously blending silica (40%) into 10 g of the original oil, and irradiating the sample with 4 $\times$ 10^6 r a semitransparent elastomer having a tensile strength of 1100 psi was obtained.

Another series of elastomers have been prepared by the irradiation of acrylic acid dispersions. Five grams of a commercial 60% solution of acrylic acid in water stabilized with 0.1% beta-naphthol (I) were irradiated and found to solidify after being subjected to 1.1 $\times$ 10^6 r of gamma rays. A known solid elastomer was obtained. It was found that

TABLE III. *Copolymers of methyl acrylate*

% Methyl acrylate	% Styrene	Dose	Appearance	Sp gr	Hardness
100	0	24	Clear transparent elastomer	1.19	0–5
67	33	22	Light-brown semitransparent solid	1.12	90
50	50	19	Light-brown transparent solid	1.06	65
33	67	16	Light-brown transparent solid	1.30	90
0	100	11	Straw-colored transparent solid	1.04	85

% Methyl acrylate	% Methyl methacrylate	Dose	Appearance	Sp gr	Hardness
100	0	24	Clear transparent elastomer	1.19	0–5
50	50	9.2	Straw-colored transparent plastic	1.31	90
0	100	6	Clear transparent plastic	1.20	90

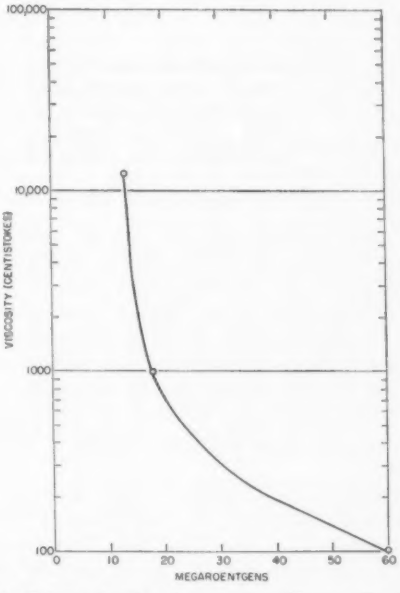

FIG. 3. Polymerization dosages for silicone oils of different viscosities.

dosages of this order 1–4 $\times$ 10^6 r could convert 50–50 mixture of (I) and styrene, acrylonitrile, methyl methacrylate, and methyl acrylate, respectively, into elastomeric bodies.

CONCLUSIONS

It would appear from the results obtained that the irradiation of monomers with gamma rays yields products differing from polymers made by conventional means. In the cases where increased density, heat distortion, or resistance to solvents is desirable, the employment of

gamma rays may be warranted. Where freedom from adulterants and additives is required, gamma radiation techniques are recommended.

Manuscript received September 6, 1955.
Any discussion of this paper will appear in a Discussion Section to be published in the December 1956 JOURNAL.

REFERENCES

1. R. L. WAKEMAN, "The Chemistry of Commercial Plastics," p. 575, Reinhold Publishing Corp., New York (1947).
2. K. H. SUN, *Modern Plastics*, **32**, 141 (1954).
3. T. D. CALLINAN, *Elec. Eng.*, **74**, 510 (1955).
4. H. RABIN AND W. E. PRICE, *Nucleonics*, **13**, 33 (1955).

Preparation of Pure Nickel by Electrolysis of a Chloride Solution

W. A. WESLEY

Research Laboratory, The International Nickel Company, Inc., Bayonne, New Jersey

ABSTRACT

Pure nickel was prepared in the form of malleable electrodeposited sheets as thick as 6 mm from purified nickel chloride-boric acid solution using iridium-platinum alloy anodes. The over-all reaction is

$$NiCl_2 = Ni(metal) + Cl_2(gas)$$

As electrolysis proceeded, purified chloride solution was added automatically to maintain the metal content of the electrolyte. The total of spectrographically detectable impurities is estimated to be about 34 ppm. Carbon content of 26 ppm was reduced to 9 ppm by heating the metal in tank hydrogen and it is believed that any hydrogen, oxygen, and chlorine in the nickel were also substantially reduced by this treatment.

INTRODUCTION

For many research purposes and for spectrographic reference standards, nickel of the highest purity is required in a massive form. The term "high purity" signifies a widely different level of total impurity content when it is applied to different metals. In the present state of the art nickel is considered of high purity if it contains less than about 100 ppm of spectroscopically detectable contaminants. Little information is available on preparations reported to date regarding their content of nonmetallic elements.

A summary of the literature to 1938 on preparation of pure nickel is available (1). No descriptions of preparation of spectrographically pure nickel have been found in the literature since that date. It seems probable that the purest massive metal was prepared by Fink and Rohrman (2) who electrolyzed an impure solution of nickel chloride with a stationary insoluble anode and a cathode rotating at high velocity. First, copper was selectively deposited at a low cathode current density, then iron was removed chemically by oxidation and precipitation with ammonium hydroxide. The electrolyte thus purified was then electrolyzed at a higher current density to give a deposit of nickel on the rotating aluminum cathode from which it was finally stripped mechanically. Purity of the product was assessed only spectrographically because "chemical analytical methods were found inadequate to detect and determine any traces of impurities remaining."

Nickel prepared in this laboratory by the procedure described below has been used as a reference standard and for a wide variety of research purposes over the past fifteen years by more than one hundred research workers in universities, industrial laboratories, and other institutions. No question has been raised by the recipients which would throw doubt on the assumed purity of the metal, namely, a total content of 34 ppm of metallic impurities.

CHOICE OF METHOD

The object was to produce a malleable nickel 6 mm thick and in pieces weighing 1–5 kg each. By analogy with attempts to prepare pure iron it seemed unlikely that any pyrometallurgical or sintering process could be devised which would produce nickel of better than 99.85% purity (1500 ppm impurities) (3). Regardless of how pure the metal could be made in some particulate form it was not believed possible to melt it or otherwise consolidate it to a massive form without contamination, since nickel has a melting point of 1455°C. Such recent developments as levitation melting and drip melting may alter this picture and permit wider choice of methods in the future.

The distillation of nickel chloride in a stream of hydrogen chloride gas, a procedure used in purifying nickel chloride for atomic weight determination, would be cumbersome and hazardous to operate on a larger scale. A nickel carbonyl process would suffer from the same disadvantages. It was concluded that the following procedure was best suited in principle for operation on the desired scale to produce directly a pure malleable nickel.

Commercial nickel refined by the carbonyl process, hence low in cobalt, is dissolved in hydrochloric acid to

form a concentrated solution of nickel chloride. Copper is removed by a hydrogen sulfide treatment. Cobalt, iron, and zinc are removed by treatment with an excess of nickel peroxide. The purified, concentrated nickel chloride solution then serves as the stock to feed an electrolysis cell in which the electrolyte is a more dilute, hot solution of the pure nickel chloride containing boric acid. The latter is added as a buffer to improve physical properties of the deposit. Insoluble iridium-platinum anodes are used with a flat, nonreactive cathode sheet but without a diaphragm of any kind. As electrolysis proceeds the electrolyte becomes depleted in nickel and chlorine in nearly equivalent amounts. These are replaced by addition of the stock purified nickel chloride solution. The *p*H reaches a steady-state value determined by the boric acid content and the fact that the electrolyte is maintained saturated with chlorine by the anode reaction. The net cell reaction is

$$NiCl_2 = Ni(\text{metal}) + Cl_2(\text{gas})$$

Hydrated nickel peroxide was selected as the oxidizing reagent to be used for purification because it combines four necessary properties, namely, it is a noncontaminating reagent which can safely be added to the electrolyte in excess to oxidize iron and cobalt (4), its reduction products are harmless in a nickel plating solution, it raises the *p*H of the solution to assist in removal of iron and zinc, and it is a colloid which can adsorb impurity cations.

Details of Preparations

Preparation of the high purity nickel was carried out three times, first in 1932 when a batch of about 3 kg was prepared, then in 1940 with about 6 kg, and finally in 1952 with 32 kg. Details of only the most recent preparation are given.

Dissolving Mond pellets.—For the 1952 preparation it was necessary to dissolve a large quantity of the impure material, namely, about 50 kg. This was obtained from the Mond Nickel Co., Ltd., in the form of pellets made by the carbonyl process. This metal is the best starting material because it is substantially free from cobalt which is a most difficult impurity to remove. The principal impurities are iron, carbon, copper, and silicon.

It is not as easy to dissolve 50 kg of nickel in a large tank as to dissolve a few kilos in laboratory glassware. The process was accelerated by anodic dissolution in contact with an iridium-platinum electrode, the electrolyte being initially 35 liters of 4.7*N* chemically pure hydrochloric acid. Eventually all the desired nickel was dissolved and 375 liters of nickel chloride solution obtained with the following composition: nickel, 127 g/l; copper, 5.3 mg/l; iron, 37.8 mg/l; cobalt, 1.2 mg/l; manganese, <0.1 mg/l; lead, 0.6 mg/l; zinc, $\ll$5 mg/l; *p*H, 0.3.

Chemical purification.—Sufficient hydrogen sulfide was introduced to precipitate the copper. Copper sulfide was removed by filtration and the excess hydrogen sulfide blown out by a stream of clean air.

A batch of nickel peroxide sufficient to neutralize the acid of the chloride solution was prepared by chilling a solution of 14 kg of C.P. caustic soda in 150 liters of water, chilling this solution to −8°C, dissolving 5.1 kg chlorine gas in it, chilling 46 liters of the nickel chloride solution to 5°C and mixing the two solutions by pumping the hypochlorite solution into the nickel solution with rapid agitation. The black nickel peroxide slime thus formed was filtered, washed, and added to the main tank of nickel chloride solution. The *p*H of the latter rose to 4.5 but, since most of the peroxide had dissolved, a fresh small batch of the black slime was prepared, quickly added to the solution, and then the solution was filtered. This was stored in clean glass carboys. Plant-type equipment was used throughout.

The nickel chloride solution was analyzed spectrographically in direct comparison with a sample of nickel chloride made from the 1940 high purity nickel. The results indicated that the new solution could yield nickel as pure as the earlier laboratory preparation, the only difference in the spectrographic results being the presence of a small amount of sodium and a trace of calcium and magnesium in the large new nickel chloride solution.

Electrodeposition of massive nickel.—A 39-liter Koroseal-lined steel tank was selected to serve as a plating cell in the first run. In later runs a 10-liter Pyrex battery jar of rectangular cross section was used to permit observation of the growing cathode and to correct early any tendency for warping due to unequal current distribution on the cathode surface. The cathode was cut from Inconel or stainless steel (type 316) sheet, 0.8 mm thick, in a rectangular shape which substantially filled the central vertical cross section of the cell. Two anodes of 10% iridium-platinum alloy sheet were suspended at opposite sides of the cell in such a way that any condensed or spattered liquid reaching the outside metal connector or supports could not drip back into the cell. The submerged areas of the anodes gave an effective anode area of 877 cm². Sheets of glass were mounted over the cell to reduce danger of contamination of the solution by falling or wind-blown particles. The cell was set up within a chemical hood to exhaust the chlorine gas evolved at the anodes.

In a typical run the plating cell was filled with the purified nickel chloride solution, diluted to about 2*N*, and sufficient chemically pure boric acid was dissolved in it to provide a concentration of 30 g/l. With the electrolyte at 50°C the cathode was first coated all over, including those portions later to extend above the solution to serve as connectors, with pure nickel to a thickness of one or two hundred microns. The cathode was then mounted exactly midway between the anodes and parallel to them. Separate ammeters were connected to the anodes so that exactly equal currents could be supplied to each side of the cathode and thus prevent warping.

Since 5 or 10 days of uninterrupted electrolysis were required to grow the cathode deposits, automatic control of conditions in the plating cell was desirable. This was made easy by the nature of the over-all cell reaction, namely, the production of almost equivalent quantities of nickel and chlorine at the cathode and anode, respectively. Even though the cathode efficiency was less than 100% the excess anode efficiency simply caused evolution of a little more chlorine from the already saturated electrolyte and the *p*H did not fluctuate much. By arranging a constant-level jar device and filling it with pure nickel chloride solution the latter entered the plating cell at a rate equal to the

TABLE I. *Electrodeposition data*

Run	5-29-52	6-27-52	11-20-52	12-5-52	12-18-52
Plating cell	Koroseal	Koroseal	Pyrex	Pyrex	Pyrex
Capacity, liters	39	39	10	10	10
Cathode area, dm^2	23.4	20.0	12.1	12.1	12.1
Electrolyte					
$NiCl_2$ g/l†	280–140	280–100	100–120	130–80	90–110
H_3BO_3 g/l	30	26–30	34	36	37
*p*H	2.5–3.3	2.4–2.8	2.6–2.7	2.3–2.9	1.7–3.8
Cath. cur. density, amp/dm^2	2.6–3.4	2.5–4.2	3.0	2.6	2.6
Duration, hr	51	220	41	244	242
Approx. cathode efficiency, %	90			80	87
Pure nickel					
No. of pieces	2	2	2	2	2
Weight,* kg	2.7	10.5	1.1	5.4	6.0
Thickness, mm	1.4	6.6	1.0	5.6	6.3
Condition	Warped	Good	Warped	Excellent	Excellent

* Estimated weight after shearing edges and removing starting sheet.
† Roughly estimated from sp gr readings at bath temperatures.

rate of evaporation of water from the electrolyte. Evaporation rate was controlled automatically by regulating the temperature and the rate of deposition of nickel by controlling the electrolysis current. It was thus necessary only to balance temperature and current flow so that nickel chloride was decomposed at exactly the same rate as that at which fresh chloride feed entered the cell.

Quantitative data relating to the several runs are presented in Table I. The total amount of usable metal prepared was about 32 kg. This included an estimated 6 kg of edge scrap which is not in the desired form but is useful for many research purposes.

Purity of Product

The accurate analysis of metals of high purity poses difficulties which require intensive research to overcome.

TABLE II. *Spectrographic examination of high purity nickels*

Element	Amounts in nickel prepared in		
	1932	1940	1952
Al	NF	NF	2–11 ppm
Sb, Ba, Bi, Cr, Co, Ge, Au, In, Ir, Mn, Hg, Mo, Os, Pt, K, Rh, Ru, Sc, Sr, Ta, W, Y	NF	NF	NF
As, B, Pd, Na	NF	VST	VST
Cd, P	NF	NF	
Cs, Ga, La, Li, Nb, Rb, Te, Tl		NF	NF
Fe, Ag	Trace	Trace	Trace
Ca	NF	<1 ppm	<1 ppm
Cu	Present	≪4 ppm	≪4 ppm
Pb	NF	4 ppm	4 ppm
Mg	NF	1 ppm	1 ppm
Re	NF		
Si	NF	NF	2 ppm
Sn	NF	3 ppm	3 ppm
Ti	NF	NF	<1 ppm
V	NF	VST	<1 ppm
Zn	NF	≪1 ppm	≪1 ppm
Zr		<1 ppm	<1 ppm

NF = None found. VST = Very slight trace.

TABLE III. *Results of wet chemical analysis of pure nickels*

Element	Results in 1952		1952 Accuracy	In 1932	In 1940
	12-5-52	12-18-52			
	ppm	*ppm*		*ppm*	*ppm*
Cobalt	5	3	±0.8	3	4
Copper	4	4	±2	8	2
Iron	10	10	±5	5	11

There has not been sufficient need thus far for exact knowledge of the composition of the nickel made here to justify such research. The spectrographic data recorded in Table II represent results obtained in three different decades by different spectrographers. It can be seen that there is little doubt of the absence of metallic impurities except aluminum, cobalt, copper, iron, lead, silicon, and tin. Repeated analyses by standard colorimetric methods in 1932, 1940, and 1953 yielded the data of Table III. Procedures were similar to those approved by the A.S.T.M. (5) and commonly known as the thiocyanate method for iron, the hydrobromic acid method for copper, and the nitroso-R salt method for cobalt. A large sample of 10 or 20 g was taken for each determination. Blanks for aluminum, lead, gold, silicon, and tin were too large in comparison with the amounts of these elements present to permit their determination by standard wet methods.

Nonmetallic impurities.—Of the nonmetallic impurities whose presence might be suspected, other than those included in Table II, there remain carbon, sulfur, oxygen, hydrogen, nitrogen, and chlorine to be considered.

Sulfur could not be detected.

For carbon determinations the greatest care must be exercised to avoid contamination of the sample by particles of steel in the cutting tools and by contact with the fingers or even with wax on the cap of a sample bottle. In addition, the carbon level is low enough that low precision was inevitable with conventional methods. The data of Table IV indicate a carbon level of 20–30 ppm in the nickel in its as-deposited condition. A conductometric method was employed in making these carbon determinations.

TABLE IV. *Removal of carbon from pure nickel by annealing in hydrogen*

Time of heating	Avg carbon content* in ppm ±2	
	12-18-52 nickel	12-5-52 nickel
None	28	24
24 hr	26	15
48	25	15
72	20	15
96	10	8

* As determined by the Laboratory Equipment Co. in their conductometric apparatus for determination of very low carbon values.

It is known that the carbon, oxygen, and hydrogen contents of pure iron can be reduced greatly by merely heating it in undried hydrogen at 400°–500°C to remove surface carbon and then in dry hydrogen at 1100°C to remove oxygen (3). With nickel it should be unnecessary to use dry hydrogen. Accordingly, small pieces of the 12-5-52 nickel and millings of the 12-18-52 nickel were placed on trays of pure nickel and heated in tank hydrogen at 540°C. Each day a portion of the nickel was removed from the furnace and retained for analysis. The data of Table IV show that the carbon content was indeed lowered by the heating treatment.

At present this laboratory is not equipped for vacuum fusion gas analysis and no information is available on the gas content of the pure nickel. By analogy with results published by the National Bureau of Standards for commercial nickel deposited at *p*H 3 from a nickel chloride plating bath (6) there might be as much as 150 ppm oxygen, 10 ppm hydrogen, and 15 ppm chloride in such nickel. It is reasonable to assume that the long treatment of the pure nickel in hot hydrogen reduced its content of these gases below 10 ppm at the same time that the carbon was eliminated. The solubility of hydrogen in nickel at 540°C is probably less than 5 ppm (7).

Probable purity.—Weighing all the evidence in Tables II, III, and IV it can be concluded that nickel can be prepared by the electrolysis of purified nickel chloride on a rather large scale with the following purity:

Metallic impurities		Nonmetallic impurities		
			As-deposited	Annealed
	ppm		ppm	ppm
Al	6			
Co	4	C	26	9
Cu	4			
Fe	10	H*	(10)	(<10)
Pb	4	O*	(150)	(10)
Mg	1	Cl*	(15)	(<10)
Si	2			
Sn	3			
	34			

* Not determined, see text.

Properties of Pure Nickel

As deposited from the chloride solution the nickel was very smooth of surface even at the relatively great thickness of 6 mm. The metal retains high residual internal stresses and these should be reduced by annealing before proceeding with cold forming operations in using it. In some of the individual deposits a lamellar structure occurred which could be detected by the growth of blisters within the metal upon heating. These faults are believed to have been due to occasional accidental interruption in the direct current supply during deposition.

Specimens of the 1932 batch of pure nickel have been employed by workers in a number of laboratories for research purposes. Many of these data were included in a paper by Wise and Schaefer (8). Table V lists significant values for interesting properties of the 1932 nickel.

Acknowledgment

The author wishes to express his thanks to N. B. Pilling for guidance in the earlier preparations, to E. G. Mohling and E. J. Roehl for assistance in the earlier preparations, and to R. G. Lomell, H. B. Canada, and N. E. Gordon for analytical data.

TABLE V. *Properties of the 1932 pure nickel*

	Value communicated	Reference
Lattice constant	3.5168 A.U. at 24.8°C	(9)
Density	8.908 computed from lattice constant	(8)
Avg. coef. of thermal expansion	10.22×10^{-6}/°C at −180 to 0°C	(8)
	13.3×10^{-6} 0 to 100	
	14.63×10^{-6} 0 to 300	
	15.45×10^{-6} 0 to 500	
Thermal diffusivity	0.15885 ± .00009 cm²/sec at 25°C	(10)
Thermal conductivity	0.618 watt/cm °C at 25°C	(10)
Electrical resistivity	6.141 microhm cm at 0°C	(8)
	6.844 microhm cm at 20°C	
Temp. coef. of electrical resistivity	0.00682/°C at 0 to 100°C	(8)
	0.00692 (vacuum annealed)	
Coercive force	2.73 oersteds	(8)
Tensile strength	Annealed: 46,000 psi	(8)
Yield strength	0.2% offset; annealed 8,500 psi	(8)
Recrystallization temperature	After cold rolling 50%: 370°C	(8)

Manuscript received September 30, 1955. This paper was prepared for delivery before the Pittsburgh Meeting, October 9 to 13, 1955.

Any discussion of this paper will appear in a Discussion Section to be published in the December 1956 JOURNAL.

REFERENCES

1. A. E. VAN ARKEL, "Reine Metalle," p. 349, Julius Springer, Berlin (1939).
2. C. G. FINK AND F. A. ROHRMAN, *Trans. Am. Electrochem. Soc.*, **58**, 403 (1930); **59**, 359 (1931).
3. G. A. MOORE, *Trans. Am. Inst. Mining Met. Engrs.*, **197**, 1443 (1953).
4. R. L. SUHL, J. W. SANDS, AND O. B. J. FRASER, Canadian Pat. 264,172, Sept. 7, 1926.
5. "A.S.T.M. Methods of Chemical Analysis," American Society for Testing Materials, Philadelphia (1950).
6. V. ZENTNER, A. BRENNER, AND C. W. JENNINGS, *Plating*, **39**, 865 (1952).
7. C. J. SMITHELLS, "Metals Reference Book," Vol. 2, p. 535, New York (1955).
8. E. M. WISE AND R. H. SCHAEFER, *Metals & Alloys*, **16**, 424 (1942).
9. E. R. JETTE AND F. J. FOOTE, *J. Chem. Phys.*, **3**, 605 (1935).
10. C. STARR, *Rev. Sci. Inst.*, **8**, 61 (1937).

Determination of the Activity of Sodium in Sodium-Lead Alloys at High Temperatures

BERNARD PORTER AND MORRIS FEINLEIB

Chemical Research Department, Kaiser Aluminum & Chemical Corporation, Permanente, California

ABSTRACT

The activity of sodium in sodium-lead alloys was determined by the concentration cell method. The emf of cells

$$\text{Na (pure)}/\text{Na}^+/\text{Na in Pb}$$

was directly measured up to 820°C, using alumina containers impregnated with Na_2CO_3 in an argon atmosphere. Results were converted to activities and extrapolated to 1010°C. To check the extrapolation, emf's of cells of the type

$$\text{Na}(a_1) \text{ in Pb}/\text{Na}^+/\text{Na}(a_2) \text{ in Pb}$$

were measured up to 1010°C The a_2/a_1 ratios calculated from the measurements were compared with those obtained by extrapolation. Fair agreement was found.

INTRODUCTION

In connection with a study of sodium-aluminum equilibria (1) it was necessary to determine the activity of sodium in various sodium-lead alloys at temperatures up to 1010°C. Few published data are available on the activity of sodium in sodium-lead alloys at elevated temperatures. Hauffe and Vierk (2) determined these activities at temperatures ranging from 425° to 475°C. They measured the emf of cells consisting of pure sodium on one hand and various sodium-lead alloys on the other.

The activity of sodium in the alloy was obtained from the Nernst equation:

$$E = \frac{RT}{n\mathbf{F}} \ln \frac{a_{\text{Na(Pb)}}}{a_{\text{Na(pure)}}} = 1.984 \times 10^{-4} T \log a_{\text{Na(Pb)}} \qquad \text{(I)}$$

since the activity of pure sodium is unity at any temperature. E is expressed in volts and T in °K. Wide departures from ideal solutions were observed.

In Hauffe and Vierk's studies, the pure sodium and the alloys were contained in sodium glass, which also furnished the electrolytic path between the two half-cells. At higher temperatures, glass is not suitable, as it was necessary to find a material that would not react with sodium or lead, yet would provide an electrolytic path for sodium ions.

EXPERIMENTAL

The cell material selected was fused-cast alumina Monofrax MH (Carborundum Co.). It is 99+% alumina, and contains sodium aluminate. In order to insure a good electrolytic path for Na^+ and to reduce the possibility of Na^+ concentration gradients, the cells were impregnated by fusing anhydrous Na_2CO_3 in the cell cavities for several hours at 1000°C.

Cells (Fig. 1) were fabricated from Monofrax MH bricks as follows: a block of the desired size was cut with a diamond saw and was carefully examined to make sure that no large blowholes were present. Block dimensions were approximately 3 in. high x 2⅛ in. long x 1⅛ in. wide, but were not critical. A slot was next cut down the center of the block, to within about ¾ in. to 1 in. of the bottom. Two ½ in. D. cavities were then drilled with a diamond core drill to a depth of about 1½ in.; a 3/16 in. D. thermocouple hole was also drilled in one side. The blocks were oven-dried, then impregnated as mentioned above.

In order to get reliable emf data, it is necessary that the sodium concentration should remain constant throughout a run. This can only be accomplished in a sealed chamber, in which the liquid sodium or alloy is in equilibrium with sodium vapor, with no chance of vapor escape. This

becomes especially important at the elevated temperatures of these experiments, where sodium has a high vapor pressure (its boiling point is 880°–890°C).

In order to provide an electrical connection to the liquid metals and to seal the cell cavities, metal caps were used. The caps need only withstand the action of sodium vapor, and therefore were made of mild steel. Since the thermal expansion coefficient of steel is considerably higher than that of alumina, the caps had to be machined undersize, so that, at the highest temperature of a given run, they would just seal the cavity. Experience showed that sufficient Na_2O was present so that, once the cavities were sealed at a high temperature, the seal remained intact upon cooling.

The electrical lead-in wire had to withstand the action of both lead and sodium up to 1000°C; molybdenum was chosen as one of the few suitable metals. (Graphite was unsuitable because of carbide reactions with sodium.) Since molybdenum wire becomes brittle when welded, it was joined to the cap as illustrated in Fig. 1. A small hole was drilled through the cap, and the wire inserted through this hole and welded at the top of the cap, so as to completely seal the hole at the same time. Thus the cap itself furnished protection against bending of the wire. A Nichrome wire was also welded to the outside of the cap for connection to a potentiometer.

In view of the ease with which sodium is oxidized, the experiments were run in an inert atmosphere. This was most readily accomplished in a vacuum apparatus provided with electrical connections and a furnace.

A typical run was carried out as follows.

Sodium and lead were weighed out in approximately the desired proportions and placed in one cavity; pure sodium was placed inside the other cavity. The caps were inserted, and the cell positioned inside the furnace. An Inconel thermocouple protection tube was inserted into the thermocouple well in the Monofrax block, and a thermocouple put inside the tube. The fused-cast alumina is a fair conductor of heat and will reach a uniform temperature rather fast; therefore, by locating the well within the block itself, a representative measurement of cell temperature could be achieved.

Next, all thermocouple and electrical connections were completed. The vacuum apparatus was closed and pumped down to approximately 150 μ. Argon was then led into the vacuum chamber until the pressure approached atmospheric. The chamber was again evacuated to about 150 μ while the temperature was raised to approximately 200°C. The apparatus was refilled with argon to almost atmospheric pressure. The temperature was then raised to the maximum level at which measurements were to be taken. With pure sodium in one of the cell cavities, this maximum temperature usually did not exceed 820°C. After temperature equilibrium was attained, emf readings were taken every two minutes until a steady value was observed. A Beckman battery-operated pH meter with a millivolt scale was used for measuring the potentials.

After a minimum of 6 steady emf readings were obtained at the highest temperature, the temperature was dropped in a number of steps, holding it at each level until thermal and emf equilibrium was attained. After the last reading, the system was allowed to cool to room temperature in argon.

The cell was removed from the chamber and the alloy compartment opened; the seal was usually so strong that considerable force was required to break it. A ½ in. drill was first used to remove the top portion of the alloy and thus avoid possible contamination of samples with Na_2O. A smaller drill was then used to get turnings from several spots in the remaining alloy for sodium analysis. In the case of high-sodium alloys, samples had to be taken and weighed rapidly to avoid air oxidation and moisture pickup. Sodium analyses were performed with a Beckman DU spectrophotometer, using a flame photometer attachment.

It is important to point out that all of this work is based on the assumption that the alloy composition does not change from the time the first emf readings are taken at the highest temperature till the end of the run. When the cap sealing was satisfactory, there is good reason to believe that the assumption was justified. If sealing was not adequate, it was not usually possible to get steady emf readings at a given temperature, and such runs were discarded.

It was mentioned above that, with pure sodium in one of the cavities, the highest practical temperature level was 820°C. Since it was necessary to know the values of sodium activity in lead alloys at temperatures ranging from 940°C to 1040°C, an extrapolation of the measured activities to these temperatures had to be made (*see* later). As a check on the validity of this extrapolation, it was decided to run a few concentration cells at temperatures up to 1010°C, using a high-sodium-lead alloy in one compartment and a lower sodium alloy in the other. Except for the temperature range, the procedure was as already described. In the case of double-alloy cells, both compartments were analyzed for sodium.

In a double-alloy cell, the Nernst equation relating sodium activities and emf's becomes:

$$E = 1.984 \times 10^{-4} T \log \frac{a_{1\,\mathrm{Na(Pb)}}}{a_{2\,\mathrm{Na(Pb)}}} \qquad \text{(II)}$$

where a_2 is the high-sodium alloy activity and a_1 that of the lower sodium alloy. Activity ratios obtained from these direct measurements were compared with those taken from extrapolated activity-concentration curves.

Results and Discussion

Results of a typical activity determination are given in Table I and for several runs in Fig. 2. The activity of sodium vs. temperature at a given concentration is almost linear on a semi-log scale, and therefore is most readily extrapolated.

The curve of limiting activity

$$a_L = \frac{1}{p^0} \qquad \text{(III)}$$

where p^0 is the vapor pressure of pure sodium, has also been plotted (Fig. 2) to show the limits beyond which the extrapolation cannot be used when working at atmospheric pressure. Fig. 3 shows the variation of sodium activity

TABLE I. *Activity of sodium in a sodium-lead alloy**

Temp		emf† mv	a = sodium activity	γ = activity coefficient
°C	°K			
827	1100	389	16.5×10^{-3}	7.78×10^{-2}
798	1071	393	14.2×10^{-3}	6.70×10^{-2}
763	1031	398	11.6×10^{-3}	5.47×10^{-2}
730	1003	400	9.77×10^{-3}	4.61×10^{-2}
695	968	405	7.78×10^{-3}	3.67×10^{-2}
664	937	408	6.38×10^{-3}	3.01×10^{-2}
622	895	409	4.98×10^{-3}	2.35×10^{-2}
552	825	409	3.17×10^{-3}	1.50×10^{-2}
502	775	404	2.36×10^{-3}	1.11×10^{-2}

* Wt % Na in Pb = 2.90 (N_{Na} = 0.212).
† Emf of pure sodium against the above alloy.

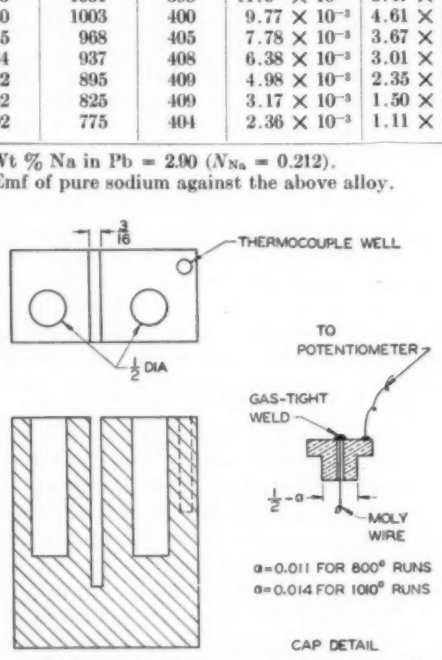

FIG. 1. Cell for the determination of sodium activity in sodium-lead alloys.

with its mole fraction in sodium-lead alloys at various temperature levels.

Fig. 2 and 3 show that the precision of the activity determinations and extrapolations is limited. In Fig. 3 there is a considerable scattering of measured activity values; this becomes even more serious for extrapolated values.

Measurement errors can account for some of the inaccuracy. The potentiometer used in the emf measurements could be read to ±1 mv, causing an uncertainty in the activity of ±1.3%. A temperature error of 1°C causes a

TABLE II. *Double-alloy cells; comparison of directly measured and calculated activity ratios*

Pb-Na alloy composition	Temp	a_2/a_1 from Fig. 3	a_2/a_1 from emf (meas)	% difference = $\left(\frac{\text{meas.} - \text{calc.}}{\text{meas.}} \times 100\right)$
	°C			
$N_1 = 0.171$	1008	2.80	2.97	+5.7
$N_2 = 0.301$	970	2.84	3.01	+5.7
	938	2.85	3.01	+5.3
	898	2.91	2.92	+0.5
	806	3.04	3.09	+1.6
	706	3.12	2.98	−4.7
	608	3.10	2.94	−5.5
$N_1 = 0.222$	1010	3.31	3.58	+7.5
$N_2 = 0.371$	968	3.41	3.78	+9.8
	936	3.41	3.84	+11.1
	894	3.42	3.75	+8.8
	801	3.67	3.90	+5.9
	700	3.84	3.99	+3.8
	597	3.80	4.01	+5.3

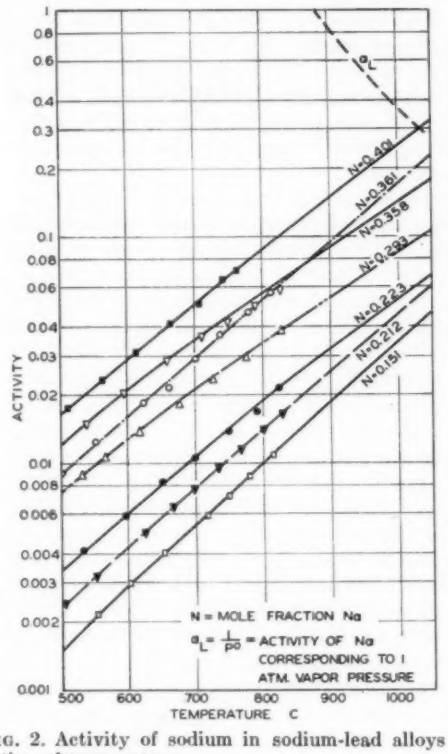

FIG. 2. Activity of sodium in sodium-lead alloys as a function of temperature.

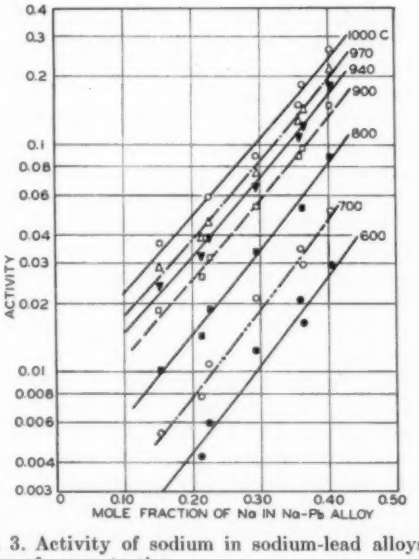

FIG. 3. Activity of sodium in sodium-lead alloys as a function of concentration.

change of 0.5% in the activity. Sodium analyses are no better than ±2% of the sodium concentration, causing a corresponding error in the mole fraction values used in Fig. 3.

A major source of error could be the establishment of metallic or electronic paths between the two cell compartments, either on top between the caps, or within the cell material itself. This was the reason for cutting the slot between the cell compartments (Fig. 1); such a slot breaks up the continuity of the top surface and at the same time lengthens the electrolytic path between the two half-cells.

Finally, whereas the assumption of constant alloy composition during a run appears to be justified, there is no way of making certain of this, other than observing the constancy of potential readings at each temperature and checking each cell at the end of the runs for cracks, etc.

To test extrapolated activity values, two double-alloy cells were run as previously described. The results of these runs were taken into account in determining the best line to draw through the extrapolated points plotted in Fig. 3.

A comparison of activity ratios calculated from double-alloy cell measurements and those taken from Fig. 3 is given in Table II.

In view of the experimental difficulties and the assumptions involved, it may be stated that the agreement between measured and extrapolated values is acceptable, and that the extrapolation of activity measurements of sodium-lead alloys against pure sodium is on the whole justified.

ACKNOWLEDGMENT

The authors wish to acknowledge the help of J. I. Davis in carrying out the laboratory work. Analytical determinations were performed by K. Lincoln and J. Winkler. The machine work was carried out by K. I. Booth and T. G. Glassey.

Manuscript received September 15, 1955. This paper was prepared for delivery before the Cincinnati Meeting, May 1 to 5, 1955.

Any discussion of this paper will appear in a Discussion Section to be published in the December 1956 JOURNAL.

REFERENCES

1. M. FEINLEIB AND B. PORTER, *This Journal*, **103**, 232 (1956).
2. K. HAUFFE AND A. L. VIERK, *Z. Elektrochem.*, **53**, 151 (1949).

Electrochemical Characteristics of Melts in the Sb-Sb_2S_3 System

TSUTOMU YANAGASE[1] AND GERHARD DERGE

Carnegie Institute of Technology, Pittsburgh, Pennsylvania

ABSTRACT

Liquid Sb and Sb_2S_3 were equilibrated at various temperatures and electrolyzed with the metal phase as anode and the sulfide phase as cathode. Current efficiencies varied below 60% and analysis of the data indicated that the balance of the current should be accounted for by the electronic character of the melt rather than losses or side reactions. This was confirmed by direct measurement of the conductivity of the melt as a function of its composition.

INTRODUCTION

The electrical conduction of molten copper sulfide, iron sulfide, and their mixtures has been shown to be electronic in character (1). Therefore, it was of interest to investigate in detail the electrical properties of molten antimony sulfide (Sb_2S_3) since early electrolysis experiments (2) indicated it has some ionic character even though current efficiencies were too low to be of commercial interest. The ionic character of solid Sb_2S_3 was also demonstrated by electrolysis (3).

Preliminary experiments showed measurable changes in composition of the anode and cathode compartments after electrolysis of molten Sb_2S_3 in a simple Vycor H-cell with graphite electrodes. Free sulfur was also observed at the anode. This confirmed the reported presence of ions in the melt. It was evident that a useful study of the system would require a more elaborate cell and control of the experimental variables. This is due chiefly to the mutual solubility of the liquid metal and sulfide phases as shown in Fig. 1. In order to measure the current efficiency for deposition of metal at the cathode, it would be necessary to have the sulfide electrolyte previously saturated with metal at the temperatures of electrolysis. The cell and the experiments developed for this study will now be described.

[1] Present address: Department of Metallurgy, Kyushu University, Fukuoka, Japan.

EXPERIMENTAL PROCEDURE

Molten antimony metal was used as the anode in order to prevent the formation of free sulfur (as observed at an inert graphite anode) which might in turn react with the metal deposited at the cathode. The electrolyte should be

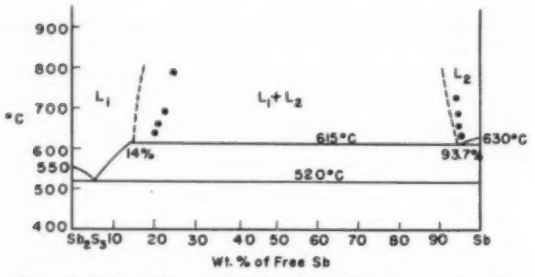

FIG. 1. Phase diagram of the Sb-Sb_2S_3 system, based on the diagram of Hansen (4) for the Sb-S system. ● = Data from this research.

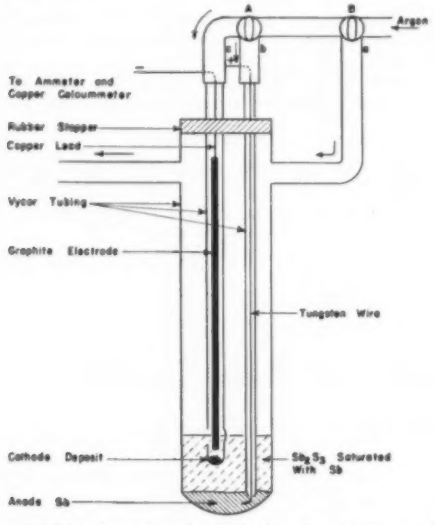

FIG. 2. Cell for the electrolysis of molten antimony sulfide.

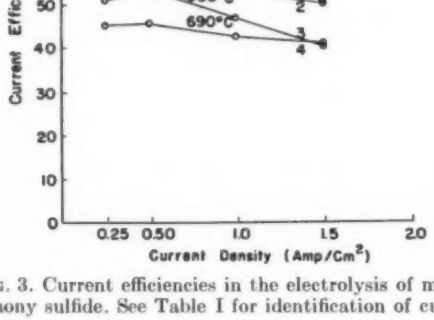

FIG. 3. Current efficiencies in the electrolysis of molten antimony sulfide. See Table I for identification of curves.

saturated with metal previously so that all antimony formed as a result of cathode reaction can be collected and weighed. These and related considerations form the basis for the cell and technique.

The cell is shown in Fig. 2. It is constructed of Vycor, connected to the Pyrex stopcock system A and B so that argon can be introduced as the cell atmosphere or bubbled through the anode holder to provide stirring. The cathode consisted of a graphite electrode in a perforated chamber which collected the liquid antimony deposit as formed. Other features become evident in the description of the procedure. The antimony metal was C.P. grade and the Sb_2S_3 was Fisher, Technical.

The liquid metal and sulfide phases were presaturated in a similar cell without electrical connections by bubbling argon for 3 hr at selected temperatures.

The Vycor cell, with electrodes elevated, was charged with 30 g of Sb_2S_3 and 15 g of Sb, previously equilibrated as above, and the charge melted under argon.

The anode tube was lowered into the melt and argon bubbled at constant temperature for 1 hr in order to insure equilibrium between phases. The bubbling was stopped for 15 min to allow Sb droplets to settle from the sulfide layer.

The cathode tube (*c*) was then lowered into the melt with argon flowing through it to maintain the neutral atmosphere. Electrolysis was started and the amount of current measured by a copper coulometer connected in series.

The cathode tube was raised out of the cell and cooled rapidly with an air blast. The metal button was separated and weighed.

The current efficiency was calculated on the assumption that all ions discharged were Sb^{+3}.

The results of such experiments in the temperature range 635°–690°C, with current densities increasing to 1.5 amp/cm², are shown in Fig. 3 and listed in Table I. They show that the current efficiency decreases with increasing current density and higher temperature. Since the melting point of antimony is 630°C, the curve for 635°C represents the limiting temperature for these experiments. The points at 0.25 amp/cm² are believed to be the least reliable because only a small amount of metal was deposited and

TABLE I. *The electrolysis of molten* Sb_2S_3

Run No. in Fig. 3	Temp.	Current density	Volt	Time	Cathode deposit	Current efficiency	Remarks
	°C	amp/cm²		min	g	%	
1	635	0.25	1.0	120	0.4075	53.3	
	635	0.5	1.7	90	0.6400	56.6	
	635	1.0	2.8	60	0.8086	53.5	
	635	1.5	3.8	40	0.7648	50.6	
2	635	0.25	1.0	120	0.4234	53.3	Bubbling
	635	0.5	2.2	90	0.6300	55.7	during
	635	1.0	2.6	60	0.7992	52.9	elec-
	635	1.45	3.5	60	1.0942	50.0	trolysis
3	660	0.25	0.6	120	0.3740	51.1	
	660	0.48	1.3	90	0.5816	53.3	
	660	1.0	2.2	60	0.7014	46.6	
	660	1.5	2.7	40	0.6050	40.0	
4	690	0.25	0.8	120	0.3530	45.1	
	690	0.5	0.9	90	0.5105	45.2	
	690	1.0	1.6	60	0.6414	42.4	
	690	1.5	2.0	40	0.6200	41.0	

all measurements involved high percentage error. If these are ignored, and the data extrapolated to zero current density it would seem that, even under optimum conditions, the maximum attainable current efficiency is only about 60%. In order to understand the reasons for this low value a number of factors have been considered.

Several possible sources of error in the experiment were considered. The data for curve 2 of Fig. 3 were obtained by bubbling argon continuously during the electrolysis. In other cases this procedure gave erratic results due to disturbance of the metal-sulfide interface and it was not generally used, but it is believed that the evidence at hand is sufficient to show that failure of the liquids to remain saturated was not a source of serious error.

The possibility of loss of antimony from the cathode by vaporization during electrolysis was checked by blanks with 1 g of metal in the cathode chamber. The maximum loss observed was 0.5% of the metal after 1 hr at 690°C. This is negligible in comparison to the changes observed during electrolysis.

Analysis of the cathode metal button showed that it contained from 2–4% Sb_2S_3, or less than 1%S, which is less than the equilibrium solubility of Fig. 1 and is too small to be important.

The presence of Sb^{+5} in the system could account for the observed low current efficiencies. However, this does not seem likely in the presence of metallic antimony for the reaction:

$$2Sb + 3Sb^{+5} \rightleftarrows 5Sb^{+3}$$

will not only prevent the formation of appreciable amounts of the pentavalent ion, but will become more effective with increase in temperature. This is contrary to the trend of current efficiency.

Since the sources of experimental error did not appear to be great, it was desirable to seek another explanation for the low observed current efficiencies by examining the electrical characteristics of the molten sulfide through direct measurement of conductivity as influenced by the dissolved metal, according to Fig. 1. It might be expected that a part of the conductance is by an electronic mechanism.

Influence of Dissolved Antimony on the Electrical Conductivity of Molten Antimony Sulfide

Conductivity measurements were made with the four terminal cell, a-c potentiometer circuit developed and described in connection with studies of other sulfide systems (1). Sulfides were prepared with varying amounts of dissolved antimony by equilibrating the sulfide and metal at various temperatures as already described for the electrolysis experiments. After equilibration the sulfide layer was separated and its conductivity measured. The analyses of both layers are shown in Table II for identification in connection with the conductivity data. These analyses are also plotted as solid points on Fig. 1 since they define the two-liquid region of this system, which has previously been uncertain, as indicated by the dashed lines of Fig. 1. Conductivity data are plotted as a function of temperature in Fig. 4 where it is evident that the conductivity of the system is very sensitive to small amounts of dissolved metal. For all compositions measured, the positive temperature coefficient of conductivity is large and the specific conductance is above 5 $\Omega^{-1}cm^{-1}$ at temperature above 800°C. These high values certainly indicate that a large part of the conductance in this system must be electronic.

TABLE II. *Analysis of sulfide and metal equilibrated at various temperatures*

Run No. in Fig. 4	Temp	Metal layer		Sulfide layer	
		%S	%Sb_2S_3 (calcd.)	%S	%Sb† (calcd.)
	°C				
1	635	1.46	5.2	22.5	21
—	660	1.52	5.4	22.4	21.5
2	690	1.65	5.9	22.0	22
3	735	1.76	6.2	21.7	23
4	790	1.27 (?)	—	21.3	24
5*	—	—	—	24.6	12.8

* Prepared by fusion of C.P. grade Sb_2S_3 powder. Sulfur loss observed.

† Sb in excess of that required for Sb_2S_3.

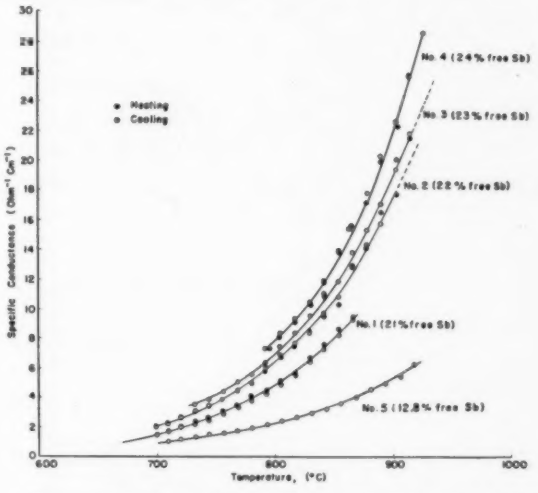

FIG. 4. Specific conductance of antimony sulfide with dissolved antimony. See Table II for complete identification of melts. Curve No. 1, 21% dissolved Sb; curve No. 2, 22% dissolved Sb; curve No. 3, 23% dissolved Sb; curve No. 4, 24% dissolved Sb; curve No. 5, 12.8% dissolved Sb.

Discussion

The electrolysis of molten antimony sulfide is characterized by low current efficiencies (never observed to exceed 60%) even when the experiment is carefully controlled to remove disturbing side reactions by the use of sulfide saturated antimony anode and antimony saturated sulfide electrolyte. This is attributed to the fact that the solution of antimony in the Sb_2S_3 causes an increasing amount of electronic conduction in the electrolyte. This is demonstrated by measurements of conductivity, showing that it increases with dissolved antimony and with temperature and exceeds the magnitude normally associated with simple ionic conduction. This explanation of the observed data is preferred by the authors as it cor-

relates with the major controlled changes in the system and the known behavior of other sulfides. It is of course possible that unknown impurities could be partially responsible, but there is no compelling reason for not accepting the more direct explanation.

Although not directly related to the electrolysis of antimony sulfide, the conductivity of the metal layer equilibrated with sulfide at 790°C was also measured. It is interesting to note that, unlike pure metal, this has a slight positive temperature coefficient, increasing from about 9200 $\Omega^{-1}cm^{-1}$ at 800°C to about 9300 $\Omega^{-1}cm^{-1}$ at 900°C.

Acknowledgments

The authors appreciate helpful discussions of this work with Drs. G. M. Pound, M. Simnad, L. Yang, and M. Bourgon and the analytical assistance of N. A. Mooney.

The work was done under Contract No. AT(30-1)-1024 with the United States Atomic Energy Commission.

Manuscript received August 1, 1955. This paper was prepared for delivery before the Cincinnati Meeting, May 1 to 5, 1955.

Any discussion of this paper will appear in a Discussion Section to be published in the December 1956 JOURNAL.

REFERENCES

1. G. M. POUND, G. DERGE, AND G. OSUCH, *Trans. Am. Inst. Mining Met. Engrs.*, **203**, 481 (1955).
2. R. E. VIVIAN, *Trans. Electrochem. Soc.*, **69**, 637 (1936).
3. G. S. SON FREY, *Arkiv. Kemi Mineral. Geol.*, **11A**, No. 4, 1 (1932).
4. M. HANSEN, "Aufbau der Zweistofflegierungen," p. 1033, Springer, Berlin (1936).

FUTURE MEETINGS OF
The Electrochemical Society

Cleveland, September 30, October 1, 2, 3, and 4, 1956

Headquarters at the Statler Hotel

Sessions will be scheduled on

Batteries, Corrosion, Electrodeposition,
Electrothermics and Metallurgy, Theoretical
Electrochemistry (joint with Electrodeposition),
and Theoretical Electrochemistry

★ ★ ★

Washington, D. C., May 12, 13, 14, 15, and 16, 1957

Headquarters at the Statler Hotel

★ ★ ★

Buffalo, October 6, 7, 8, 9, and 10, 1957

Headquarters at the Statler Hotel

★ ★ ★

New York, April 27, 28, 29, 30, and May 1, 1958

Headquarters at the Statler Hotel

★ ★ ★

Ottawa, September 28, 29, 30, October 1, and 2, 1958

Headquarters at the Chateau Laurier

★ ★ ★

Papers are now being solicited for the meeting to be held in Cleveland. Triplicate copies of each abstract (*not exceeding 75 words in length*) are due at the Secretary's office, 216 West 102nd Street, New York 25, N. Y., *not later than June 15, 1956* in order to be included in the program. *Please indicate on abstract for which Division's symposium the paper is to be scheduled.* Complete manuscripts should be sent in triplicate to the Managing Editor of the JOURNAL at the same address.

Current Affairs

Tennessee Products & Chemical Corp.—ECS Sustaining Member

Tapping standard ferromanganese at the Alton Park, Chattanooga, plant of Tennessee Products & Chemical Corp.

In November 1917 the "Southern Ferro Alloys" Co. began manufacturing 50% ferrosilicon in their plant at Chattanooga, Tenn. Three 800 kva single-phase electric furnaces were installed in the original plant. "Southern Ferro Alloys," as the company was known to the trade, grew steadily in size and reputation during the next three decades until, in 1947, there were six electric furnaces in operation at Chattanooga having a total installed capacity of 30,000 kva.

In 1947 "Southern Ferro Alloys" was purchased by Tennessee Products & Chemical Corp. Under the leadership of Tennessee's President, Mr. Carl McFarlin, the growth of the Ferro Alloys Division has been rapid. Two new electric furnace plants have been built; one at Alton Park, Chattanooga, in 1948, comprising four furnaces with a total installed capacity of 18,000 kva. The other plant, built at Houston, Texas, in 1951, is known as Tenn-Tex Alloy & Chemical Corp., comprising three furnaces with a total installed capacity of 18,000 kva. The Houston plant is a joint venture of Tennessee and the Sheffield Division of Armco Steel Corp.

Still another electric furnace plant is now under construction in Roane County (near Rockwood, Tenn.) with the first of six large electric furnaces scheduled to begin operation in October 1956. When completed in early 1957 the Roane electric furnace plant will have an installed capacity of 73,000 kva. The original Chestnut St. plant in Chattanooga will be incorporated into the Roane electric furnace plant. The new plant will represent an increase in installed capacity of approximately 90% for the company's electric furnace operations in the state of Tennessee.

The growth in size and capacity of Tennessee's ferroalloys operations has been accompanied by diversification in the products manufactured. Tennessee was a major producer of standard ferromanganese in blast furnaces in the early 1940's, long before Southern Ferro Alloys was acquired. The manufacture of ferromanganese in electric furnaces was begun in 1949 at the Alton Park plant. In 1953 this diversification continued with the initial production of the silico-manganese family of alloys at Alton Park. In 1954 boron-silicon alloys became major products at the Chestnut St. plant in Chattanooga. Early in 1955 the corporation began manufacturing the entire family of high carbon ferrochromium alloys. The rapid acceptance of these by the steel industry has already placed them in Tennessee's classification of major products. Plans are under way to add other alloys.

Tennessee's growth in ferroalloys has been marked by a steady increase in the size of furnaces employed. In 1917 there were three 800 kva single-phase furnaces; in 1918 a three-phase furnace of 2000 kva was installed, and in 1929 one 3300 kva furnace was added. A 6000 kva furnace was installed in 1930. One of the new furnaces at the Roane electric furnace plant will have a capacity of 13,000 kva; the remainder will be 12,000 kva.

All of Tennessee's furnaces are of the stationary type, submerged arc, charged and operated continuously, tapped intermittently. Carbon and graphite electrodes are employed, varying in size according to the size of the furnace. The smallest electrodes are 24 in. in diameter, while the large furnace has 35 in. diameter carbon electrodes. Both single-phase and three-phase furnaces are available, with the choice dependent upon the type of product to be manufactured.

Electric energy is supplied to all plants at 60 cycles, three-phase, 13,000 volts. Each furnace is equipped with a multitap furnace transformer to step-down the voltage to that desired at the furnace, within the range of 80 to 170 v.

The ferroalloy processes are of the reduction-smelting type. Reducing agents are generally carbon or silicon, but others such as aluminum are employed at times. Carbonaceous reducing agents consist of by-product coke, petroleum coke, charcoal, and coal. Each of these materials is used in at least one of the processes. The choice depends upon price, physical and chemical quality, and electrical resistivity.

Raw materials for these various alloys are obtained from a variety of sources throughout the world. In the manufacture of manganese alloys, metallurgical ores are purchased largely from India, Cuba, and Africa in lots of 2000 to 10,000 tons. For chromium alloys, metallurgical ores come from Turkey, New Caledonia, Africa, and Cuba. Silicon for the silicon alloys is derived from domestic metallurgical quartzite that is available from a number of locations. The selection of raw materials for these processes is an involved procedure and requires a detailed study of the price and characteristics of various ores, with a further consideration of world market price and the cyclical trend in these prices.

In 1955 the common stock of Tennessee Products & Chemical Corp. was acquired by the Merritt-Chapman & Scott Corp. by an exchange of stock, and it is now a unit in the Chemical, Paint, and Metallurgical Dept. of Merritt. Tennessee's President, Mr. Carl McFarlin, is Executive Vice-President for this department. Under his continuing leadership, Tennessee's past record of growth and diversification in ferroalloys seems well assured.

NEWS ITEMS

Perkin Medal Award Nominations due June 1

The Electrochemical Society is one of five societies responsible for nominating the recipient of the Perkin Medal, an award which was founded in commemoration of the 50th anniversary of the coal-tar color industry 1856–1906. The other societies responsible for selection of the medalist are The Society of Chemical Industry, The American Chemical Society, The American Institute of Chemical Engineers, and the Societe de Chimie Industrielle. The award is granted to anyone residing in the United States who is actively engaged in the chemical profession and who, in the judgment of the Medal Award Committee, has done outstanding work at some time during his career. The medal is usually awarded at the regular January meeting of the American Section of The Society of Chemical Industry.

Members of The Electrochemical Society who wish to suggest nominees for the award are urged to do so. Suggestions should be sent to Secretary Henry B. Linford at Society Headquarters, 216 West 102 St., New York 25, N. Y., accompanied by a statement setting forth the reasons for presenting the candidate, and a description of the work the candidate has done. All suggestions received will be reviewed by a committee consisting of the President, Past-President, and senior Vice-President of the Society who are responsible for sending in one or two names to the Perkin Medal Award Committee which will select the final candidate.

The Perkin Medal is one of the highest honors that can be bestowed on an American chemist. Several members of our Society have won the medal in past years, the most recent of whom is Dr. R. M. Burns, Past-President of the Society and currently Chairman of the Publication Committee.

H. H. Uhlig, *President*

New Sustaining Member

Michelin Tire Manufacturing Co., Clermont-Ferrand, Puy-de-Dome, France, recently became a Sustaining Member of the Society.

"Zinc Controls Corrosion"

A new 16-mm sound and color motion picture, "Zinc Controls Corrosion," has been produced by The American Zinc Institute, Inc., national trade association for the zinc industry. Available at no charge for showing before agricultural, industrial, technical, and educational groups, the film dramatically tells how zinc in its role of "protector" controls corrosion to lengthen life and to minimize maintenance and replacement costs.

Bookings are now being accepted at The American Zinc Institute, Inc., 60 East 42 St., New York 17, N. Y. Special booking forms available on request.

Also available for showing is another AZI film, "Die Casting: How Else Would You Make It?," which was released about a year ago.

Enthone Trade Name Change

Enthone, Inc., New Haven, Conn., announces a change in name only of their acid activating compound "Actane" (trademark registered). In view of their addition of Actane 70 to this line of acid activators for various uses, it has been decided that the use of a suffix number to designate the original product will eliminate confusion for those customers using both products. There has been no change in the formulation or manufacture of Actane 22 (formerly called Actane).

Actane 22 is a neutral activating compound for addition to hydrochloric or sulfuric acid pickles to remove colloidal films from metal surfaces. It is particularly useful prior to bright plating operations.

Actane 70 is an acidic fluoride-containing compound used as a replacement for liquid hydrofluoric acid. It is much less hazardous to handle, being a crystalline solid. While it may also be used for the removal of colloidal films in normal acid pickles, it is also extensively used alone or with sulfuric or nitric acids for pickling titanium, etching and cleaning of aluminum, etching of glass, removal of sand from castings, and pickling of nickel-chromium alloy steels and many magnesium alloys. Literature is available upon request.

Olin Mathieson to Enter Aluminum Industry

Details of Olin Mathieson Chemical Corp.'s plans to enter the aluminum industry with an initial investment of $120,000,000, and with the world's first fully integrated aluminum plant, were announced recently by Thomas S. Nichols, President.

The new operation will mark the first time in the history of the aluminum industry when coal, mined directly on the site, is used to provide the large power requirements for the reduction of alumina to pig aluminum.

Investment in the new operation includes approximately $90,000,000 for the aluminum plant and $30,000,000 for the power facilities needed for the aluminum plant. The aluminum plant will be financed from the company's own resources and a newly negotiated long-term loan from the Prudential Insurance Co. in the amount of $60,000,000. The power plant will be financed entirely through a long-term loan of $30,000,000 from Prudential to the power subsidiary corporation, of which Olin Mathieson will have a 50% interest.

The new facilities will be located in the Ohio River Valley. The alumina plant, the reduction plant, and the rolling mill will be on the Ohio River near Clarington, Ohio. The power plant to be engineered and built by American Gas and Electric will be slightly upstream on the West Virginia side at Cresap Bottom and will be connected to the aluminum facilities by a high tension transmission line. The power plant will be built on a new major coal mine which will be constructed, owned, and operated by the Pittsburgh Consolidation Coal Co.

The power plant, which will be known as the Kammer Plant, will consist of two units of 225,000 kw each. One unit will be owned by the Ohio Power Co., a subsidiary of the American Gas and Electric Co., the other by a joint subsidiary of Olin Mathieson Chemical Corp. and Pittsburgh Consolidation Coal Co. Both power units will be operated by the Ohio Power Co. and integrated into the American Gas and Electric Co. System. The plant will be designed for development up to 1,350,000 kw capacity.

The plants are being built under certificates of necessity from the U. S. Government issued in order to help increase the supply of primary aluminum.

The alumina plant will have a capacity of 230,000 tons per year. The capacity of the aluminum plant will be 60,000 tons per year. At first, only about 115,000 tons of alumina will be required for the aluminum plant and the other 115,000 tons of surplus alumina will be available to the market. Most of the 60,000 tons of finished aluminum will be consumed by the Metals Division of Olin Mathieson. However, in view of the need of flexibility, the

corporation will be both a buyer and a seller of prime aluminum in order to keep the fabricating facilities in balanced supply.

Bauxite, the major raw material required, will be shipped to the United States from Surinam (Dutch Guiana). Olin Mathieson has signed a long-term supply contract for its initial requirements. First shipments for stockpiling of the raw material are scheduled for arrival early in 1957.

It was pointed out that this major investment of $120,000,000 is indicative of the corporation's confidence in the future for aluminum. While new capacity is being added by the expansion plans of other companies at this time, there is still great need for additional new domestic capacity in view of the potential future expansion in the use of aluminum in such fields as construction, appliances, transportation, and others.

Forum Shifts Site of 1956 Atomic Industry Trade Fair

The Atomic Industrial Forum has announced that heavy demand for space in the second annual Trade Fair of the Atomic Industry has caused the site of the Fair to be shifted from the Morrison Hotel in Chicago to the Navy Pier, Chicago. The Fair will run from September 24 through 28, concurrent with a major Forum meeting on "management and technology for the atomic industry," September 25, 26, and 27. The Morrison Hotel will remain as conference headquarters and primary meeting location.

Emphasis in the Trade Fair is on those products and services directly related to the application of atomic energy, either through power generation, heat utilization, or wide use of radiation in manufacturing processes, research, agriculture, medicine, and food sterilization. The Fair is wholly managed by the Forum with the guidance of an 18-man Exhibit Committee, representing a broad cross section of interests from the atomic industry.

Armour Research Foundation Expansion

A $5,000,000 building program was announced on January 10 which will give Armour Research Foundation of Illinois Institute of Technology "one of the most complete industrial research centers in the world." The expansion program calls for the construction of three buildings and substantial additions to two buildings over the next 10 years. The plans were outlined by Dr. Haldon A. Leedy, Foundation Vice-President and Director, at a press dinner commencing ARF's 20th anniversary observance.

New buildings planned, and their dates of completion, are: Physics and Electrical Engineering Research building (now under construction), 1956; Chemistry Research building, 1959; Administration building, 1966.

Additions scheduled for completion in 1961 are to the Mechanical Engineering Research building, and to the Metals Research building.

The five construction projects will consolidate, modernize, and enlarge Armour Research Foundation's physical plant, now scattered over 15 buildings on the Illinois Tech campus, according to Dr. Leedy. When completed, the Foundation's facilities will be concentrated in six buildings in a two-block area.

New Norelco Office in Newark

Effective January 1, the Research & Control Instruments Division, North American Philips Co., Inc., 750 So. Fulton Ave., Mt. Vernon, N. Y., established a new office at 96 Bloomfield Ave., Newark, N. J., it has been announced by C. J. Woods, National Sales Manager.

John O'Connor is District Manager, Frank Cavanaugh is Sales Engineer, and Frank Stein is Service Engineer. The new office will serve Norelco customers in New Jersey and eastern Pennsylvania, the territory formerly covered by the F. J. Mullowney X-Ray Co. of Trenton. Edward Champaygne, Al Gobus, and Joseph Ladd from Mt. Vernon headquarters have been assigned to assist with technical problems at the Newark office. Champaygne will deal with electron microscopes and x-ray diffraction instruments while Gobus and Ladd will devote their attention to x-ray radiographic units.

Resources Research, Inc.

Formation of Resources Research, Inc., a firm of consultants specializing in solving air and stream pollution problems for industry and federal and state governmental agencies, has been announced by Dr. Louis C. McCabe, formerly Scientist Director in the United States Public Health Service.

Dr. McCabe, who served as the first Director of the Los Angeles Air Pollution Control District, will be joined in the new enterprise by Frederick S. Mallette, Executive Secretary of the Committee on Air Pollution Controls and Research Manager of the American Society of Mechanical Engineers, and William S. McCabe, consulting geologist of Casper, Wyo.

The company will handle research and development in geology, mining, industrial wastes, water resources, and the economics and supply of conventional and atomic fuels. It will deal with such specialized problems as fuel sources and their evaluation for power, metallurgy and chemistry; research and engineering in air and stream pollution; water treatment and supply problems; and the development of fuel resource properties.

The main office of Resources Research, Inc., will be in the Wisconsin Bldg., 4435 Wisconsin Ave., N.W., Washington 16, D. C., with offices in New York City at 55 W. 42nd St., and in Casper, Wyo., c/o P. O. Box 1861.

Corrosion Resistance of Aluminum Alloys

The National Bureau of Standards, Washington, D. C., has found that some aluminum alloys can resist corrosion in either a marine or inland atmosphere for at least 20 years. These results were obtained in a long-range study conducted by F. M. Reinhart and G. A. Ellinger of the NBS staff for the Navy Bureau of Aeronautics. Besides determining the corrosion resistance of a large number of aluminum alloys, the study also provides data regarding the effects of heat treatment and protective coatings on corrosion rates.

Dow Manufacturing Operation

Plans for a new $20,000,000 manufacturing operation, to be located in the Baton Rouge area of Louisiana, have been announced by the Dow Chemical Co.

Options have been taken on three tracts of land on the west bank of the Mississippi with the expectation of building facilities to produce chlorine, caustic soda, and several organic chemicals. The availability of water transportation stimulated the company's interest in a Mississippi river site.

Molybdenum Chemical Research

Battelle Memorial Institute, Columbus, Ohio, will conduct for Climax Molybdenum Co. certain phases of an expanded molybdenum chemical research program now under way at Climax, according to a joint announce-

(*Continued on page 120C*)

Officers of Local Sections of the Society

Boston
F. C. BENNER, Chairman
L. B. ROGERS, Vice-Chairman
CHARLES LEVY, Sec.-Treas.
61 Central St.
Auburndale 66, Mass.
Representatives on Council of Local Sections:
H. BANDES AND C. W. JEROME

Chicago
ERNEST KOEHLER, Chairman
R. D. MISCH, Vice-Chairman
R. J. HOVEY, Treasurer
D. V. LOUZOS, Secretary
735 Arbor Lane
Glenview, Ill.
Representatives on Council of Local Sections:
C. A. HAMPEL (1 year) AND HOWARD FRANCIS

Cleveland
W. H. STOLL, Chairman
K. S. WILLSON, Vice-Chairman
D. E. KINNEY, Treasurer
P. S. BROOKS, Secretary
National Carbon Co.
P. O. Box 6087
Cleveland, Ohio
Representatives on Council of Local Sections:
N. C. CAHOON (1 year) AND K. S. WILLSON (2 years)

Detroit
A. W. LIGER, Chairman
G. V. KINGSLEY, 1st Vice-Chairman
MANUEL BEN, 2nd Vice-Chairman
MANUEL SHAW, Sec.-Treas.
Chrysler Engineering
Dept. 487, 12800 Oakland
Highland Park 3, Mich.
Representatives on Council of Local Sections:
FRANK PASSAL AND L. O. CASE

Midland
M. P. NEIPERT, Chairman
P. R. JUCKNIESS, Vice-Chairman
H. W. SCHMIDT, Sec.-Treas.
1313 Helen St.
Midland, Mich.
Representatives on Council of Local Sections:
H. A. ROBINSON (1 year) AND F. W. KOERKER (2 years)

New York Metropolitan
M. B. DIGGIN, Chairman
C. V. KING, Vice-Chairman
K. B. MCCAIN, Sec.-Treas.
Wilbur B. Driver Co.
1875 McCarter Highway
Newark 4, N. J.
Representatives on Council of Local Sections:
A. C. LOONAM AND F. A. LOWENHEIM (1 year)
M. F. QUAELY (2 years)

Niagara Falls
JOHN CURREY, Chairman
R. B. MACMULLIN, Vice-Chairman
L. A. STOYELL, Sec.-Treas.
Electro Metallurgical Co.
Niagara Works, 137 47th St.
Niagara Falls, N. Y.
Representatives on Council of Local Sections:
M. S. KIRCHER AND W. D. SHERROW

Pacific Northwest
G. H. KISSIN, Chairman
E. C. PITZER, Vice-Chairman
J. F. MURPHY, Sec.-Treas.
Dept. of Metallurgical Research
Kaiser Aluminum & Chemical Corp.
Spokane 69, Wash.
Representatives on Council of Local Sections:
G. H. KISSIN AND J. F. MURPHY

Philadelphia
E. L. ECKFELDT, Chairman
G. F. TEMPLE, Vice-Chairman
A. A. WARE, Treasurer
G. W. BODAMER, Secretary
Rohm & Haas Co.
Philadelphia, Pa.
Representatives on Council of Local Sections:
J. F. GALL (1 year) AND J. F. HAZEL (2 years)

Pittsburgh
R. A. WOOFTER, Chairman
R. B. HOXENG, Vice-Chairman
A. J. CORNISH, Sec.-Treas.
Rectifier Dev. 4N-N
Westinghouse Electric Corp.
East Pittsburgh, Pa.
Representatives on Council of Local Sections:
R. A. WOOFTER (1 year) AND E. A. GULBRANSEN (2 years)

San Francisco
C. W. TOBIAS, Chairman
MORRIS FEINLEIB, Vice-Chairman
R. A. ZIMMERLY, Treasurer
H. F. MYERS, Secretary
Columbia-Geneva Steel Co.
Russ Bldg.
San Francisco, Calif.
Representatives on Council of Local Sections:
R. F. BECHTOLD AND S. H. DREISBACH

Washington-Baltimore
FIELDING OGBURN, Chairman
D. T. FERRELL, JR., Vice-Chairman
GWENDOLYN B. WOOD, Treasurer
JEANNE B. BURBANK, Secretary
Naval Research Laboratory
Washington, D. C.
Representatives on Council of Local Sections:
D. T. FERRELL, JR. (1 year) AND J. C. WHITE (2 years)

Ontario-Quebec
A. F. G. CADENHEAD, Honorary Chairman
P. J. ENSIO, Chairman
A. C. HOLM, Vice-Chairman (Programs)
JOHN SUMNER, Vice-Chairman (Membership)
J. U. MACEWAN, Chairman Junior Members Committee
R. R. ROGERS, Sec.-Treas.
552 Booth St.
Ottawa, Ont., Canada
Representatives on Council of Local Sections:
P. J. ENSIO (1 year) AND R. R. ROGERS (2 years)

India
M. S. THACKER, Chairman
S. RAMASWAMY, Vice-Chairman
A. JOGA RAO, Vice-Chairman
T. L. RAMA CHAR, Sec.-Treas.
Indian Institute of Science
Bangalore 3, India
Representatives on Council of Local Sections:
B. K. RAM PRASAD AND V. M. Dokras

Officers of Divisions of the Society

Battery

N. C. Cahoon, Chairman
U. B. Thomas, Vice-Chairman
E. J. Ritchie, Sec.-Treas.
The Eagle-Picher Co.
Joplin, Mo.

Corrosion

T. P. May, Chairman
J. E. Draley, Vice-Chairman
C. V. King, Sec.-Treas.
Dept. of Chemistry
New York University
New York 3, N. Y.

Electric Insulation

L. L. Deer, Chairman
D. A. Lupfer, Vice-Chairman
L. J. Frisco, Sec.-Treas.
The Johns Hopkins University
1315 St. Paul St.
Baltimore 18, Md.

Electrodeposition

C. A. Snavely, Chairman
Sidney Barnartt, Vice-Chairman
Abner Brenner, Sec.-Treas.
National Bureau of Standards
Washington, D. C.

Electronics

C. W. Jerome, Chairman
J. H. Schulman, Vice-Chairman
(Luminescence)
Channing Dichter, Vice-Chairman
(General Electronics)
F. J. Biondi, Vice-Chairman
(Semiconductors)
M. F. Quaely, Sec.-Treas.
90 Mt. Hebron Rd.
Montclair, N. J.

Electro-Organic

H. M. Scholberg, Chairman
Stanley Wawzonek, Vice-Chairman
G. W. Thiessen, Sec.-Treas.
Dept. of Chemistry
Monmouth College
Monmouth, Ill.

Electrothermics and Metallurgy

A. C. Haskell, Jr., Chairman
A. U. Seybolt, Vice-Chairman
G. M. Butler, Vice-Chairman
E. M. Sherwood, Sec.-Treas.
Battelle Memorial Institute
Columbus 1, Ohio

Industrial Electrolytic

Milton Janes, Chairman
W. D. Sherrow, Sec.-Treas.
Great Lakes Carbon Corp.
Niagara Falls, N. Y.

Theoretical Electrochemistry

E. B. Yeager, Chairman
Paul Delahay, Vice-Chairman
Ralph Roberts, Sec.-Treas.
Office of Naval Research
Washington, D. C.

News Items

(*Continued from page 118C*)

ment by Clyde Williams, Battelle President, and Alvin J. Herzig, Climax Vice-President—research, and President of the subsidiary company, Climax Molybdenum Co. of Michigan.

Under the terms of a one-year contract, Battelle will conduct research aimed at finding new applications for existing molybdenum chemicals. The first phase of this work will be directed at broadening the use of phospho- and silicomolybdates, now used in the organic pigment industry. Battelle will also evaluate the technical feasibility of new applications for such molybdenum chemicals as the normal molybdates, the cyanomolybdates, and molybdenum disulfide. It will also survey potential markets represented by new uses for these chemicals.

Acheson Builds Plant in Holland

Plans to construct the first colloidal graphite manufacturing plant in The Netherlands have been announced by Acheson Industries, Inc., New York, N. Y. Construction and operation of the factory, located near the harbor of Eexta, Borough of Scheemda, will be supervised by Acheson Colloids Ltd., the firm's British affiliate. Estimated cost of construction is over 470,000 Dutch guilders, approximately $135,000.

Postwar expansion of Dutch industry, particularly in the electronic, metalworking, and foundry fields, has created a substantial market for colloidal dispersions. The Scheemda production unit will have sufficient capacity to satisfy all requirements of the Continental market as well as the Dutch.

The new ultramodern plant will manufacture products paralleling those of other units of Acheson Industries; Acheson Colloids Co. of Port Huron, Mich.; Acheson Dispersed Pigments Co. of Philadelphia, Pa.; and Gredag, Inc., of Niagara Falls, N. Y. In addition to the internationally known 'dag' dispersions, these include dispersions of carbon black and other pigments in various media employed by the graphic arts and the plastics industry, and graphited greases.

RCA Special Laboratory Apparatus

Precision electronic test apparatus that facilitates the design, development, and production of complex electronic equipment and systems has been

placed on the market by the Radio Corp. of America.

Introduction of 13 different instruments marked RCA's full-scale entry into the field of electronic test equipment for industrial and laboratory applications.

RCA will sell the new test apparatus nationally and will appoint manufacturers' representatives or distributors of industrial electronic equipment in each major market area. Additional instruments and equipment developed and planned by RCA for this specialized market also will be offered through these channels.

The instruments include: a pulse generator, two RF power meters, two null-reading d-c voltmeters, a vacuum tube voltmeter, two impedance bridges, four types of signal generator, and a deluxe multimeter.

Crane and Vitro Joint Operation

Crane Co. and Vitro Corp. of America have entered into a joint operation to produce thorium, rare earths, and heavy minerals from monazite, as well as rutile, ilmenite, zircon, and kyanite. The two companies will assume equal ownership of Heavy Minerals Co., its mining subsidiary Marine Minerals, Inc., and associated operations. By the end of 1956, the combined investment in this operation will approximate $6,000,000.

A subsidiary of the French chemical group of Pechiney, known as STR, continues to hold a minority interest. Heavy Minerals Co. has an exclusive North American license to numerous patents held by STR on the processing of thorium, rare earths, and heavy minerals.

Heavy Minerals Co., organized by Crane in 1953, will proceed with plans to build processing facilities on a site now owned near Chattanooga, Tenn. Mark K. Wilson Co., of Chattanooga, will be the general contractor. Among other products a large quantity of monazite will be processed annually.

Marine Minerals, located near Aiken, S. C., is now mining rutile for sale as a raw material in the production of titanium metal; ilmenite for sale as a raw material in the production of titanium pigments; zircon for sale and for processing by Heavy Minerals; and monazite, also to be processed by Heavy Minerals.

An associated operation has developed minable areas along the Gulf Coast between Panama City and Pensacola, Fla. It will dredge-mine a mineral concentrate which will be separated principally into rutile, ilmenite, zircon, and kyanite. Facilities will be built near Panama City for these purposes.

SECTION NEWS

Washington-Baltimore Section

The Section held its 38th technical meeting on February 16 at the National Bureau of Standards. Preceding the talks by the principal speakers of the evening, Dr. John Taylor presented an outline of the extensive activities of the local Technical and Scientific Societies in promoting scientific interest in the secondary schools of the area. The effort has been coordinated through a joint committee of the societies.

Mr. E. L. Brancato of the Naval Research Lab. spoke on Thermal Evaluation of Electric Insulation. The degradation of insulation in actual use is a complex function of temperature, humidity, dielectric stress, and mechanical strength. Several testing procedures were described that have been devised to measure service performance of electric insulation. These are being correlated with actual service performance at the present time.

Dr. Mary Jo Boehm, Naval Research Lab., spoke on the Physical and Chemical Properties of the Corrosion Products of Iron. The several compounds of iron with oxygen and/or hydroxyl ions were characterized in detail. Dr. Boehm showed models of the crystal structures of some of the compounds, and described the conditions under which each would be stable in the corrosion products of iron.

The third speaker of the evening was Dr. J. J. Lambe, Naval Research Lab., whose topic was Photoconductivity and Luminescence. The mechanisms of these two phenomena were briefly described and these effects were vividly illustrated by demonstrations. Data were presented showing the quantitative aspects of these phenomena.

JEANNE BURBANK, *Secretary*

Philadelphia Section

On March 7 the Philadelphia Section was addressed on the topic "Corrosion Inhibition" by Dr. H. H. Uhlig, President of the Society. This was preceded by a dinner at the Lenape Club at which Dr. Uhlig commented on the excellent status of Society affairs.

In his technical presentation Dr. Uhlig pointed out the industrial importance of corrosion inhibition in

MANUSCRIPTS AND ABSTRACTS FOR FALL MEETING

Papers are now being solicited for the Fall Meeting of the Society, to be held at the Statler Hotel in Cleveland, September 30, October 1, 2, 3, and 4, 1956. Technical sessions will be scheduled on Batteries, Corrosion, Electrodeposition, Electrothermics and Metallurgy, Theoretical Electrochemistry (joint symposium with Electrodeposition), and Theoretical Electrochemistry.

To be considered for this meeting, triplicate copies of abstracts (not to exceed 75 words in length) must be received at Society Headquarters, 216 West 102nd St., New York 25, N. Y., *not later than June 15, 1956. Please indicate on abstract for which Division's symposium the paper is to be scheduled.* Complete manuscripts should be sent in triplicate to the Managing Editor of the JOURNAL at the same address.

***

The Spring 1957 Meeting will be held in Washington D. C., May 12, 13, 14, 15, and 16, at the Statler Hotel. Sessions will be announced in a later issue.

pickling, slushing, vapor phase work, and many other processes in the metal industries. The two largest classes of inhibitors are organic compounds and the passivators.

The organic substances that serve as effective inhibitors are those which possess a polar group at the extremity of a molecule. This polar group may readily be adsorbed on a metal surface which it then protects by physically shielding the surface from corrodents. Typical of such polar groups are —OH, —SH, —NH_2, and —COOH.

Dr. Uhlig presented evidence that many of the passivators or polarizing inhibitors which render more noble the anodic areas of a metal surface function in a similar fashion. Measurements of surface tension indicate that on the surface of metals such as tungsten and chromium are not oxide films but chemisorbed oxygen. Indeed, such inhibitors as $CrO_4^=$ on iron were found to follow the Langmuir adsorption isotherm.

Passivators which function in this manner must have high chemical affinity for the metal (to provide high energy of adsorption) and a high activation energy (to prevent actual chemical reaction with the surface). It was mentioned that the pertechnetate ion is the most powerful inhibitor in this class.

In a lengthy question and answer period following the lecture it was brought out that, even in the case of some metals which are protected by diffusion barrier layers of oxide such as aluminum, the chemisorption of molecules on the metal surface still plays a part in corrosion inhibition.

HARRY C. MANDELL, JR.

NEW MEMBERS

In March 1956 the following were approved for membership in The Electrochemical Society by the Admissions Committee:

A recent action of the Board of Directors of the Society requires that, commencing January 1, 1956, all prospective members include first year's dues with their applications for membership.

Also, please note that, if sponsors sign the application form itself, processing can be expedited considerably.

Active Members

PAUL L. ASNIS, Wilbur B. Driver Co.; Mail add: 16 Mandeville Ave., Pequannock, N. J. (Electrothermics & Metallurgy)

ANTON DEŠ. BRASUNAS, American Society for Metals; Mail add: 7301 Euclid Ave., Cleveland 3, Ohio (Corrosion)

GENE BROST, Cowles Chemical Co.; Mail add: 174 East Genesee St., Skaneateles, N. Y. (Corrosion, Electrodeposition, Electro-Organic, Theoretical Electrochemistry)

FRANCIS F. CARINI, General Electric Co.; Mail add: 1033 Westcott Rd., Schenectady 6, N. Y. (Battery, Electrodeposition, Electrothermics & Metallurgy, Theoretical Electrochemistry)

CLARE B. CARLSON, Pittsburgh Lectromelt Furnace Corp.; Mail add: 602 Edgehill Drive, R. # 5, Gibsonia, Pa. (Electrothermics & Metallurgy)

PETER FABER, Electrizitäts-Actien-Gesellschaft vorm. W. Lahmeyer, Frankfort; Mail add: Niederwaldstr. 46, Wiesbaden, Germany (Battery)

ROBERT M. FOWLER, Metals Research Labs. Electro Metallugical Co., Box 580, Niagara Falls, N. Y. (Electrothermics & Metallurgy)

THOMAS C. FRANKLIN, Chemistry Dept., Baylor University, Waco, Texas (Theoretical Electrochemistry)

DONALD P. GENTRY, Engineering Dept., Delco Battery Operations, Delco-Remy Div., General Motors Corp., W. Willard St., Muncie, Ind. (Battery)

ARTHUR P. HAAG, Stauffer Chemical Co., 1375 So. 47 St., Richmond, Calif. (Electrothermics & Metallurgy)

RICHARD E. JOHNSON, National Carbon Research Labs.; Mail add: 12511 Clifton Bldg., Apt. 30, Lakewood 7, Ohio (Battery)

H. EDWARD KLEIN, Watertown Arsenal Lab.; Mail add: 28 Regent St., West Newton 65, Mass. (Corrosion)

MEIR E. MEER, Yardney Electric Corp.; Mail add: 5 Peter Cooper Rd., New York 10, N. Y. (Battery, Corrosion, Electronics, Theoretical Electrochemistry)

JAMES R. MEYER, R. B. MacMullin Associates; Mail add: 1051 Ridge Rd., Lewiston, N. Y. (Industrial Electrolytic)

CORNELIUS B. MURPHY, General Engineering Lab., General Electric Co., Rm. 299–44, Bldg. 37, Schenectady, N. Y. (Electric Insulation, Electrothermics & Metallurgy)

EMERSON H. NEWTON, Arthur D. Little, Inc.; Mail add: 39 Virginia Rd., Arlington, Mass. (Corrosion, Electrodeposition, Industrial Electrolytic)

RICHARD A. PEAK, Arthur D. Little, Inc.; Mail add: 22 Ewell Ave., Lexington 73, Mass. (Electrodeposition, Industrial Electrolytic, Theoretical Electrochemistry)

EUGENE PEARLMAN, Yardney Electric Corp.; Mail add: 1859 Bergen St., Brooklyn 33, N. Y. (Battery, Corrosion, Theoretical Electrochemistry)

DERROL E. PENNINGTON, Tektronix, Inc.; Mail add: Box 831, Portland 7, Oreg. (Electronics)

ALFRED RUDIN, Central Research Lab., Canadian Industries Ltd., McMasterville, Que., Canada (Corrosion, Industrial Electrolytic)

D. R. SPINK, Carborundum Metals Co., Inc., P.O. Box 32, Akron, N. Y. (Corrosion, Electrodeposition, Elec-

DECEMBER 1956 DISCUSSION SECTION

A Discussion Section, covering papers published in the January–June 1956 JOURNALS, is scheduled for publication in the December 1956 issue. Any discussion which did not reach the Editor in time for inclusion in the June 1956 Discussion Section will be included in the December 1956 issue. Those who plan to contribute remarks for this Discussion Section should submit their comments or questions in triplicate to the Managing Editor of the JOURNAL, 216 W. 102nd St., New York 25, N. Y., *not later than September 1, 1956*. All discussions will be forwarded to the author, or authors, for reply before being printed in the JOURNAL.

trothermics & Metallurgy, Industrial Electrolytic)

JOSEPH P. SWEENEY, Research Div., Aircraft-Marnie Products Inc.; Mail add: 152 So. 31 St., Camp Hill, Pa. (Corrosion, Electrodeposition, Electrothermics & Metallurgy, Theoretical Electrochemistry)

SHELDON A. TAYLOR, National Carbon Co.; Mail add: 65 French St., Berea, Ohio (Industrial Electrolytic)

THEODORE L. TREITLER, Corning Glass Works; Mail add: 10 Fulton St., Corning, N. Y. (Corrosion, Theoretical Electrochemistry)

HAROLD C. WEBER, Massachusetts Institute of Technology; Mail add: 67 Vose Hill Rd., Milton, Mass. (Industrial Electrolytic)

REUBEN E. WOOD, George Washington University; Mail add: 3120 No. Pershing Dr., Arlington 1, Va. (Theoretical Electrochemistry)

Associate Members

SAMUEL L. COOKE, JR., Chemistry Dept., Baylor University; Mail add: Box 123, Baylor University Station, Waco, Texas (Electronics, Theoretical Electrochemistry)

JOHN R. PIKE, Duro-Test Corp.; Mail add: 73 Fairmount Ave., Maywood, N. J. (Electronics, Theoretical Electrochemistry)

Student Associate Members

ANDREW G. B. CZEMPINSKI, Research & Development Dept., Norton Co.; Mail add: 513 First St., Chippawa, Ont., Canada (Electrothermics & Metallurgy)

RAJENDRA P. KHERA, Dept. of Metallurgy, Cambridge University, Pembroke St., Cambridge, England (Corrosion)

Reinstatements to Active Membership

HECTOR D. DOUGLAS, JR., Fansteel Metallurgical Corp.; Mail add: 3626 Warren Rd., Cleveland 11, Ohio (Corrosion, Electro-Organic, Industrial Electrolytic)

R. H. LESTER, Pabco Products, Inc.; Mail add: 2366 Virginia St., Apt. 1, Berkeley 9, Calif. (Corrosion, Electrodeposition, Electro-Organic, Theoretical Electrochemistry)

FAUSTINO G. PRADO, Prado y Asociados; Mail add: Monte 211, Havana, Cuba (Electrothermics & Metallurgy, Industrial Electrolytic)

KENNETH C. RULE, Food Machinery & Chemical Corp., 161 East 42 St., New York 17, N. Y. (Industrial Electrolytic)

ECS Membership Statistics

The following two tables give breakdown of membership as of April 1, 1956. The Secretary's Office feels that a regular accounting of membership will be very stimulating to membership committee activities. In Table I it should be noted that the totals appearing in the right-hand column are *not* the sums of the figures in that line since members belong to more than one Division and, also, because Sustaining Members are not assigned to Divisions. But the totals listed are the total membership in each Section. In Table I, Sustaining Members have been credited to the various Sections.

TABLE I. *ECS Membership by Sections and Divisions*

Section	Division												
	Battery	Corrosion	Electric Insulation	Electrodeposition	Electronics	Electro-Organic	Electrothermics & Met.	Industrial Electrolytics	Theoretical Electrochem.	No Division	Totals as of 4/1/56	Totals as of 1/1/56	Net Change
Boston				1			1				1	0	+1
Chicago	9	34	2	47	16	8	11	15	20	19	106	105	+1
Cleveland	46	35	4	47	33	10	20	26	39	13	174	171	+3
Detroit	6	16	5	35	5	7	4	3	19	20	78	73	+5
India	7	1	3	13	2	5	4	10	8	3	26	23	+3
Midland	5	12	0	3	1	2	6	15	8	4	38	38	0
New York	64	101	19	129	78	28	49	58	79	75	442	427	+15
Niagara Falls	7	19	1	19	2	5	58	50	18	24	152	141	+11
Pacific Northwest	4	12	0	10	0	2	7	12	12	6	45	40	+5
Philadelphia	19	30	4	38	45	15	19	14	14	29	160	160	0
Pittsburgh	3	34	3	23	14	5	24	14	29	10	95	85	+10
San Francisco	6	10	2	13	9	3	8	17	13	5	46	43	+3
Washington-Baltimore	33	39	9	32	19	3	11	12	28	7	115	108	+7
Ontario-Quebec	7	11	0	13	1	3	24	20	7	12	60	59	+1
U.S. Non-Section	76	148	28	157	94	56	94	96	145	97	638	622	+16
Foreign Non-Section	33	39	8	48	19	24	26	53	52	53	182	175	+7
Total as of April 1, 1956	325	541	88	629	340	177	366	414	490	371	2358		
Total as of Jan. 1, 1956	309	518	88	609	312	172	341	401	476	377		2270	
Net Change	+16	+13	0	+20	+28	+5	+25	+13	+14	−6			

DONALD A. SWALHEIM, E. I. du Pont de Nemours & Co., Inc., Buffalo Ave., Niagara Falls, N. Y. (Electrodeposition)

Transfers from Student Associate to Active Membership

RALPH J. BRODD, National Bureau of Standards, Section 18, Washington, D. C. (Theoretical Electrochemistry)

WILLIAM N. VANDERKOOI, Dow Chemical Co., Midland, Mich (Electronics)

WILLIAM H. WADE, Radiation Lab., University of California; Mail add: 33 Sunset Dr., Berkeley 7, Calif. (Theoretical Electrochemistry)

Transfer from Associate to Active Membership

JOSEPH RAIMONDO, D. E. Makepeace Co.; Mail add: 94 Gray St., Providence, R. I. (Corrosion, Electric Insulation, Electrodeposition, Electronics)

Deceased—Reported in February

GUSTAV EGLOFF, Des Plaines, Ill.

TABLE II. *ECS Membership by Grade*

	Total as of 4/1/56	Total as of 1/1/56	Net Change
Active	2095	2013	+82
Life	14	14	0
Emeritus	36	34	+2
Associate	48	49	−1
Student	57	53	+4
Honorary	5	5	0
Sustaining	103	102	+1
Total	2358	2270	+88

J. C. JONES, New York, N. Y.
JOHN W. MAGLY, Cincinnati, Ohio
CLARENCE C. ROSE, Cleveland, Ohio

PERSONALS

EDWARD R. WEIDLEIN formally announced his retirement as President of the Mellon Institute of Industrial Research, Pittsburgh, Pa., effective March 31, at a testimonial dinner given him by the members of the Institute on March

19. Dr. Weidlein has been prominently and actively identified with the Institute for over 40 years, serving as a senior fellow 1912–16, and then as an executive staff member from 1916 to 1951, when he was made President. He is noted internationally as a scientist, research administrator, and author. Following his retirement he will spend several months in Europe on a Federal Government mission. Dr. Weidlein will continue to serve the Institute as a member of the Board of Trustees and will be available in an advisory capacity in the administration of research programs.

ALBERT H. COOPER has joined the American Hard Rubber Co., New York City, as assistant to W. M. Bergin, Director of Research & Development. A well-known authority on organic and inorganic chemicals, Dr. Cooper will devote the major part of his time to furthering American's accelerated chemical research and allied production programs. He is the owner and manager of Pilot Engineering Co., industrial consultants on plant design and production problems; he also is head of the Dept. of Chemical Engineering at Pratt Institute in Brooklyn.

J. J. LANDER has resigned as chemist with the Naval Research Lab., Washington, D. C., to assume the position of Director of Research of the Storage Battery Division, Electric Auto-Lite Co., Toledo, Ohio.

J. S. DEWAR recently was promoted to President of National Carbon Co. Ltd., Toronto, Ont., Canada. He has the distinction of being the youngest chief executive in the history of the company.

S. C. OGBURN, JR., Vice-President—Research & Development, Foote Mineral Co., Philadelphia, Pa., retired as an officer of the company on March 1. He will continue to serve as a management consultant. Dr. Ogburn joined Foote Mineral in 1948 as Manager of Research & Development, became a member of the board in 1949, and was named Vice-President in 1951. He is the author of several patents and over 25 technical papers dealing with chemical research and research management.

KASIL POTASSIUM SILICATE BINDERS

Kasil #1 molecular ratio 1:3.9 (7.8% K_2O, 19.5% SiO_2); 28° Baume
Kasil #22 molecular ratio 1:3.45 (8.6% K_2O, 18.9% SiO_2); 28.6° Baume

These Kasil Potassium Silicates meet the high standards needed for TV tube production. Spectographic analyses indicate the high degree of purity—absence of copper, nickel and other elements which might cause contaminated screens.

Kasil's uniform quality is dependable—shipped in drums, tanktrucks and tankcars.

• Ask for helpful publications: Potassium silicate binders for cathode ray tube formulas • Colloidal and surface phenomena in the preparation of cathode ray screens.

PHILADELPHIA QUARTZ COMPANY
Established 1831

1156 Public Ledger Bldg.
Philadelphia 6, Pa.
Trademarks Reg. U. S. Pat. Off.

BOOK REVIEWS

TABLES OF THERMAL PROPERTIES OF GASES by J. Hilsenrath, C. W. Beckett, W. S. Benedict, L. Fano, H. J. Hoge, J. F. Masi, R. L. Nuttall, Y. S. Touloukian, and H. W. Woolley. Circular 564, published by National Bureau of Standards, Government Printing Office, Washington 25, D. C., 1955. 478 pages, $3.75.

Covers air, argon, carbon dioxide, carbon monoxide, hydrogen, nitrogen, oxygen, and steam. The properties tabulated are compressibility factor, density, entropy, enthalpy, specific heat, specific heat ratio, sound velocity, vapor pressures and transport properties, thermal conductivity, viscosity, and Prandtl number.

PLASTICS PROGRESS 1955. Phillip Morgan, Editor. Published by Iliffe & Sons Ltd., London, and Philosophical Library, Inc., New York, N. Y., 1956. vii + 432 pages, $17.50.

Technical papers and discussions at the British Plastics Convention, June 1955.

STEELS FOR THE USER, 3rd edition, by R. T. Rolfe. Published by Philosophical Library, Inc., New York, N. Y., 1956. xvi + 399 pages, $10.00.

A discussion for the practical man of the effects of composition, heat treating, and other factors on properties; methods of testing and interpreting tests, principles of selection for various purposes.

SPECTROSCOPY AT RADIO AND MICROWAVE FREQUENCIES by D. J. E. Ingram. Published by Butterworths Scientific Publications, Ltd., London, W. C. 2, England, 1955. xii + 332 pages; 45 shillings + postage.

A general outline for the nonspecialist. Production and detection of radiation from 1 mc to 500,000 mc, techniques of measurements, discussion of results and theory, a chapter on applications including chemical analysis, study of free radicals, nature of semiconductors.

INFORMATION PROCESSING EQUIPMENT. M. P. Doss, Editor. Published by Reinhold Publishing Corp., New York, N. Y., 1955. 270 pages, $8.75.

Papers presented at an American Chemical Society Symposium. Covers typing, stenciling, hectographing, photographic copying, microcopying, xerography, letterpress and offset printing, figure preparation, slide preparation, projection equipment; audio methods, punched cards, numerical data-handling machines, and other topics.

MATERIALS FOR NUCLEAR POWER REACTORS by Henry H. Hausner and Stanley B. Roboff. Published by Reinhold Publishing Corp., New York, N. Y., 1955. 224 pages, $3.50.

An elementary exposition of the problems encountered in design, materials, and construction.

HORNER'S DICTIONARY OF MECHANICAL ENGINEERING TERMS, 7th edition. Revised by Staton Abbey. Published by Philosophical Library, Inc., New York, N. Y., 1955. 417 pages, $6.50.

AIRCRAFT TODAY. J. W. R. Taylor, Editor. Published by Philosophical Library, Inc., New York, N. Y., 1955. 96 pages, $4.75.

Nontechnical.

C. V. KING

MODERN PHYSICS by Robert L. Sproull. Published by John Wiley & Sons, Inc., New York 16, N. Y., 1956. VII + 491 pages, $7.75.

The purpose of this book is to provide the reader with an analytical introduction to modern physics and its applications. Although offered as a textbook for engineers, it covers much more of the mathematical details of atomic and nuclear physics than most engineers outside of the electronics and nuclear fields would normally be expected to find useful.

The philosophy of the author is to develop an understanding of the nature of nuclei, atoms, molecules, and crystalline solids. In general, he has succeeded. A modern treatment is given of the principles of quantum physics, well illustrated by many examples of experimental data which convincingly support these principles. The author shows very clearly how relativity and quantum physics extend rather than supplant the classical physics of Newton and Maxwell.

The material is well organized. Physical phenomena due to the nuclei of atoms and those due to the planetary electrons are compared and systemized. Each chapter contains a good list of pertinent references and problems.

The chapter on semiconductors is most informative and of particular interest at this time because of the rapidly increasing use of transistors and other semiconductor devices in industry and communication. One omission was noted. This was the lack of any description of photovoltaic cells.

The book will be of considerable value to those who desire to understand the physics underlying modern electronic devices.

HENRY S. MYERS

AUTOMATIC PROCESS CONTROL FOR CHEMICAL ENGINEERS by Norman H. Ceaglske. Published by John Wiley & Sons, Inc., New York 16, N. Y., 1956. x + 228 pages, $6.75.

The book emphasizes the growing importance of automatic control in the chemical process industries. A grounding in the principles of automation and some of its elementary practice is most essential in the career of today's chemical engineer. The book imparts such information concisely and should be of definite assistance both to the student and to the practicing engineer.

The subject matter is divided into two general categories. The introductory chapters describe the various types of control systems and instruments, and include a short history of automatic control, descriptions of typical systems, standards of measurements, explanations of apparatus, and details of various control systems. Topics are well illustrated, with many excellent sketches, diagrams, and photographs.

The remaining chapters discuss mathematical treatments of various phases of the subject. They cover derivations of equations, solutions by differential equations, transient analysis of control systems, frequency response of control systems, and the analysis of simple control systems. Laplace transforms have been used throughout the mathematical section.

A number of illustrative problems are given at the end of most chapters. Following each chapter is an extensive list of references.

This book provides an excellent introduction to the vital field of automation, which certainly is becoming increasingly important in all our technologies.

HENRY S. MYERS

HOW TO

GET THE MOST OUT OF YOUR B.S. DEGREE IN CHEMISTRY OR CHEMICAL ENGINEERING

Take advantage of this unique combination:

THE COMPANY: A world leader—both in the success of current products, and in the quality of its advanced and diversified research program for the future.

THE PLACE: Southern California, with a climate and a way of living second-to-none.

THE JOB: Electro-Chemical research on new materials and processes: fascinating work—as personally satisfying as it is professionally rewarding.

This is your chance to realize your full potential. Act now. Write: BOX A-263, c/o this publication.

ANNOUNCEMENTS FROM PUBLISHERS

CHEMICAL INDUSTRY FACTS BOOK. Published by the Manufacturing Chemist's Association, Inc., 1625 Eye St., Northwest, Washington 6, D. C., 1955.

A fourfold chemical industry sales growth, 1939 through 1954, is reported in the new edition of the Facts Book.

1950–1951 BIBLIOGRAPHIC SURVEY OF CORROSION. Published by the National Association of Corrosion Engineers, 1061 M & M Bldg., Houston 2, Texas, 1955. 430 pages; price—nonmembers NACE $12.50, members NACE $10.00.

Summaries of 4454 corrosion and corrosion prevention articles, books, and brochures published in 1950–1951 are compiled in this volume. Bulletins published by 30 abstracting agencies were canvassed regularly for material taken from more than 500 sources the world over. This is the fourth in a series of NACE bibliographies on corrosion literature. The preceding three volumes, covering 1945 through 1949, contained 7960 abstracts.

ALKALINE DERUSTING OPERATIONS. Prepared by Rock Island Arsenal, U. S. Army, June 1955. Available as report PB 111744.* 11 pages, 50 cents.

TECHNICAL DIGESTS. Monthly publication of the Organization for European Economic Cooperation, a multigovernment agency set up to stimulate economic growth of member nations. Price: $24.00 a year, $2.50 a single issue. Subscriptions handled by: O.E.E.C. Mission Publications Office, 2000 P St., N. W., Washington 6, D. C.

Periodical, averaging 140 pages, contains the best articles from European technical and industrial journals, translated and digested. The U. S. Dept. of Commerce, through its Office of Technical Services, is cooperating with O.E.E.C. in making this new source of information known to American industry.

PROCEEDINGS OF THE CONFERENCE ON DIELECTRIC MATERIALS. Prepared by the Naval Research Laboratory, Washington, D. C., 1955. Available as Publication No. PB 111863.* v + 169 pages, $4.25.

Volume contains papers on many aspects of radiation effects in organic and inorganic materials presented at the Dec. 14, 1954 Conference sponsored jointly by the Naval Research Laboratory and the Air Research and Development Command.

SCALING OF TITANIUM AND TITANIUM ALLOYS. Prepared by the University of Kentucky for the Wright Air Development Center in March 1955. Available as report PB 111731.* 137 pages, $3.50.

THE EXTRUSION OF TITANIUM. Prepared by the Wright Air Development Center, 1955. Available as report PB 111696.* 77 pages, $2.00.

PHOSPHATING MATERIALS AND PROCESS. Prepared by the Rock Island Arsenal Laboratory. Available as report PB 111726.* 88 pages, $2.25.

* Order from Office of Technical Services, U. S. Dept. of Commerce, Washington 25, D. C.

LITERATURE FROM INDUSTRY

"CORROSION PROOFING." Brochure on corrosion proofing materials and techniques, containing detailed information on cement mortars, interliners for masonry construction, and protective coatings and linings for surface treatment, is offered. *Pennsylvania Salt Manufacturing Co.*, Corrosion Engineering Dept., 3 Penn Center Plaza, Philadelphia 2, Pa.

STOPPING CORROSION WITH PVC LININGS. How to choose the best polyvinyl chloride protection for any given corrosive environment is discussed at length in a new booklet. The three most commonly used types of PVC protection are covered individually. *Kaykor Industries, Inc.*, Yardville, N. J.

"THE USE OF SELENIUM PHOTOCELLS AND SUN BATTERIES." Technical booklet contains 58 pages of information and over 35 illustrations, charts, and diagrams. Copies available through electronic parts distributors throughout the country, at a net cost of $1.50 each, or may be ordered, by including check or money order, from *International Rectifier Corp.*, Product Information Dept., El Segundo, Calif.

To receive further information on any New Product or Literature from Industry listed, write directly to the company at the address given in each item.

RADIOISOTOPE CATALOGUE. Revised catalogue is available on request to scientific institutions, medical centers, industrial laboratories, and other qualified persons. Nearly 100 different radioactive preparations, together with specifications and price, are listed. *Oak Ridge National Lab., Union Carbide Nuclear Co.*, Radioisotope Sales Dept., P. O. Box P, Oak Ridge, Tenn.

ADVERTISERS' INDEX

Bell Telephone Laboratories, Inc. 114C
Enthone, Incorporated ..... Cover 4
Great Lakes Carbon Corporation ..... Cover 2
Mallinckrodt Chemical Works 110C–111C
Philadelphia Quartz Company 124C
Stackpole Carbon Company .. 112C

EMPLOYMENT SITUATIONS

Please address replies to box shown % The Electrochemical Society, Inc. 216 W. 102nd St., New York 25, N. Y.

Positions Wanted

CHEMIST, 36, 11 years' experience, including batteries, electroplating, general physical and chemical commerical testing, seeks New Jersey, Philadelphia, New York City position. *Reply to Box 357.*

CHEMICAL ENGINEER, 40, B.S. degree, 14 years' experience, including materials engineering and research, electrodeposition processes, product engineering and development work involving capacitors. *Reply to Box 358.*

CHEMICAL ENGINEER, experience in high temperature process development, including fused salt electrolysis, electric furnaces, metals extraction, B.Ch.E. 1939, married, age 38, seeking challenging, mature position. *Reply to Box 359.*